ASSESSMENT OF PHOTOCATALYTIC PERFORMANCE OF ALUMINUM-SUPPORTED TITANIUM DIOXIDE THIN FILMS PRODUCED BY FLAME ASSISTED CHEMICAL VAPOUR DEPOSITION

by

Eric Edward Potter

A thesis submitted to the Department of Chemical Engineering

In conformity with the requirements for

the degree of Master of Applied Science

Queen's University

Kingston, Ontario, Canada

(December, 2010)

Abstract

Titanium dioxide films were deposited on aluminum by flame assisted chemical vapour deposition. The photocatalytic performance of these films when the air flow rate to the flame and thickness of silicon oxides under-layer were varied, was compared against a film of electrophoretically deposited Degussa P25, a titanium dioxide powder. At a high air flow rate, only powder was deposited on the substrate and the films had no measurable photocatalytic activity. When the air flow rate was lower, and the flame cooler, titanium dioxide was successfully deposited. Samples with a silicon oxides under-layer had more titanium dioxide deposited than with no undercoating, but titanium dioxide content did not increase as the layer of silicon oxides thickness increased. Films deposited at a low air flow rate, and with a silicon oxides under-layer, were shown to act as self-cleaning surfaces through the mineralization of a stearic acid film, successfully removed organic compounds from water through the oxidation of methylene blue as a model compound, and effectively inactivated *Vibrio fischeri* in water. However, in all cases the performance was found to be moderate when compared to Degussa P25 films. The successful use of films produced under these conditions in various applications suggests that they may also be effective in an air sterilization unit. An air sterilization reactor system was designed with considerations to reactor geometry, relative humidity and air flow rate. Bioaerosol generation and capture experiments were performed while varying pressure supplied to a Collison Nebulizer, the nebulizer optical density of *Bacillus subtilis*, and the sample period using a modified AGI-4 impinger. A model was developed to correlate these parameters to expected bacterial capture. Different methods of assessing cell viability in the capture solution were examined, and the use of the Live/Dead assay was recommended over traditional plate counts because of lower associated error.

Acknowledgements

Special thanks are owed to my supervisors, Dr. Juliana Ramsay and Dr. Aristides Docoslis, for their expert guidance, understanding, and constant support throughout the project. I am grateful.

This project was done in cooperation with Novelis Inc., and would not have been possible with Novelis Inc. and its employees, especially Florina Truica-Marasescu, John Hunter, and Robert Jones. Novelis Inc. supplied the flame assisted chemical vapour deposition films (produced by Pamina Lin and Megan Wright) used in this study, as well as the SEM/EDS, GD-OES (Pamina Lin and Megan Wright), and stearic acid results (Pamina Lin).

I would like to thank Pamina Lin, the Masters student continuing the project, for her expeditiousness when carrying out the stearic acid tests at Novelis Inc., and for providing me with the additional information I needed to write my thesis.

I would like to thank all of my lab group members for their help, encouragement, and friendship. It has been a pleasure working with you. Special thanks to Jeff Wood for his constant willingness to help. I would also like to thank the lab of Dr. Ron Neufeld for allowing me use of their plate reader.

I would also like to thank many people in the department for their friendship and support and in some cases for their homes while I was completing my thesis. Thank you.

Finally I would like to thank the Ontario Centers of Excellence, Novelis Inc., and Queen's University for the funding required for my project.

Table of Contents

List of Figures

List of Tables

Chapter 1

Introduction

Titanium dioxide is a semiconductor and photocatalyst that can be activated by UV light (< 384 nm) (Carp et al., 2004; Fujishima et al., 2008). When light with sufficient energy is absorbed by titanium dioxide in the presence of oxygen, an electron-hole pair is generated. The valence band electron hole can react with water to produce highly oxidizing hydroxyl radicals, while the conduction band electron can react with oxygen to form super oxide species. These radical species are capable of mineralizing most organic compounds. Titanium dioxide photocatalysis can be used for applications such as self-cleaning surfaces, for the removal of organic compounds, and the inactivation of biological organisms.

Recently, there has been much industrial interest in the production of titanium dioxide thin films for a range of applications. Traditional methods of film deposition, such as the sol-gel method, are slow and not suited for continuous industrial production of films. Chemical vapour deposition (CVD) or related processes are normally better suited for industrial applications. Novelis Inc., a world leader in aluminum rolling and recycling, is in the process of optimizing a flame assisted chemical vapour deposition (FACVD) system for the generation of titanium dioxide films, with the goal of producing value added products to their existing product lines. FACVD has long been recognized by industry as the most cost effective way to produce metal oxide powders like titanium oxide, but to the author's knowledge, no titanium dioxide films have been previously deposited using FACVD (Choy, 2003). Novelis Inc. is interested in developing an in-line process for the rapid deposition of mechanically robust titanium dioxide films on

aluminum substrate, with specific interest towards the development of photocatalytic films for the destruction of bioaerosols.

Bioaerosols may consist of bacteria, cellular fragments, fungal spores, viruses, and microbial metabolites such as endotoxin. Exposure to bioaerosols can lead to serious diseases, such as influenza, tuberculosis, and meningitis and has been found to be responsible for asthma incidences. Two of the most common technologies used to improve air quality are Ultraviolet Germicidal Irradiation (UVGI) and High Efficiency Particulate Air (HEPA) filters. However, each technology has inherent limitations. For example, neither UVGI nor HEPA filters will remove endotoxin (Grinspun et al., 1997).

The purpose of this study is to compare the performance of films produced under different process conditions by Novelis Inc.'s FACVD process against a standard benchmark titanium dioxide film. The performance of Novelis Inc.'s films as self-cleaning surfaces, for the destruction of aqueous phase organic compounds, and for the inactivation of aqueous phase microorganisms was tested. Additionally, a photocatalytic reactor system for bioaerosol inactivation was designed to test the performance of the FACVD films. The thesis was organized as follows:

- A literature review was performed and used to design the experiments in this study (Chapter 2).
- Deposition procedures were described, and the produced films analyzed (Chapter 3).
- The performance of Novelis Inc.'s films was tested as self-cleaning surfaces, for the destruction of aqueous phase organic compounds, and for the inactivation of aqueous phase and compared to a standard film (Chapter 4).

- A photocatalytic reaction system for the inactivation of bioaerosol was designed. Bioaerosol generation and capture procedures were also developed (Chapter 5).

Chapter 2

Literature Review

2.1 Basic Properties of Titanium Dioxide

Titanium dioxide is a semiconductor with three main crystal structures: rutile, anatase, and brookite (Carp et al., 2004; Fujishima et al., 2008). It has high chemical stability, is non-toxic, and inexpensive (Carp et al., 2004; Legrini et al., 1993). When a semiconductor is struck with a photon that has a greater energy than the band gap energy, an electron is promoted from the valence band to the conduction band forming an electron-hole pair (de Lasa et al., 2005). The band gap energy was found to be 3.0 eV for rutile and 3.2 eV for anatase (Fujishima et al., 2008; Mardare et al., 2000). The maximum wavelength of light needed to promote an electron from the valence band to the conduction band is 410 nm and 384 nm respectively (Carp et al., 2004). Electron-hole pairs can be used for many applications such as the degradation of organic compounds. The use of light to provide the energy for a reaction to occur in the presence of a catalyst is commonly referred to as photocatalysis.

2.2 Photocatalysis

Investigation into the photocatalytic use of titanium dioxide began after it was observed that pigments were being degraded in paints containing titanium dioxide (Jacobsen, 1949). Since then, much investigation has been done on titanium dioxide photocatalysis and its mechanism. The photocatalytic oxidation of organic compounds using light activated titanium dioxide can either take place due to indirect oxidation via hydroxyl radicals (Mills and Hoffman, 1993; Terzian et al., 1991; Turchi and Ollis, 1990) or by direct interaction with valence band holes (Carraway et al., 1994; Draper and Fox, 1990). Some have suggested that the primary

mechanism of oxidation depends on the nature of the substrate (Moa et al., 1991). The rate of oxidation also depends on the crystal phase of titanium dioxide.

Anatase is the crystal structure that generally shows the greatest photocatalytic activity, but the rutile crystal structure is also employed (Ding et al., 2000; Tanaka et al., 1991; Fox et al., 1993). In photocatalytic reactions, the interfacial reactions involving the generated electron-hole pairs (microseconds to milliseconds) compete with the deactivation process of electron-hole recombination (picoseconds to nanoseconds) (Carp et al., 2004; de Lasa et al., 2005; Hoffman et al., 1995). The difference in photocatalytic performance between rutile and anatase has been attributed to the higher band gap energy of anatase leading to slower electron-hole recombination (Tanaka et al., 1991; Wold, 1993; Bickley et al., 1991; Bessergenev et al., 2006).

In order for a photocatalytic reaction to proceed there must be a catalyst surface, an oxidizing agent (usually oxygen), and photons of the appropriate wavelength (de Lasa et al., 2005; Legrini et al., 1993; Hoffman et al., 1995). A generalized reaction scheme can be described as follows (de Lasa et al., 2005; Hoffman et al., 1995):

Light with a wavelength less than 384 nm ($h\nu$>3.2 eV, anatase) strikes the titanium dioxide and generates an electron (e^-)-hole (h^+) pair:

$$TiO_2 \xrightarrow{h\nu > 3.2\ eV} e^- + h^+$$

An electron is donated from adsorbed water (H_2O), adsorbed hydroxyl ions (OH^-), or adsorbed substrates (A) to fill the valence band hole.

$$h^+ + H_2O \longrightarrow OH^\bullet + H^+$$
$$h^+ + OH^- \longrightarrow OH^\bullet$$

$$h^+ + A \longrightarrow A^+$$

Oxygen molecules act as acceptors of electrons to form super-oxide anions which can participate in further generation of reactive oxygen species or additional radical species (de Lasa et al., 2005).

$$e^- + O_2 \longrightarrow O_2^-$$

Previously generated hydroxyl radicals can oxidize substrates near the catalyst surface (de Lasa et al., 2005).

$$OH^\bullet + A \longrightarrow Intermediate$$

The general concept provided by this simple mechanism has been applied to various applications in both the gaseous and liquid phase. Such applications include synthesis of organic compounds, production of self-cleaning surfaces, removal of organic and inorganic compounds, and inactivation of biological organisms (Fujishima et al., 2008; Carp et al., 2004). The photocatalytic nature of titanium dioxide can also be used to make light induced superhydrophilic (a term often used when talking about titanium dioxide surfaces with near 0^o water contact angle) surfaces (Fujishima et al., 2008). Superhydrophilicity is caused when trapped holes weaken the bond between titanium and the lattice oxygen, liberating oxygen and producing an oxygen vacancy. Water adsorption at these sites hydroxylates the surface, enhancing the wetting of water on the surface (Mills et al., 2003).

Titanium dioxide photocatalysis is not frequently used for selective organic synthesis. However, a variety of chemical compounds can be synthesized including alkanes/alkenes (Ohno

et al., 2001), alicyclic hydrocarbons (Maeda et al., 2004), aromatic compounds (Kanno et al., 2001), ketones and aldehydes (Mohammed et al., 2002), and many other classes of compounds. The other major applications of titanium dioxide photocatalysis will be discussed in detail later in the chapter.

2.3 Titanium Dioxide Films

2.3.1 Influence of Film Properties on Photocatalytic Performance

For many commercial applications, the use of titanium dioxide films is more practical than the use of powders (Mills et al., 2003). Many of the factors that determine the efficiency of titanium dioxide powders also apply to films, including morphology, crystal phase, specific surface area, particle aggregate size, and surface density of OH ions (Mills and Hunte, 1997). Film thickness can also affect the efficiency depending on the wavelength used for activation. Thin (about <100 nm) titanium dioxide films typically absorb a large amount of the UVC spectrum but little of the UVA (Mills et al., 2003). Thus, thin films typically have a lower efficiency in UVA light than UVC light (Mills et al., 2002).

Substrate-film interactions are another major factor which can affect photocatalytic efficiency. Efficiency can be affected by direct interaction with the substrate, by the migration of ions from the substrate, or by changes in deposition mechanism caused by various substrates. Direct interaction occurs through chemically bonding with the support material and can cause changes in the energy band structure of titanium dioxide, negatively impacting photocatalytic activity (Pozzo et al., 1997).

The migration of sodium, iron/chromium, and aluminum ions can occur under some conditions when titanium dioxide films are coated on glass, stainless steel, and aluminum respectively (Wantanabe et al., 1999; Evans and Sheel, 2007; Zhu et al., 2001; Ho et al., 2007).

The degree of ion migration is related to temperature of film deposition (Evans and Sheel, 2007). All of these ions are known to act as charge recombination sites, lowering the life span of electron-hole pairs, and decreasing photocatalytic efficiency (Wantanabe et al., 1999; Evans and Sheel, 2007; Cho et al., 1994; Ho et al., 2007). Kwon et al. (1994) showed that as the film thickness of titanium dioxide on aluminum substrate increased, the impact of the aluminum substrate diminished. The use of an inert, shielding under-layer, normally SiO_2, has been shown to block the migration of these detrimental ions, and increase photocatalytic efficiency (Wantanabe et al., 1999; Evans and Sheel, 2007).

Film activity can also be altered by substrate interaction during the film deposition process. Using a specific precursor, when titanium dioxide was deposited on SiO_2 coated stainless steel, anatase was the primary phase (Evans and Sheel, 2007). When the same precursor and deposition conditions were used, rutile was the primary phase when the coating was done on bare stainless steel. Therefore, the substrate can have an effect on the crystal structure of titanium dioxide films. This study also demonstrated that an undercoating of SiO_2 decreased the grain size compared to deposition on bare stainless steel by providing more favorable nucleation sites. It can be seen that there are many factors to ensure high photocatalytic activity which must be considered when depositing titanium dioxide films.

2.3.2 Methods of Titanium Dioxide Film Deposition

Titanium dioxide film deposition can be broadly categorized into methods using previously made titanium dioxide powder, and methods where titanium dioxide is generated during support coating (Pozzo et al., 1997). Common films deposition methodologies for each category are discussed in the following sections.

2.3.3 Powder Deposition

When films are deposited using a pre-made titanium dioxide powder, the powder of choice is most often Degussa P25 (Maness et al., 1999). Degussa P25 particles are produced by high temperature hydrolysis of $TiCl_4$ in the presence of hydrogen and oxygen to form a mixture of approximately 80% anatase/20% rutile (Mills and Le Hunte, 1997). Titanium dioxide photocatalytic films are normally compared to Degussa P25 because of its high photocatalytic activity, which has led to widespread use (Mill and Le Hunte, 1997). The high photocatalytic activity of Degussa P25 is due to slow electron-hole recombination, which is thought to be caused by the mixed anatase-rutile structure of Degussa P25 (Hoffman et al., 1995; Bickley et al., 1991). The high activity of Degussa P25 is typically independent of the support material partially due to the low temperature conditions associated with powder deposition (Byrne et al., 1998).

Many methods have been used to coat substrates with powdered titanium dioxide. Some of the most commonly used methods are dip coating, spray coating, wash coating, and electrophoretic deposition (Fretwell and Douglas, 2001; Pozzo et al., 1997; Mills and Wang, 1998; Mills et al., 2002; Byrne et al., 1998; Fernandez et al., 1995; Matthews et al., 1994). When these methods were compared, electrophoretic coating typically resulted in higher photocatalytic activity and more reproducible activity (Byrne et al., 1998).

One major drawback of titanium dioxide films made by powder deposition is their low mechanical robustness. Although there is no clear understanding of the bonding between titanium powder and support material, it is thought that electrostatic interactions may play a major role, but chemical bonding may also occur (Pozzo et al., 1997). Powder based films are usually not destroyed by washing, but it has been found that mechanical abrasion can easily remove the photocatalyst (Mill et al., 2002).

2.3.4 Sol-Gel Deposition Method

The sol-gel process is most frequently used for the deposition of titanium dioxide films where a pre-formed powder is not utilized (Mills et al., 2003; Carp et al., 2004). Most sol-gel film deposition methods use titanium alkoxides as precursors (Sivakumar et al., 2002). Titanium ethoxide, titanium isopropoxide, and titanium tert-butoxide are the most common titanium alkoxides used in the sol-gel process (Carp et al., 2004; Okudera et al., 2001; Mills et al., 2003). Some sol-gel film deposition methods have also used inorganic compounds instead of alkoxides (Sivakumar et al., 2002).

Sol-gel methods can produce films with high purity and homogeneity while exhibiting high levels of control over the films produced and can be used to coat large and complex surfaces (Carp et al., 2004). In contrast to powder deposition, the sol-gel process can make films that are very mechanically robust and scratch resistant (Fretwell and Douglas, 2001; Mills et al., 2002). Many deposition methods have been used with the sol-gel process such as dip coating, spin coating, and spray coating (Fretwell and Douglas, 2001; Byun et al., 2000). Following deposition, the films must be annealed at high temperatures to crystallize the titanium dioxide (Byun et al., 2000; Carp et al., 2004). The sol-gel process typically makes thin films (<100 nm) which have high absorbance in the UVC range, but low absorbance in the UVA range (Mills et al., 2003). However, thick films can also be produced, some of which have higher efficiency than films made from Degussa P25 (Fretwell and Douglas, 2001).

2.3.5 Chemical Vapour Deposition of Titanium Dioxide

Recently, chemical vapour deposition (CVD) methods have been investigated for the deposition of titanium dioxide films (Mills et al., 2002; Heft et al., 2006; Evans and Sheel, 2007; Bessergenev et al., 2002; Hitchman and Tian, 2002; Kaliwoh et al., 2002). CVD methods involve

the formation of a stable solid product from gas phase reactants in an activated (heat, light, plasma) environment (Choy, 2003; Xu and Yan, 2010). Common sources of titanium for CVD are $TiCl_4$ and titanium alkoxides such as titanium isopropoxide, titanium tert-butoxide, and titanium ethoxide (Ritala et al., 1993). Water, atmospheric oxygen, and oxygen in the precursor can be used to provide the oxygen needed for the generation of titanium dioxide films (Ritala et al., 1993). The crystallinity of films formed using CVD is dependent on the precursors used and the substrate material. For example, the crystallinity of films deposited directly on stainless steel by CVD was dependent on the precursor used (Bessergenev et al., 2006; Evans and Sheel, 2007). However, when there was a SiO_2 under-layer, the films were found to be anatase regardless of the precursor (Evans and Sheel, 2007). Some studies have found that whether deposition was done on glass, quartz, or ceramic, the crystal phase was not affected and the results relied solely on the precursor (Bessergenev et al., 2006).

Advantages to using CVD are the production of uniform films, high adhesion of the deposited film to the substrate, controllable crystal structure, easily adjusted deposition rate, relatively low deposition temperatures (compared to annealing in the sol-gel process), and the ability to coat complex surfaces (Choy et al., 2003; Xu and Yan, 2003). CVD processes may also result in a relatively high rate of film formation compared with other methods because these processes do not require any external energy to cause film solidification after deposition (Xu and Yan, 2010; Byun et al., 2000). For these reasons CVD methods, especially variants that occur at atmospheric pressure, are often the preferred deposition methods for industrial production of films (Mill et al., 2003)..

2.3.6 Flame Assisted Chemical Vapour Deposition

Flame assisted chemical vapour deposition (FACVD), a variant of CVD, has long been recognized as one of the most cost effective way to produce metal oxide powders like TiO_2 and SiO_2 (Choy, 2003). It is a relatively new and innovative method of producing films (Evans and Sheel, 2007) and typically produces films in a much shorter period than traditional CVD processes (Choy, 2003). To the author's knowledge, no titanium dioxide films have been previously deposited using FACVD. However, other studies have used FACVD to deposit an under-layer of SiO_2 by FACVD before coating the substrate with titanium dioxide using another variant of CVD (Evans and Sheel, 2007).

In FACVD the precursors needed to make the film are mixed with the fuel source, and injected into a flame system where they are combusted to form a coating (Xu and Yan, 2010; Choy et al., 2003). In CVD processes, the substrate is often heated to enhance the surface mobility on the substrate during deposition (Choy, 2003). In the FACVD process the flame provides the heat required for both the precursor to react and to heat the substrate, which makes it more efficient than conventional CVD processes (Choy, 2003).

In FACVD, there are many factors which determine the crystal structure, morphology, and grain size such: flame temperature profile, choice of precursor, residence time in the flame, ratio of fuel to precursor and fuel to air, the distance between the substrate and the flame, and the cooling of the deposited film (Choy, 2003; Xu and Yan, 2010). Dopants may also greatly affect the properties of the deposited film. In the production of titanium dioxide powders by FACVD, dopants such as silicon and phosphorus can drastically alter the morphology of titanium dioxide powders by increasing the extent of aggregation, increasing the specific surface area, decreasing the specific particle size, and decreasing the rutile content (Akhtar et al., 1992). All of these

effects typically enhance the photocatalytic activity of titanium dioxide. However, doping with aluminum caused irregular titanium dioxide crystals to form and generated pure rutile (as opposed to 90% anatase without aluminum) (Akhtar et al., 1994).

The major advantages of FACVD is the ability to coat complex substrates, the formation of product in a single step without need for annealing, reduced processing time compared to conventional CVD, high control of stoichiometry, high deposition rate, and relatively low cost compared to other CVD methods (Choy et al., 2003; Xu and Yan, 2010).

The major drawback of the FACVD method is the large temperature fluctuation in the flame source (Choy, 2003). This makes it difficult to produce uniform, dense thin films, but adherent porous coatings can be made (Choy et al., 2003; Choi et al., 1998). Effort has also been made to improve flame stability using various burners such as the counterflow flame burner and reduced pressure flat flame burner (Choy, 2003). Another difficulty associated with many FACVD processes is that since the flame temperature is very high, it can lead to a homogeneous gas phase reaction and the deposition of powder (Choy, 2003). To avoid this, the flame temperature can be reduced by adjusting factors such as the ratio of fuel to precursor (Choy, 2003).

2.4 Applications of Titanium Dioxide Photocatalysis

Titanium dioxide photocatalysis has many potential applications. Such applications include synthesis of organic compounds, production of self-cleaning surfaces, removal of organic and inorganic compounds, and inactivation of biological organisms (Carp et al., 2004).

2.4.1 Removal of Organic Compounds from Aqueous Solution

Titanium dioxide photocatalysis has many potential benefits over conventional methods of wastewater and drinking water purification. Conventional wastewater treatment typically involves an activated sludge process which requires high contaminant concentration to ensure microbial growth (Carp et al., 2004). Therefore, conventional methods cannot be applied to treat water with low concentrations of organics. Furthermore, these processes produce a sludge by-product and risk microbial death due to toxic shock (Carp et al., 2004). They have also been shown to be ineffective in the degradation of some synthetic compounds such as chloroorganics (Gogate and Pandit, 2004; Baird and Cann, 2005). Need exists for an economical and environmentally benign process to mineralize organic compounds left behind by conventional water treatment methods (Carp et al., 2004). Titanium dioxide photocatalysis has been shown to be a relatively low cost, non-toxic process capable of mineralizing a wide variety of organic compounds at near ambient conditions (Bhatkhande et al., 2001; Legrini et al., 1993).

In aqueous systems, chemical degradation typically occurs through indirect oxidation involving the generation of hydroxyl radicals from water or hydroxyl ions adsorbed to the surface (Legrini et al., 1993). Hydroxyl radicals are strong oxidizing species that primarily initiate oxidation of organic species through hydrogen abstraction (Legrini et al., 1993). Oxidation can also occur by addition to an atom of a multiple bond or the extraction of an electron from an ion (Baird and Cann, 2005).

The use of titanium dioxide photocatalysis to remediate contaminated water was first reported by Carey et al. in 1976. Since then, studies have shown the titanium dioxide photocatalytic degradation of many other types of compounds, including: aromatic hydrocarbons (Soana et al., 2000), halogenated compounds (Crittenden et al., 1997), hydroxylated compounds

(Chen and Ray, 1999), ethers (O'Shea and Cardona, 1994), aldehydes (Parra et al., 2003), organic acids (Al-Rasheed and Cardin, 2003), sulfur containing compounds (Liu et al., 2003), oestrogen compounds (Coleman et al., 2000), dyes (Ozkan et al., 2004), herbicides (Konstantinou et al., 2001), and insecticides (Herrmann et al., 1999). A more comprehensive list can be seen in review articles (Carp et al., 2004; Legrini et al., 1993; Hoffman et al., 1995; Mills and Le Hunte, 1997). In many cases, complete mineralization is reported (Hoffman et al., 1995).

2.4.1.1 Removal of Organic Compounds from Aqueous Solutions as a Means to Quantify Photocatalytic Performance

A model organic compound is often chosen to evaluate the performance of a photocatalyst or a reactor (de Lasa et al., 2005). Methylene blue, a cationic thiazine dye with a maximum absorbance at 660 nm (de Tacconi et al., 1997), is often used as a test substrate (Wang et al., 2007; Inagaki et al., 2001; Mills and Wang, 1999; de Lasa et al., 1997) because it absorbs little light in the wavelengths between 300 and 400 nm (Mills and Wang, 1999) and its disappearance can easily be evaluated using a spectrophotometer (de Lasa et al., 2005).

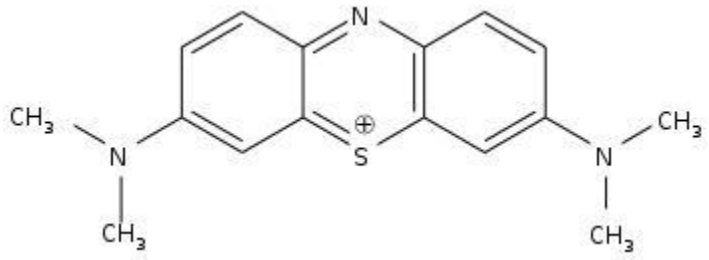

Figure 2.1 Chemical Structure of methylene blue.

Previous studies have determined the likely oxidation pathway of methylene blue exposed to light-activated titanium dioxide. The reaction is initiated by attachment of the cationic

functional group of methylene blue to the catalyst surface, followed by the opening of the central ring as a result of the attack of the C-S^+=C functional group by hydroxyl radicals. This led to the mineralization of methylene blue to CO_2, NH_4^+, NO_3^-, and SO_4^{2-} (Houas et al., 2001). The overall mineralization of methylene blue in the presence of illuminated TiO_2 can be expressed by the following chemical equation (Mills and Wang, 1999):

$$C_{16}H_{18}N_3SCl + \frac{25}{2}O_2 \xrightarrow{TiO_2,\ h\nu>3.2\ eV} HCl + H_2SO_4 + 3HNO_3 + 16CO_2 + 6H_2O$$

Titanium dioxide photocatalysis can also lead to the reduction of methylene blue through interaction with conductance band electrons (de Tacconi et al., 1997). The singly reduced form of methylene blue readily disproportionates to form methylene blue and the colourless, twice reduced form, *leuco*-methylene blue (de Tacconi et al., 1997;Karyakin et al., 1993). The overall equation can be summarized as follows (de Tacconi et al., 1997):

$$C_{16}H_{18}N_3S^+ + 2e^- + H^+ \xleftrightarrow{TiO_2,\ h\nu>3.2\ eV} C_{16}H_{19}N_3S$$

Leuco-methylene blue is stable under oxygen limited and acidic conditions, but otherwise the reduction reaction is reversible (de Tacconi et al., 1997;Karyakin et al., 1993).

Many groups have correlated the amount of dye bleaching (i.e. loss of colour) to dye mineralization, but this may not always be accurate (Mills and Wang, 1999). The oxidation reaction irreversibly bleaches methylene blue, but the reversible reduction reaction has been shown to have a similar effect (Mills and Wang, 1999). Mills and Wang (1999) demonstrated that under conditions where the formation of *leuco*-methylene blue was favorable, such as at low oxygen concentrations during photocatalysis, the bleaching process could be reversed in the dark

through addition of oxygen. Therefore, when using methylene blue bleaching to quantify photocatalytic activity, it is import to ensure that the reduction reaction has no significant effect on the reaction.

2.4.2 Self-cleaning Surfaces

Titanium dioxide can be applied to materials as a self-cleaning coating. Self-cleaning surfaces typically take advantage of the ability of titanium dioxide to degrade organic compounds and its superhydrophilic properties which allow dirt to be washed away (Carp et al., 2004). The majority of self-cleaning surfaces are designed to use available solar light, or the small amount of UV light emitted from fluorescent sources (Fujishima et al., 2008).

In order to test the self-cleaning properties of photocatalytic surfaces, a variety of test compounds can be chosen. Stearic acid is often used as it provides a good representation of organic solid films, and is easily analyzed by transmission FTIR (Mills et al., 2003; Sawunyama et al., 1997). The IR bands at 2960, 2925, and 2850 cm^{-1} measure the C-H stretching in CH_3, CH, and CH_2 respectively (Sawunyama et al., 1997; Minabe et al., 2000). From CO_2 analysis, it was found that the disappearance of stearic acid, as measured by FTIR, is a direct measure of photocatalytic mineralization of stearic acid (Mills et al., 2003; Minabe et al., 2000). The overall process proceeds in a heterogeneous manner and can be summarized as follows (Mills et al., 2003; Sawunyama et al., 1997):

$$C_{17}H_{35}COOH + 26O_2 \xrightarrow{TiO_2,\ h\nu>3.2eV} 18CO_2 + 18H_2O$$

It has been shown that many other compounds can be mineralized on titanium dioxide surfaces including high molecular weight organic compounds and oils (Minabe et al., 2000; Heller) as well as liquid and semi-solid films (Minabe et al., 2000).

In order for a titanium dioxide surface to be self-cleaning, the photocatalytic degradation rate must be greater than the deposition rate of organic compounds (Fujishima et al., 2008). Studies have shown that some organic contaminants can be degraded at a rate sufficient to keep a surface clean under normal conditions (Heller, 1995). However, when this is not the case, titanium dioxide can still perform well as a self-cleaning surface if there is water flow because of titanium dioxide's light-activated superhydrophilic properties (dirt can easily be washed away by rain) (Wang et a., 1998). For this reason it has been suggested that outdoor applications may be appropriate for titanium dioxide photocatalytic surfaces (Hashimoto et al., 2005). Titanium dioxide self-cleaning surfaces are already widely used in outdoor applications in Japan and gaining popularity elsewhere (Fujishima et al., 2008).

2.4.3 Photocatalytic Disinfection of Water

Contamination of water by viable biological microorganisms is a major concern and often causes more immediate sickness and death than chemical contamination (Baird and Cann, 2005). Additionally, endotoxin from bacterial cells can have negative health impacts even at low concentrations (ng per mL in blood) and will remain even after cells are killed (Sunada et al., 1998). For this reason it is essential to have water treatment methods that can kill a wide range of microorganisms, as well as destroy cellular components. Traditional chemical sterilization methods such as chlorination and ozonation are inefficient at the inactivation of certain pathogens and may lead to the production of harmful byproducts (Dunlop et al., 2002). Membrane filters can remove the microbial cells, but the process is very energy intensive and endotoxins may still

remain (Baird and Cann, 2005; Blake et al., 1999). Titanium dioxide photocatalysis has neither of these limitations, it can potentially kill a wide range of bacteria and destroy the endotoxins.

Disinfection through photocatalytic oxidation was first demonstrated by Matsunaga et al. in 1985. Since then, titanium dioxide photocatalysis has been shown to be an effective method for the complete inactivation of various types of bacteria and spores, as well as the destruction of endotoxin and biofilm components (Vohra et al., 2005; Sunada et al., 1998; Wolfrum et al., 2002). A comprehensive list can be seen in review articles (Blake et al., 1999). The complete destruction of bacterial cell mass has been shown by TEM (Saito et al., 1992) and total oxidation to carbon dioxide (Jacoby et al., 1998).

The first mechanism of sterilization proposed was the inactivation of cells through the destruction of Coenzyme A and the consequent inhibition of cell respiration (Matsunaga et al., 1985). It is now generally agreed that microbial inactivation arises from damage to the cellular membrane by hydroxyl radicals and subsequent loss of membrane functionality (Sunada et al., 1998, Saito et al., 1992; Kuhn et al., 2003). Hydroxyl radicals are strong oxidizers and non-selectively react with organic matter (Mills and Le Hunte, 1997). These short lived radicals, valence band holes, and other reactive oxygen species produced from titanium dioxide photocatalysis first attack the outer surface of the cell (Blake et al., 1999). More specifically, they react with the polyunsaturated phospholipids, a major component of the cell membrane (Maness et al., 1999). Radical attack initiates a chain reaction of lipid peroxidation, destroying the membrane's polyunsaturated phospholipids and other important biological molecules (Maness et al., 1999). Once these molecules are destroyed, the membrane structure is damaged and functions such as semipermeability, respiration, and oxidative phosphorylation are diminished (Maness et al., 1999). The leakage of potassium ions and other cellular components reported in

the literature is consistent with this reaction mechanism (Saito et al., 1992; Maness et al., 1999). Ultimately cell viability is lost and eventually the entire cell mass is mineralized, including endotoxins (Saito et al,. 1992; Maness et al; 1999; Sunada et al., 2003; Jacoby et al., 1998).

2.4.4 Air Disinfection

The disinfection of air is another potential application of titanium dioxide photocatalysis. Biological contaminants in air are known as bioaerosols which may consist of bacteria, fungi, viruses, and cellular components (e.g., cell wall fragments, flagella, and genetic material). Bioaerosols may exist as particulates or droplets of different sizes ranging from 0.5 to 30 μm in diameter (Pal et al., 2005; Stetzenbach, 1997; Griffiths and DeCosemo, 1994; Henningson et al., 1990).

Since the discovery that *Legionella pneumophila* caused the outbreak of Legionnaires' disease in Philadelphia in 1976, the awareness of diseases caused by bioaerosols has greatly increased (Stetzenbach, 1997). It is now generally accepted that microorganisms are directly involved in Sick Building Syndrome (Heidelberg et al., 1997). Many types of airborne microorganisms have been documented as infectious airborne pathogens (Jacoby et al., 1998). Exposure to these viable pathogens can cause diseases such as tuberculosis, cough and cold, mumps, measles, rubella, pneumonia, meningitis, influenza, small pox, and scarlet fever (Pal et al., 2005; Lin and Li, 2003b; Jacoby et al., 1998). Exposure to bioaerosols, whether viable or not, can also lead to an allergic or toxic response (Griffiths and DeCosemo, 1990; Jacoby et al., 1998; Henningson et al., 1988). Humans can be exposed to microorganisms through inhalation, ingestion, and dermal contact, however, inhalation of bioaerosols is the major pathway resulting in adverse health effects (Stetzenbach, 1997; Griffiths and DeCosemo, 1990).

Bioaerosols can be generated from a variety of outdoor and indoor sources. There are many natural and human generated outdoor sources such as fresh and marine surface waters, soil, plants, and wastewater treatment facilities (Stetzenbach, 1997). Bacteria are naturally released into air through methods such as rain splashing, spray irrigation, or wind or wave action on water surfaces (Reponen et al., 1997). A major source of indoor bioaerosols is human activity such as coughing, sneezing, disturbing surfaces, washing, talking, and toilet flushing (Stetzenbach, 1997; Kalogerakis et al., 2005). Buildings components can act as sites of microbial contamination including wallboard, ceiling tiles, carpet and vinyl flooring, painted surfaces, upholstery and drapery, wallpaper, plastics, wood, cement, and brick (Stetzenbach, 1997). Heating, ventilation, and air conditioning systems can also act as breeding and distribution systems for microorganisms (Pal et al., 2005). As a result, some studies have found that residential indoor bioaerosol levels were always higher than outdoor levels (Kalogerakis et al., 2005). Volatile substances generated from biological sources have also been found to accumulate in indoor air to levels that cause disease (Burge and Solomon, 1987). Many energy conservation techniques which involve reducing the amount of air exchange between indoors and outdoors have increased bioaerosol contamination (Burge and Solomon, 1987). Due to all the negative health effects associated with bioaerosols, numerous methods exist to remove viable microorganisms from air.

The most common methods of bioaerosol removal or inactivation are filtration, ultraviolet germicidal irradiation (UVGI), and ozone sterilization (Lin and Li, 2003; Foarde et al., 1997; Grinshpun et al., 2007). However, there are problems associated with each of these approaches. Filtration does not kill bacteria, but instead transfers them to another surface that must later be sterilized (Goswami et al., 1997). High efficiency particulate air (HEPA) filters may also become a source of microbes if the trapped microbes proliferate (Chuaybamroong et al.,

2010; Jankowska et al., 2000). UVGI is effective at reducing the viability of microbes, but does little to remove toxins and allergens present in bacteria (Grinspun et al., 1997). Additionally, UVGI becomes less effective as relative humidity increases above about 50% and has high energy costs associated with it (Riley and Kaufman, 1972; Peccia et al., 2001; Grinshpun et al., 2007). Ozone generators can effectively inactivate bioaerosols, but the ozone levels required significantly exceed health standards (Grinshpun et al., 2007; Foarde et al., 1997). Due to the above limitations of existing methods, recently there have been many studies which test the ability of titanium dioxide photocatalysts for sterilizing air (Grinshpun et al., 2007).

2.4.4.1 Bioaerosol Generation and Capture

To test the ability of titanium dioxide films to sterilize air, methods must be developed to generate and capture bioaerosols in laboratory settings. Some common techniques of aerosol generation include compressed air nebulizers, ultrasonic nebulizers, fluidized bed aerosol generators, vibrating orifice aerosol generators, and many others (Mitchell, 1995). The main methods of aerosol capture include gravitational sedimentation, inertial impactors, centrifugation, and filtration (Juozaitis et al., 1994; Burge and Solomon; 1987). All have limitations, but Collison Nebulizers (a compressed air nebulizer) are often used for bioaerosol generation (Stone and Johnson, 2002; Reponen et al., 1997; Johnson et al., 1999; Grinshpun et al., 2007; Lin and Li, 2003) due to stable bioaerosol production rate (Terziva et al., 1996; Juozaitis et al., 1994; Ding and Wang, 2001). All-glass impingers (an inertial impactor) are widely used as aerosol capture devices because they have a small cutoff size diameter (Terziva et al., 1996; Jensen et al., 1992; Nevalainen et al., 1992; May and Harper, 1957; Grinshpun et al., 1997), are generally accepted as a reference sampler (Jensen et al., 1992; Brachman et al., 1964; Ding and Wang, 1997; Ginshpun et al., 1997; Henningson et al., 1988; Burge and Solomon, 1987), can sample a wide range of

concentrations (Chang et al., 1995; Chang et al., 1994; Buttner and Stetzenbach, 1991; Zimmerman et al., 1987; Nevalainen et al., 1992; May and Harper, 1957; Grinshpun et al., 1997), can quantify single cells and not aggregates (Jensen et al., 1992; Henningson et al., 1988; May and Harper, 1957; Terziva et al., 1996), and a variety of methods can be used to analyze the collected suspension (Zimmerman et al., 1987; Terziva et al., 1996; Seshadri et al., 2009; Yoon et al., 2010).

There are many factors that must be considered when generating and capturing bioaerosols with Collison Nebulizers and all-glass impingers. Perhaps the three most critical factors are the sampling flow rate, sampling duration, and method of sample analysis as described below.

The sample flow rate can affect the physical and biological collection efficiency of impingers. If the flow rate is too low (below around 6 L/min for a standard AGI-30 or AGI-4) then there will not be sufficient force to capture the bioaerosol particles and the physical efficiency of the impinger will be low (Willeke et al., 1995; Juozaitis et al., 1994). As the flow rate increases to the recommended level (12.5 L/min for a standard AGI-30 or AGI-4), the air jet in the impinger approaches sonic velocity (Jensen et al., 1992; Grinshpun et al., 1997). This increases physical capture efficiency to nearly 100%, but causes shear stress on bacteria and subsequent loss of viability (Walter et al., 1990; Stewart et al., 1995; Reponen et al., 1997; Jensen et al., 1992; Juozaitis et al., 1994). The physical efficiency is also affected by re-aerosolization of the bacteria due to bubbles forming and bursting in the impinger. Re-aerosolization occurs in impingers at flow rates as low as 5 L/min, but significant re-aerosolization occurred above 10 L/min (Ding and Wang 2001; Grinshpun et al., 1997; Willeke et al., 1995). The optimum flow rate range for the AGI-4 was found to be 6-10 L/min (Willeke et al., 1995).

The sample duration also affects the overall rate of viable bacteria capture. Long impingement times have been shown to reduce the viability of the impinged suspension due to stress from impingement and aeration (Terziva et al., 1996; Kesavan et al., 2010). Extended periods of aeration can also cause evaporation of the impingement liquid and significant liquid loss can occur within 30 min (Grinshpun et al., 1997). The capture efficiency can become irregular due to bounce effects once the liquid level becomes lower than the recommended level (Willeke et al., 1995; Grinshpun et al., 1997; Terziva et al., 1996).

The results of an aerosol generation and capture experiment are also significantly affected by the method used to analyze the liquid catch (Lembke et al., 1981). The most common method is plate count (Juozaitis et al., 1994; Rule et al., 2009) which is slow (Yoon et al., 2010) and has a high variability associated with it. Zimmerman et al. (1987) have shown that if a capture suspension is plated on two different plates, the error could be expected to be as high as 30% and Lembke et al. (1981) have reported that the error can increase with higher concentrations. Plate counts also tend to underestimate the total viable bacteria concentration of bioaerosols (DeCosemo et al., 1992; Chang et al., 1995). When cells are aerosolized and exposed to air, they may lose their culturability but still remain viable (Colwell et al., 1985; Heidelberg et al., 1997; Marthi et al., 1991) and pathogenicity can persist (Colwell et al., 1985). Therefore, it is important to quantify total viable cells and not just total culturable cells.

To assess the viable concentration of bioaerosols without culturing, molecular techniques can be utilized (Heidelberg et al., 1997). These assays have a higher minimum detection limit than plate count analysis, and this detection limit will be based on the sensitivity of the equipment used. Two assays that have been used in the assessment of bioaerosols are a luciferase assay, that quantifies viability based on cellular ATP content, and the BacLight Live/Dead assay, which is

based on membrane intactness (Seshardri et al., 2009; Yoon et al, 2010; Terziva et al., 1996). ATP analysis is rapid, but the total ATP content must be correlated to cell concentration using a different method (Yoon et al., 2010; DeCosemo et al., 1992). The ATP content also varies based on cell type and the state of the cells (Yoon et al., 2010; Seshardri et al., 2009). The Live/Dead assay is also rapid and can be applied as a direct microscopic count or by spectrophotometry (Terziva et al, 1996). However, some cells which may be counted dead because they have damaged membranes, can recover and remain viable (Terziva et al., 1996).

2.4.4.2 Photocatalytic Reactor Design and Operation

Titanium dioxide photocatalysis has been used to effectively reduce the viability of various types of bacteria in air (Grinshpun et al., 2007; Gosawmi et al., 1997; Vohra et al., 2006). However, results have been found to be highly dependent on experimental conditions. Three major factors that have been studied are flow rate, reactor design, and relative humidity as discussed below.

For bioaerosols to sufficiently inactivate, they must have time to react with the photocatalytic surface. For this reason, many studies use low flow rates for single-pass experiments ranging from about 0.1 to 10 L/min (Keller et al., 2005; Pal et al., 2008; Pal et al., 2005). These flow rates result in reactor retention times on the order of minutes. In recirculating systems, it was also found that increased flow rate decreased microbial inactivation (Goswami et al., 1997). Lin and Li (2003) reported that there was no significant inactivation of bacteria at a flow rate of 50 L/min, but at the same flow rate, Yu et al. (2008) reported efficient one-pass inactivation of bacteria when titanium dioxide photocatalysis was combined with negative air ionization. An annular photocatalytic reactor has been reported to sterilize bioaerosols in a 67 m^3 room in under 2 hours when operated at 195 L/min (retention time of under a second)

(Paschoalino et al., 2008). Therefore, low flow rates may not be required in systems where single-pass sterilization is not needed. However, for single-pass experiments, low flow rates must be maintained to provide enough contact time between the microorganisms and the catalyst.

The reactor configuration also greatly affects the bacteria-catalyst contact. Many different reactor configurations have been used such as flat plate, annular, and coated filters (Paschoalino et al., 2008; Lin and Li, 2003; Goswami et al., 1997; Yu et al., 2008; Pal et al., 2008). However, little work has been done to improve reactor design for efficient removal of bioaerosols by photocatalysis (Josset et al., 2000). Some literature indicates that reactor geometry enhanced for optimizing contact between bacteria and photocatalyst is essential (Keller et al., 2005). High one-pass bacterial inactivation (up to 90%) was reported at flow rates from 1 to 10 L/min using a reactor with enhanced tubular geometry, but no significant bacteria inactivation was observed when a simple tubular reactor with the same dimensions was used under the same conditions (Keller et al., 2005). However, others have reported that annular reactors can achieve high single-pass efficiency at similar flow rates (Pal et al., 2008; Pal et al., 2005). The main difference between the operating conditions was the relative humidity level.

Relative humidity can greatly affect photocatalytic inactivation of bioaerosols. In the study where no inactivation was seen using a simple reactor design, the relative humidity was low (<30%) (Keller et al., 2005). When high one-pass efficiency was noted with simple annular reactors, higher humidity levels were used (Pal et al., 2008; Pal et al., 2005). At low relative humidity levels (<30%), there may not be enough water to generate sufficient hydroxyl radicals to inactivate the bacteria (Goswami et al., 1997). In general, bacterial inactivation due to photocatalytic activity increases as relative humidity increases, even though without photocatalysis the bacterial survival increases at high humidity (Yu et al., 2008). However,

depending on the bacterial species and operating conditions, bacterial inactivation may increase to a maximum and then decrease with increasing relative humidity (normally above 85%) (Yu et al., 2008; Goswami et al., 1997; Pal et al., 2008).

To summarize, typically the efficiency of bioaerosol inactivation increases as flow rate decreases and relative humidity increases. Enhanced reactor geometry can also increase this efficiency.

2.5 Summary

A review of the literature has highlighted some important details about titanium dioxide photocatalysis:

- The general photocatalytic reaction mechanism can be used in many applications.
- The substrate may interact with the titanium dioxide film to affect photocatalytic efficiency. This may be avoided by having a layer of SiO_2 between the substrate and the photocatalytic film.
- Film thickness may affect the efficiency of films under UVA light.
- Degussa P25 powder is the most common reference material.
- Electrophoretic deposition is a reproducible method to deposit titanium dioxide powder.
- FACVD methods have many advantages over other deposition methods such as high deposition rate and low cost but may result in the deposition of powder under certain conditions.
- No studies were found to use FACVD to produce titanium dioxide films.

- Methylene blue is a model organic compound to easily monitor photocatalytic activity. However, it must be verified that test conditions do not allow the reduction reaction to play a significant role.
- Stearic acid degradation is commonly used to test the self-cleaning properties of surfaces.
- Bioaerosols are a significant health concern.
- The Collison Nebulizer is commonly used for bioaerosol generation. All-glass impingers are often used for bioaerosol capture.
- Bioaerosol generation and capture are complex and depend on factors such as sampling flow rate, sampling duration, and method of sample analysis.
- Analysis of captured bioaerosols can be done by plate counts, quantification of ATP using luciferase, or by using the BacLight Live/Dead assay.
- When designing a photocatalytic reactor system, the reactor geometry, test flow rate, and relative humidity levels are relevant factors to consider.

Chapter 3

Deposition and Characterization of Titanium Dioxide Films

3.1 Introduction

In many applications, after photocatalysis occurs the titanium dioxide must be removed, and therefore it is convenient to use films instead of powder (Mills et al., 2003). Methods of titanium dioxide film deposition can be broadly categorized as those that use titanium dioxide powder, and those that generate titanium dioxide during substrate coating (Pozzo et al., 1997). Films coated with Degussa P25 powder are often used as a standard for comparison (Maness et al., 1999). When different coating methods were compared, it was found that electrophoretic powder deposition typically produced a higher photocatalytic activity and more reproducible results than other powder based methods (Byrne et al., 1998).

Flame assisted chemical vapour deposition (FACVD), a variant of CVD, is a promising method for producing cost effective titanium dioxide films (Choy, 2003). The many advantages of FACVD such as high controllability, low relative cost, high deposition rate, and the ability to continuously coat a substrate have not been previously exploited to produce titanium dioxide films (Choy et al., 2003; Xu and Yan, 2010).

This chapter details the electrophoretic deposition of Degussa P25 on aluminum substrate for use as a standard film for comparison to FACVD. Films produced by FACVD are supplied by Novelis Inc. and the general deposition method utilized is described in this chapter. The effects of air flow rate during film deposition, and the use of a silicon oxides under-layer on film properties are examined. Analysis of both conventional and Novelis Inc. fabricated films is

accomplished by scanning electron microscopy (SEM), energy-dispersive X-ray spectroscopy (EDXS), glow discharge optical emission spectroscopy, and Raman spectroscopy.

3.2 Experimental

Two methods were used to produce of titanium dioxide films. "Standard" films were made by depositing Degussa P25 powder onto aluminum for comparison purpose. The films to be evaluated were provided by Novelis Inc. and made using flame assisted vapour deposition (FACVD) to coat the aluminum sheets.

3.2.1 Electrophoretic Deposition of Degussa P25

3.2.1.1 System Setup

An electrophoretic deposition apparatus was constructed using two thin sheets of flame-cleaned aluminum, approximately 21.5 cm wide and 28 cm long to act as electrodes (Figure 3.1). The sheets were aligned vertically and separated by a 1.5 mm thick, rectangular rubber gasket with an open space of 13.5 cm x 30 cm. The top section (width) of the gasket was cut out so that a titanium dioxide suspension could be added through the top. The sheets separated by the gasket were clamped tightly using non conductive clamps to avoid leakage.

3.2.1.2 Deposition Procedure

A suspension of Degussa P25 (Evonik Degussa) powder was made by sonicating (VWR Ultrasonicating Bath) 0.1 grams of powder in 100 mL of dimethylformamide (99% purity, Acros Organics) for 30 min. Approximately 60 mL was added to fill the volume between the two aluminum sheets. A potential was applied for 30 seconds by attaching the positive lead of a 9V battery to one aluminum sheet using a small wire and alligator clip, and the negative lead to the other sheet. The negatively charged aluminum sheet became coated with the Degussa P25

powder. After the liquid was removed and the system was disassembled, the titanium dioxide coated sheet was dried at room temperature, and then exposed to UVA light to remove any residual organics.

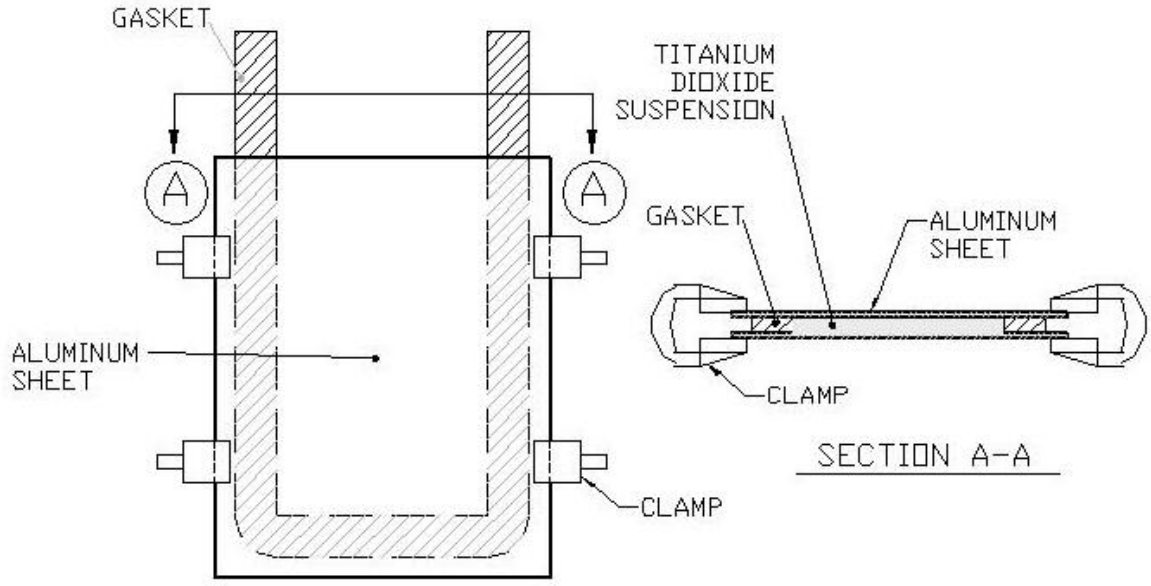

Figure 3.1 Diagram of electrophoretic deposition setup.

3.2.2 Flame Assisted Chemical Vapour Deposition

Novelis Inc. supplied films made by FACVD. Using a moving table, a sheet of cleaned aluminum was moved over a flame supplied with fuel (methane) mixed with a titanium dioxide precursor stream of titanium ethoxide and a carrier gas (nitrogen) at a fixed rate.

A variety of factors could be altered to control the deposition conditions and film properties including: air and/or methane flow rates, the speed of the moving table, number of passes over the flame, flow rate of nitrogen carrier gas, flow rate of precursor, and the substrate material. In this study, the effects of changing the air flow rate (and thus air to fuel ratio) and

substrate material were examined. Two different series of films were provided, the T65 and T68 series. For each series, a different air flow rate was used at a fixed flow rate of carrier gas and precursor with 20 passes over the flame. The substrate materials were cleaned aluminum, and aluminum coated with a layer of silicon oxides which was used to increase surface area and prevent potential interaction between the titanium dioxide film and the aluminum substrate. Three different thicknesses of silicon oxides were examined. A summary of the other run conditions is presented in Table 3.1.

Table 3.1 FACVD run conditions using fixed flow rate of carrier gas and precursor with 20 passes over the flame.

Sample	Air flow rate (SL/min)	Methane Flow Rate (SL/min)	Approximate Thickness of Silicon Oxides Layer (nm)
T65	56	8	NA
T65P1	56	8	20
T65P2	56	8	50
T65P3	56	8	100
T68	44	8	NA
T68P1	44	8	20
T68P2	44	8	50
T68P3	44	8	100

3.2.3 Film Analysis

Film analysis was done to determine the surface morphology, elemental composition, relative amounts of titanium dioxide, and crystallinity. Scanning electron microscopy (SEM) (Philips XL30 SFEG/SEI) was provided courtesy of Novelis Inc. and was used to determine the surface morphology. No additional sample preparation was needed (films viewed “as made”), and the images were acquired using a 5 kV accelerating voltage at various magnifications.

Elemental analysis of selected regions of the SEM micrographs was done by energy-dispersive X-ray spectroscopy (EDS) (Philips XL30 SFEG/EDXS). EDS spectra was detected using a 80 mm X-max silicon drift detector (Oxford Instruments) and a 8 kV accelerating voltage.

The relative amount titanium dioxide was quantified by glow discharge optical emission spectroscopy (GD-OES) (Jobin Yvon Horiba GD Profiler). GD-OES results were provided by Pamina Lin and Megan Wright (Novelis Inc.). Measurements were taken in a 4 mm diameter area with an applied voltage of 35 V and a 700 Pa argon atmosphere, over a period of 30 seconds. Measurements were performed at a spectral wavelength of 365 nm for the detection of titanium.

Raman studies were performed to assess the crystallinity of the films using a Jobin-Yvon/Horiba microRaman Spectrometer (Model: Labram), equipped with a 632 nm He/Ne laser source, 1800 1/nm grating and an Olympus BX41 microscope system. Collection of the spectra was performed in backscattered mode at room temperature under the following conditions: x100 microscope objective, 200μm pinhole size, 300 μm slit width, and 1 min exposure time. Each spectrum represents the average of two measurements.

3.3 Results and Discussion

The properties of the T65 and T68 series were examined and compared against those of the Degussa P25 films. The T68 series was deposited using a lower air flow rate to produce a cooler flame.

3.3.1 Analysis of T65 Series

3.3.1.1 Surface Morphology and Elemental Composition

The surface morphology and elemental composition of the Degussa P25 films and the T65 series was examined using SEM and EDS. The SEM micrograph of the Degussa P25 film

(Figure 3.2(B)) showed that the surface is entirely coated and had a high surface roughness which could provide a large surface area for reaction. The EDS spectrum (Figure 3.3 (A)) showed the presence of titanium, oxygen, and aluminum. Therefore, the Degussa P25 films likely provided a higher surface coverage of titanium dioxide.

In the SEM micrograph of the T65 film (no undercoating) (Figure 3.2 C), two distinct regions were visible, one consisting of white spheres and the other of grey background similar to the surface of uncoated aluminum (Figure 3.2 A). EDS revealed that the white spheres consisted mainly of titanium and oxygen, and are therefore likely titanium dioxide powder. The grey background was shown to be aluminum (Figure 3.3 C), with no trace of titanium. Therefore, it appears that titanium dioxide was only deposited as a powder, which is a common problem with FACVD processes caused by high flame temperature (Choy, 2003).

Examination of the SEM micrographs of the T65 film with silicon oxides under-layers (T65P1, T65P2, T65P3) (Figure 3.2(D-F)) also showed regions of white titanium dioxide spheres and grey aluminum. A third region of irregular white deposits was also visible, and these deposits were most apparent in the film with the thickest silicon oxides under-layer. EDS was used to show that these deposits consisted mainly of silicon and oxygen, and were therefore the silicon oxides under-layer. Thus, the rough surface of the silicon oxides layer provided a high surface area for titanium dioxide deposition, but only a disperse coating of titanium dioxide powder was deposited.

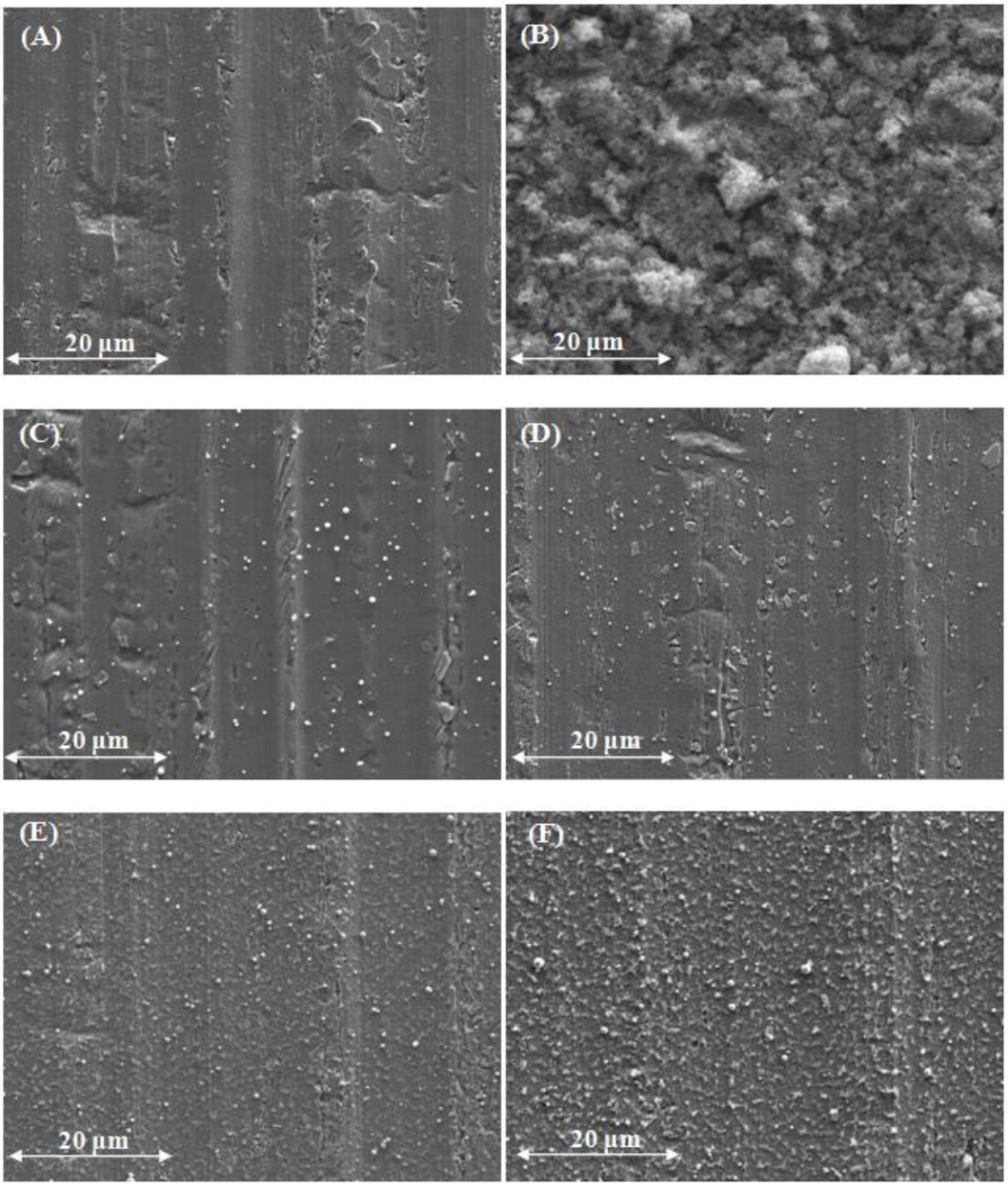

Figure 3.2 SEM micrograph of (A) blank aluminum, (B) Degussa P25 film, (C) T65, (D) T65P1, (E) T65P2, (F)T65P3.

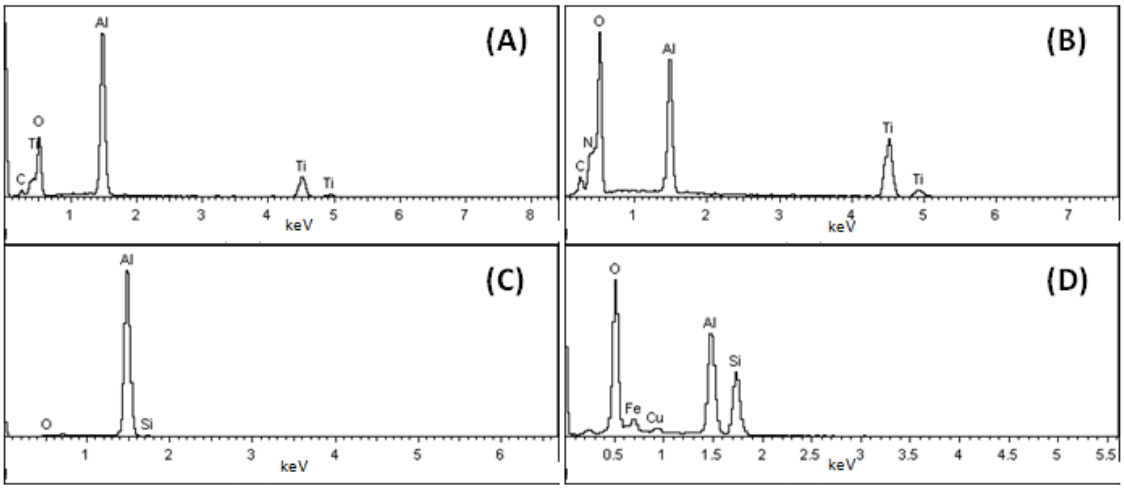

Figure 3.3 EDS spectrum of (A) Degussa film sample, (B) spheres seen on T65, (C) background of T65 sample, (D) background of the T65P3 sample.

3.3.1.2 Relative Titanium Dioxide Content

The relative amount of titanium dioxide in the Degussa P25 films and T65 series was approximated using GD-OES analysis, a technique that combines sputtering and atomic emission. It essentially erodes a sample an atomic layer at a time by sputtering using argon plasma generated by an applied voltage (Michler et al., 2004). The elements removed from the sample rapidly diffuse into the plasma where they de-excite and emit light at characteristic wavelengths. The light intensity emitted at the wavelength corresponding to titanium (365 nm) was measured over a period of time, and its integral taken in order to approximate the total titanium dioxide content. The results are displayed in Figure 3.4.

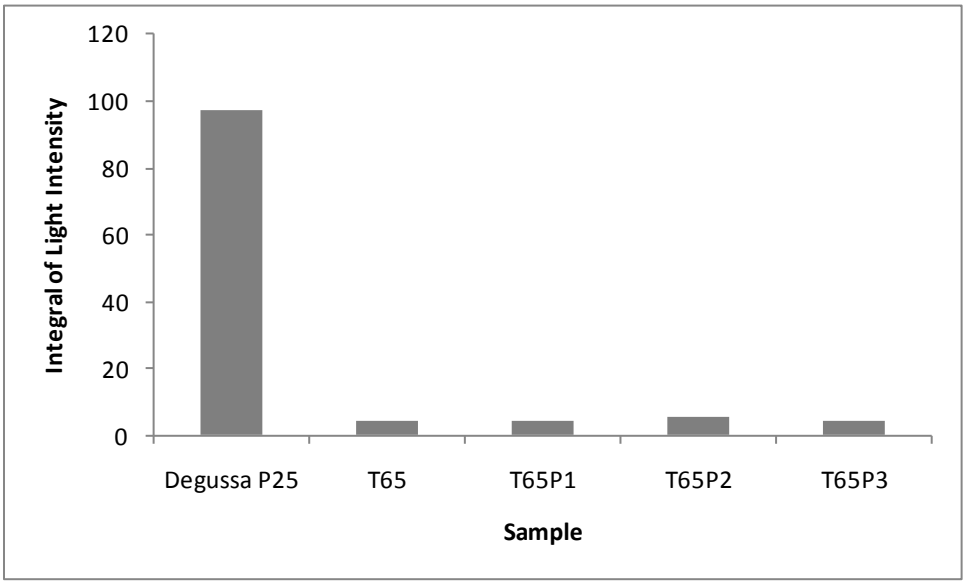

Figure 3.4 Integral of light intensity from GD-OES analysis for T65 film series.

The integrated light intensity from GD-OES analysis was much higher for the Degussa P25 films than the T65 series, indicating that there was much more titanium dioxide present in the case of Degussa P25 films. This result was expected because the T65 series was shown through SEM/EDS analysis to have a coating titanium dioxide powder coating with low surface coverage.

3.3.1.3 Crystallinity

The crystallinity of titanium dioxide films can be determined through Raman analysis. Raman peaks for anatase have been found to occur at wave numbers of 398 cm^{-1}, 515 cm^{-1}, and 639 cm^{-1}, and at 446 cm^{-1} and 610 cm^{-1} for rutile (Evans and Sheel, 2007). Raman analysis was performed on the Degussa P25 films and the T65 series, and the results are shown in Figure 3.5. The Degussa P25 films (Figure 3.5 (B)) showed the characteristic peaks of anatase. However, all other film samples (Figures 3.5 (C-F)) showed no distinctive peaks, and had similar spectra to

uncoated aluminum. The lack of detectable peaks could be due to low amounts of titanium dioxide as shown in the SEM/EDS and GD-OES analysis.

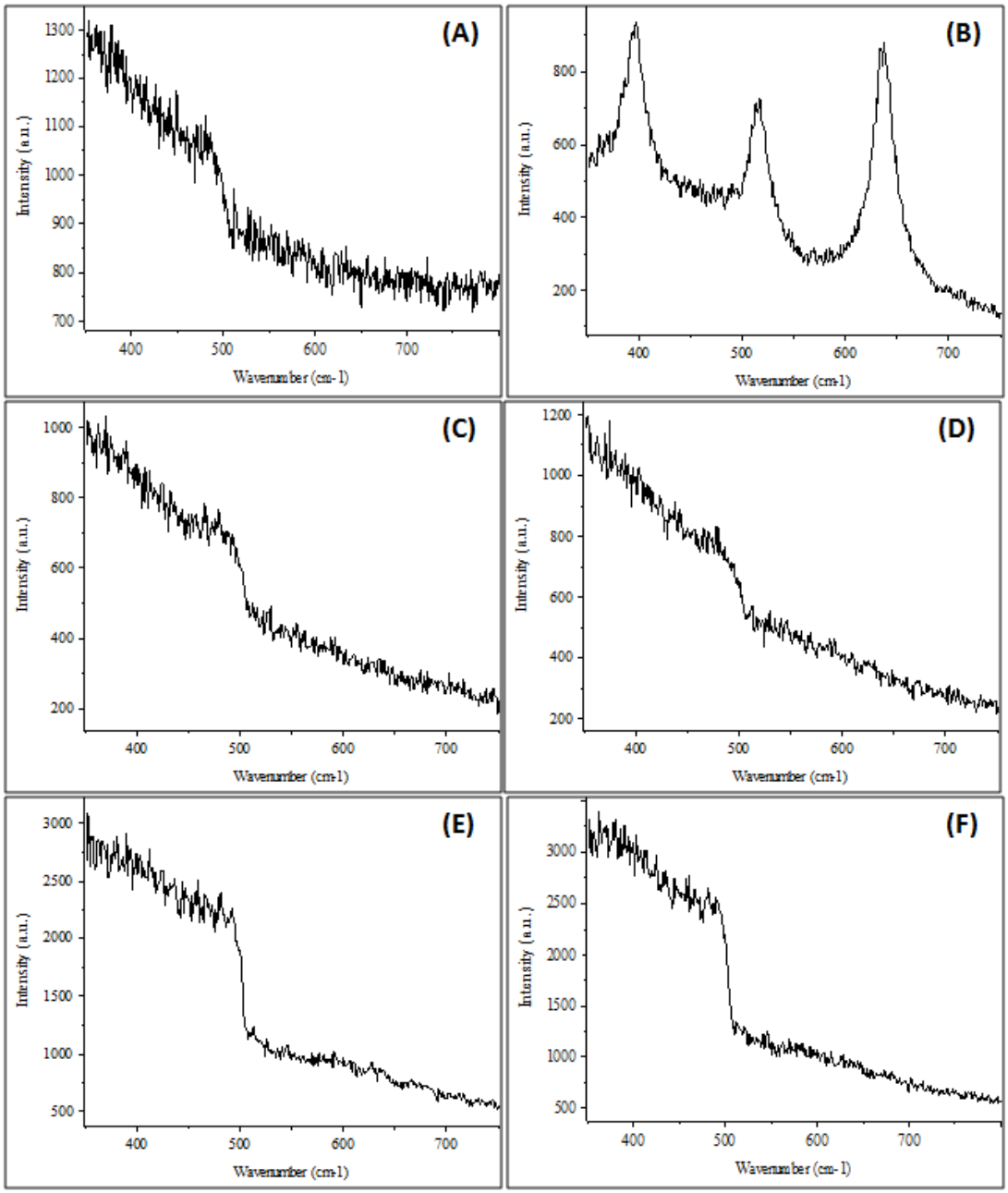

Figure 3.5 Raman spectra of (A) uncoated aluminum, (B) Degussa P25 film, (C) T65, (D) T65P1, (E) T65P2, (F) T65P3.

3.3.2 Analysis of T68 Series

3.3.2.1 Surface Morphology and Elemental Composition

SEM micrographs were taken of the T68 series and can be seen in Figure 3.6. The T68 film (no undercoating) (Figure 3.6 (C)) was seen to have two visible regions, one with white deposits, and the other with grey background. The deposits were irregular, and not spherical, suggesting that a homogeneous gas phase reaction did not occur and that the visible deposits are not powder. EDS confirmed that the white deposits (Figure 3.7 (A)) contained high amounts of titanium and oxygen, and were likely titanium dioxide. The grey areas (Figure 3.7(B)) were found to be aluminum.

The samples with silicon oxides under-layers (Figure 3.6 (D-F)) also have irregular deposits, and can be seen to have more surface coverage than the film without silicon oxides under-layer (Figure 3.6 (C)). As the thickness of the silicon oxides under-layer increased (from Figure 3.6(D) to 3.6(F)) surface coverage also increased. EDS (Figure 3.7 (C)) confirmed that the deposits contained high amounts of titanium, silicon, and oxygen and thus consisted of both the silicon oxides and titanium dioxide. The areas without visible deposits (Figure 3.7 (D) were found be mainly aluminum with a small amount of silicon. Therefore, the titanium dioxide was seen to preferentially deposit on silicon oxides surfaced as opposed to aluminum. From the SEM and EDS results it is difficult to determine whether more titanium dioxide was deposited as silicon oxides thickness increased, or if the observed increase in surface coverage was solely due to greater amounts of silicon oxides surface coverage.

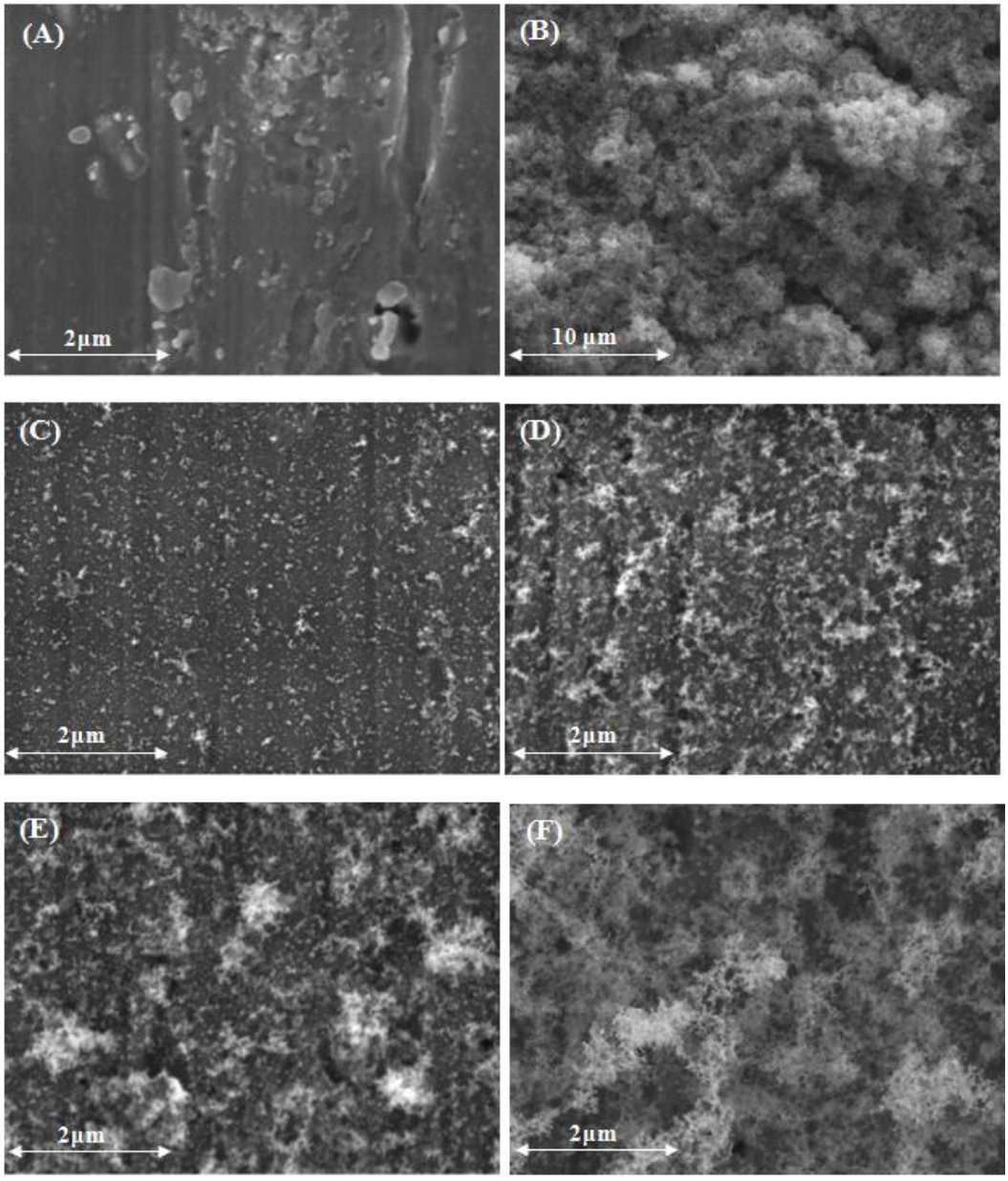

Figure 3.6 SEM micrograph of (A) uncoated aluminum, (B) Degussa P25 film, (C) T68, (D) T68P1, (E) T68P2, (F) T68P3.

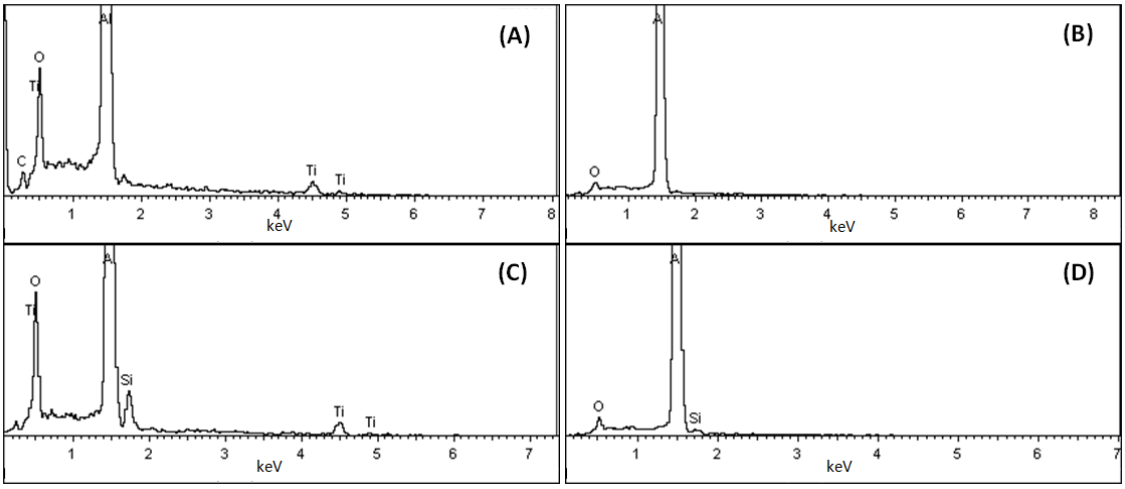

Figure 3.7 EDS spectrum of (A) white areas of T68 film, (B) grey background on T68 film, (C) white area of T68P3 film, (D) grey background of the T68P3 film.

3.3.2.2 Relative Titanium Dioxide Content

GD-OES was used to compare the amounts of titanium dioxide present in the Degussa P25 film and the T68 series and the results can be seen in Figure 3.8. The integral of light intensity measured at the wavelength of titanium was seen to be much higher for the Degussa P25 film than for the T68 series. Therefore, there was likely much more titanium dioxide on the Degussa P25 films than the T68 series. To determine if more titanium dioxide was deposited as silicon oxides thickness increased or if the observed increase in surface coverage was solely due to greater amounts of silicon oxides, triplicate GD-OES measurements were compared (Figure 3.9). Statistical comparison of means was done by hypothesis test using Microsoft Excel™, and the means are said to be statistically different if the p value is less than 0.05 (Montogomery and Runger, 2003).

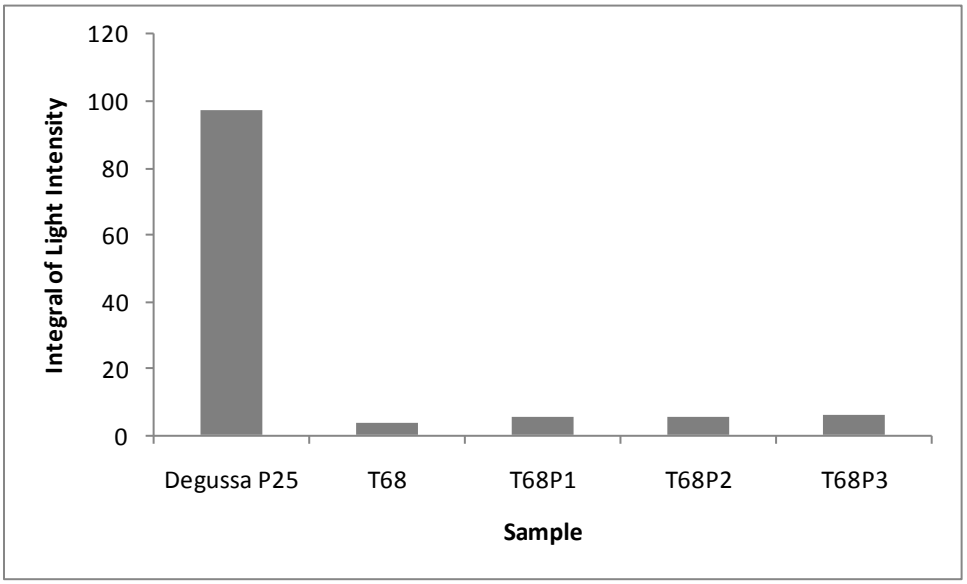

Figure 3.8 Integral of light intensity from GD-OES analysis for T68 film series and Degussa P25 film.

It was determined that the difference in the integral of light intensity, and thus titanium dioxide content, between the T68 film (no undercoating) and the films with an undercoating (T68P1, T68P2, T68P3) was statistically significant. However, the difference was small compared to the overall titanium dioxide content with the T68 sample having about 30% less than the samples with under-layers. The difference in titanium dioxide content between the three samples with under-layers (T68P1, T68P2, T68P3) was not statistically significant. Therefore, the observed increase in surface coverage as silicon oxides layer thickness increased was due solely to silicon oxides and not additional titanium dioxide deposition.

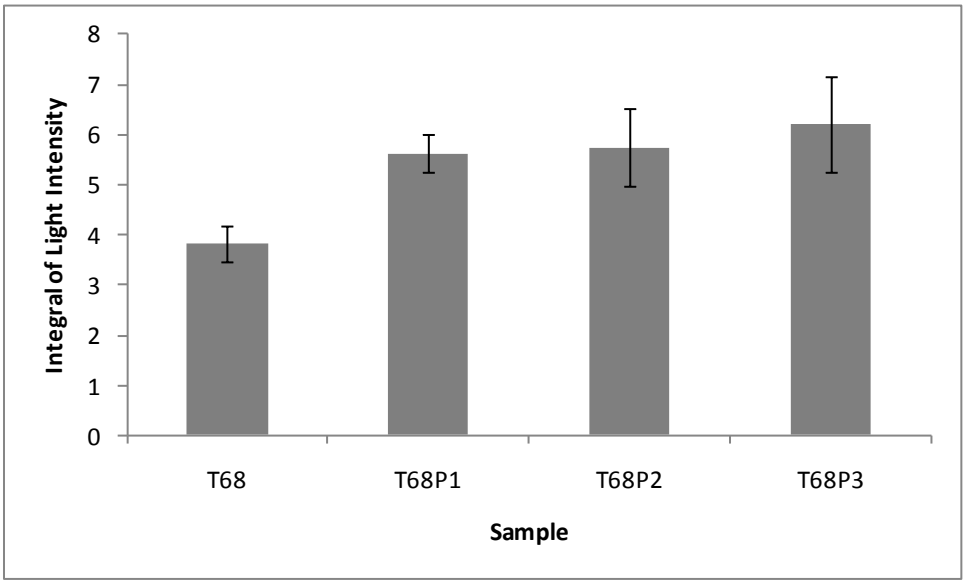

Figure 3.9 Integral of light intensity from GD-OES analysis for T68 film series

3.3.2.3 Crystallinity

The crystallinity of the T68 series was analyzed using Raman spectroscopy and the results can be seen in Figure 3.10. No characteristic peaks of crystalline titanium dioxide were present, which may indicate that the structures were amorphous. However, it is likely that there was not enough material present in these films for detection by Raman analysis using the current equipment. This is supported by the low relative amounts of titanium dioxide present in the T68 series compared to the Degussa P25 films as determined by GD-OES.

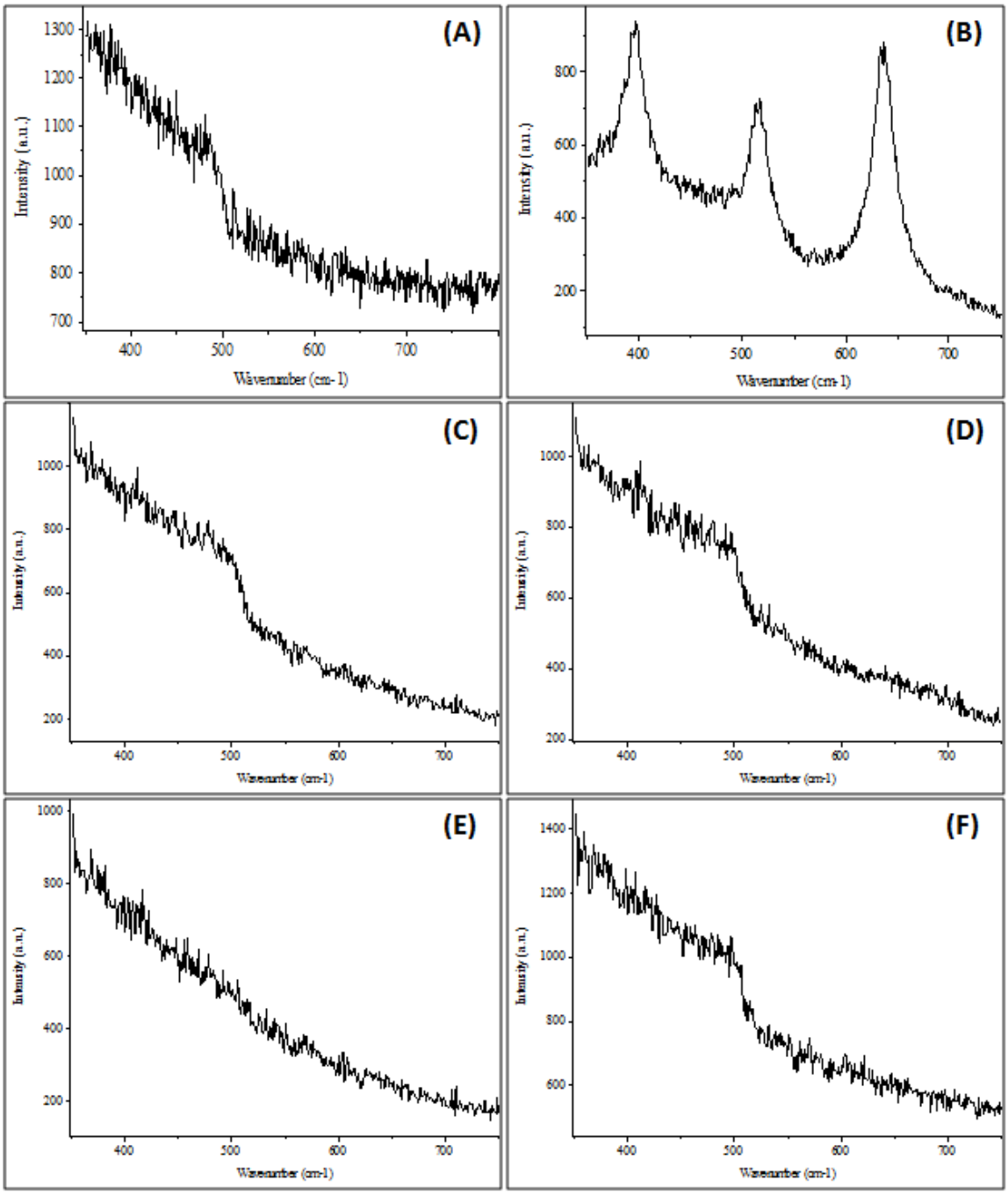

Figure 3.10 Raman spectra of (A) uncoated aluminum, (B) Degussa P25 film, (C) T68, (D) T68P1, (E) T68P2, (F) T68P3.

3.4 Conclusions

Titanium dioxide films were produced by the electrophoretic deposition of Degussa P25 on aluminum substrate to provide a standard film to compare with films deposited using FACVD produced by Novelis Inc. while varying air flow rate and thicknesses of silicon oxides under-layers. The Degussa P25 film was shown to have thick coatings of titanium dioxide primarily in the anatase form. The FACVD films series produced with a high air flow rate (T65 series) was seen to have an uneven surface coating of titanium dioxide powder. The films produced at a lower air flow rate (T68 series) were seen to have titanium dioxide deposits, however much less was present than in the Degussa P25 films, and the crystal structure could not be determined via Raman spectroscopy for the FACVD films but could be for the prepared Degussa P25 films. Films with silicon oxides under-layers were seen to have more titanium dioxide than with no under-layers, but as silicon oxides thickness increased no addition titanium dioxide was deposited.

Chapter 4

Analysis of Film Performance for the Degradation of Organic Compounds and the Inactivation of Bacteria

4.1 Introduction

The relative photocatalytic activity of titanium dioxide films can be tested in terms of performance for different applications, such as self-cleaning surfaces, for the removal of organic compounds from water, and inactivation of biological organisms by comparison to films of Degussa P25. Testing the efficacy in each of these areas will determine the potential applicability of each film, and can be used to select the films that are likely to be most effective in a photocatalytic air sterilization unit.

A common application of titanium dioxide is in the production of photocatalytic self-cleaning surfaces, which take advantage of titanium dioxide's light-induced superhydrophilicity (to allow dirt to be washed away) and its ability to degrade deposited organic compounds to stay clean. The majority of self-cleaning surfaces are designed to use UVA light present in solar light, or the small amount of UVA light emitted from fluorescent sources (Fujishima et al., 2008). Stearic acid is often used in self-cleaning tests as it is a good representative of organic solid films, and can be easily analyzed by transmission FTIR (Mills et al., 2003; Sawunyama et al., 1997).

The use of titanium dioxide photocatalysis for water purification has potential benefits over conventional methods. To assess the ability of titanium dioxide films to degrade organic compounds in aqueous solutions, a model compound is often chosen (de Lasa et al., 2005). Methylene blue is frequently used because it absorbs little light between 300 and 400 nm (Mills

and Wang, 1999) and its disappearance can easily be followed using a spectrophotometer (de Lasa et al., 2005).

Titanium dioxide photocatalysis can also be applied to the disinfection of water. Photocatalytic disinfection of water has been shown to be effective against a wide range of organisms (Vohra et al., 2005; Sunada et al., 1998; Wolfrum et al., 2002). A reference bacterial species is often chosen to determine the ability of a titanium dioxide film to disinfect water.

The degradation of some organic compounds has been shown to follow the same trend as the inactivation of microorganism when titanium dioxide properties were altered (Jang et al., 2001). Therefore, the difference in photocatalytic performance of films in one application may be similar in other applications. Thus, simple tests can be designed to evaluate which films will likely be the most effective in an air sterilization unit.

In this chapter, simple tests were developed to evaluate films as self-cleaning surfaces, in the degradation of organic compounds and the inactivation of microorganisms in water. The results of these tests were used to determine which films would likely be most effective to use in air sterilization.

4.2 Experimental

4.2.1 Stearic Acid Degradation

Stearic acid was used as a model compound to test the self-cleaning ability of the titanium dioxide films. Stearic acid results were provided by Pamina Lin (courtesy of Novelis Inc.). Thin stearic acid films were deposited on the samples using a spin coating technique. A total of 150 μL of 0.02 M stearic acid (Reagent grade, 95% purity, Aldrich) dissolved in methanol was added to the middle of a 2 x 2 cm sample. The sample was then spun at 500 rpm for 10 sec, and the methanol allowed to evaporate forming a solid film of stearic acid on the surface. The

initial amount of stearic acid was quantified using transmission FTIR (Thermo Nicolet NEXUS 470 FT-IR E.S.P.) analysis, measuring bands between 2800 and 3000 cm^{-1}. IR bands at 2960, 2925, and 2850 cm^{-1} were used to measure the C-H stretching in CH_3, CH, and CH_2 respectively (Sawunyama et al., 1997; Minabe et al., 2000). Therefore, monitoring this range will measure the degree of mineralization of stearic acid. After the samples were placed 1.5 cm from a germicidal UVC light (PURA UVB2 EPCB/SD 120v) and irradiated for two min, the light was switched off and the amount of stearic acid remaining was again quantified by FTIR. This process was repeated until the stearic acid film had been fully degraded.

4.2.2 Methylene Blue Degradation

Methylene blue (Acros Organics, Pure, Certified) was used to evaluate the ability of the titanium dioxide films to degrade organic compounds in aqueous solution. A 2.25 x 2.25 cm section was cut from each film and placed in the bottom of a round culture dish (3.5 cm diameter, 1 cm depth). A 4 mL aliquot of solution containing 0.005 g/L methylene blue in distilled water was added to each dish. The dishes were covered with an optically clear lid and left in the dark for three hours to allow adsorption equilibrium to be achieved (Houas et al., 2001). They were then placed below a UVA emitting black-light-blue lamp (Globe, F15, T8, 15 W), so that the distance between the lamp and film was approximately 4 cm. The films were exposed to UVA light for the duration of the experiment, with 100 μL samples taken periodically. The samples were added to a black-walled-clear-bottom costar 96 well multiplate and the absorbance read at 660 nm using a Spectramax $M2^e$ Microplate reader. Triplicate sections from each film were tested, as well as sections of uncoated aluminum. Dark controls were also performed.

4.2.3 Microbial Inactivation

4.2.3.1 Culture Storage and Preparation

Aqueous phase microbial inactivation was performed using *Vibrio fischeri* NRRL B-11177, a Gram negative rod shaped bacteria. Working cultures were kept on nutrient agar plates and transferred to fresh nutrient agar plates monthly. Every 6 months cultures were refreshed from slants.

A 100 mL solution of nutrient broth in a 500 mL flask was inoculated with a loopful of bacteria taken from a plate, and incubated at 30^{o}C and 200 rpm for 8 h before harvesting the culture in the exponential growth phase. The cells were resuspended in 0.9% NaCl after centrifugation at 8000 x g for 10 min. After the cells were washed once, they were resuspended in 0.9% NaCl solution to achieve an optical density of approximately 0.1 at 600 nm (Ultrospec 1000 UV/visible spectrophotometer, Pharmacia Biotech).

4.2.3.2 Microbial Inactivation Procedure

A 2.25 x 2.25 cm section was cut from each film to be tested and placed in the bottom of a round culture dish (3.5 cm diameter, 1 cm depth). A 4 mL aliquot containing the bacterial suspension was added to each dish and the dishes were covered with an optically clear lid. After the bacteria were allowed to settle for 5 h, the film sections were transferred into fresh round culture dishes (3.5 cm diameter, 1 cm depth) containing 4 mL of sterile 0.9% NaCl solution. The covered dishes were placed below a UVA emitting black-light-blue lamp (Globe, F15, T8, 15 W) for 6 h, with the distance between the lamp and film being approximately 4 cm.

The bacterial viability was assessed using the Live/Dead BacLight^{TM} (Invitrogen) cell viability assay which is based on membrane intactness. SYTO 9 (Invitrogen), a green-emitting fluorescent nucleic acid stain, labels all bacteria in a population. Propidium iodide, a red-emitting

fluorescent nucleic acid stain, labels the cells with damaged membranes and causes a reduction of SYTO 9 fluorescence in cells where both dyes are present. As a result, cells that are viable will fluoresce green and non-viable cells will stain red.

The Live/Dead assay was prepared by mixing both components of the Live/Dead kit L13152 in 5 mL of sterile filtered water to form the working stain solution. The film section to be evaluated was removed from the dish and 100 μL of stain solution was applied to the surface. Three different areas of the films sections were then photographed (Canon Rebel Xsi) through the ocular of a fluorescent microscope (Nikon Labophot-2). The number of live and dead bacteria were counted and used to calculate the average bacterial survival on each film section. Dark controls and blank aluminum samples were evaluated.

4.3 Results and Discussion

The performance of the T65 and T68 series was evaluated using the stearic acid, methylene blue, and microbial inactivation tests and compared to an aluminum sample electrophoretically coated with the industry standard, Degussa P25. Differences in mean degradation were statistically compared, and the means were said to be statistically different if the p value is less than 0.05 (>95% confidence) (Montogomery and Runger, 2003). Experiments were performed in triplicate only when time and material requirements allowed (single experiments done otherwise).

4.3.1 Performance Testing of T65 Series

The oxidation of stearic acid by the T65 series films was monitored by FTIR analysis when the samples were irradiated with UVC light. The results of the stearic acid test can be seen in Figure 4.1.

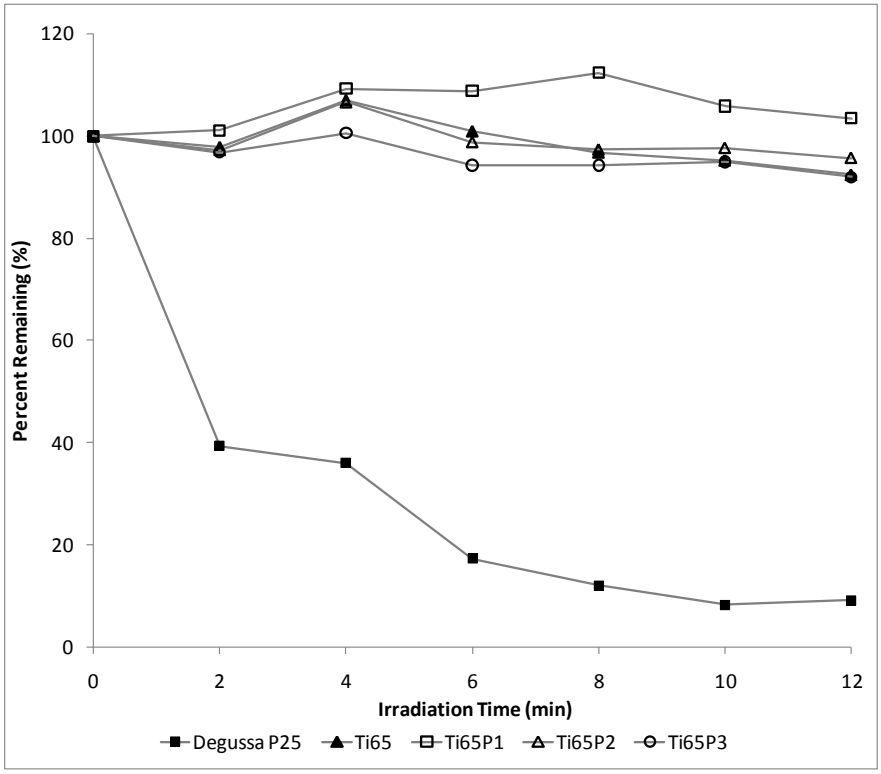

Figure 4.1 Oxidation of stearic acid on T65 sample series when exposed to UVC light.

The results of the stearic acid test were seen to be similar to the degradation of methylene blue under UVA light (Figure 4.2). In methylene blue oxidation, all films were tested in triplicate, and a dark control was performed for each sample. The electrophoretically deposited Degussa P25 films rapidly degraded stearic acid and methylene blue. Within 12 minutes, over 90% of the carbon-hydrogen bonds in the stearic acid film had been degraded, and after 38 h of exposure to UVA light, over 90% of the methylene blue was oxidized. All other samples showed no activity. This may be explained by the small amounts of titanium-containing deposits present in the T65 series compared to the large surface coverage of the Degussa P25 samples as seen in Chapter 3. Therefore, this test indicated that the T65 series did not have self-cleaning potential or the capability of degrading organic compounds in water, and therefore would not be

effective to use in bioaerosol inactivation experiments. This test also verifies the activity of the Degussa P25 films and supports their use as benchmark films.

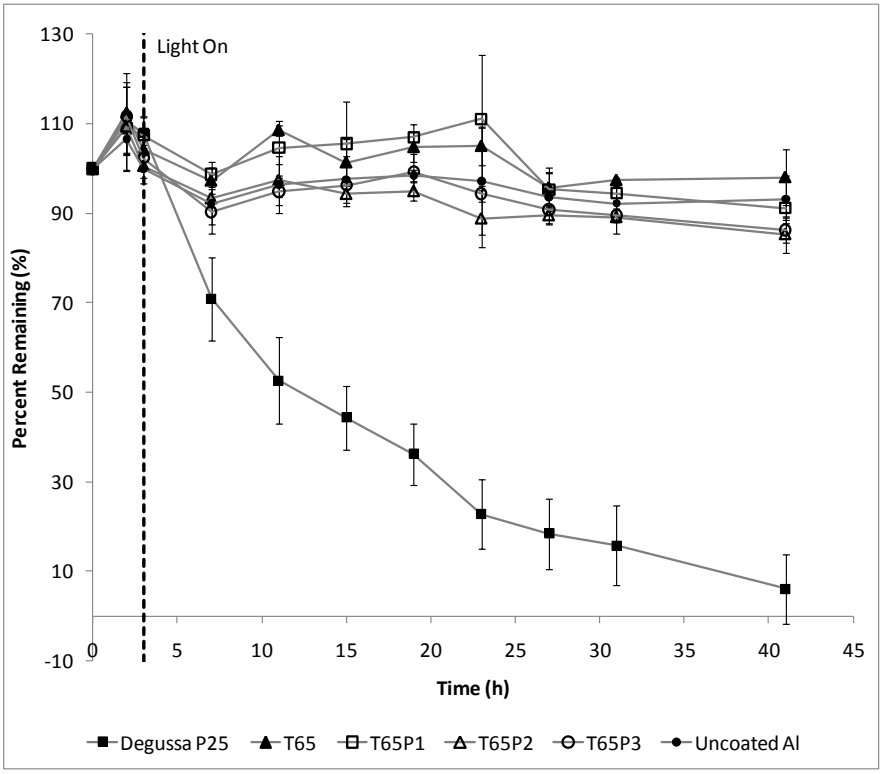

Figure 4.2 Degradation of methylene blue in aqueous solution by T65 series films exposed to UVA light. Error bars represent one standard deviation.

To ensure that the reduction in methylene blue concentration was due to photocatalytic activity, dark controls were run (Figure 4.3). It can be seen that the dark control run showed essentially no degradation of methylene blue, which confirmed that the activity was photocatalytic.

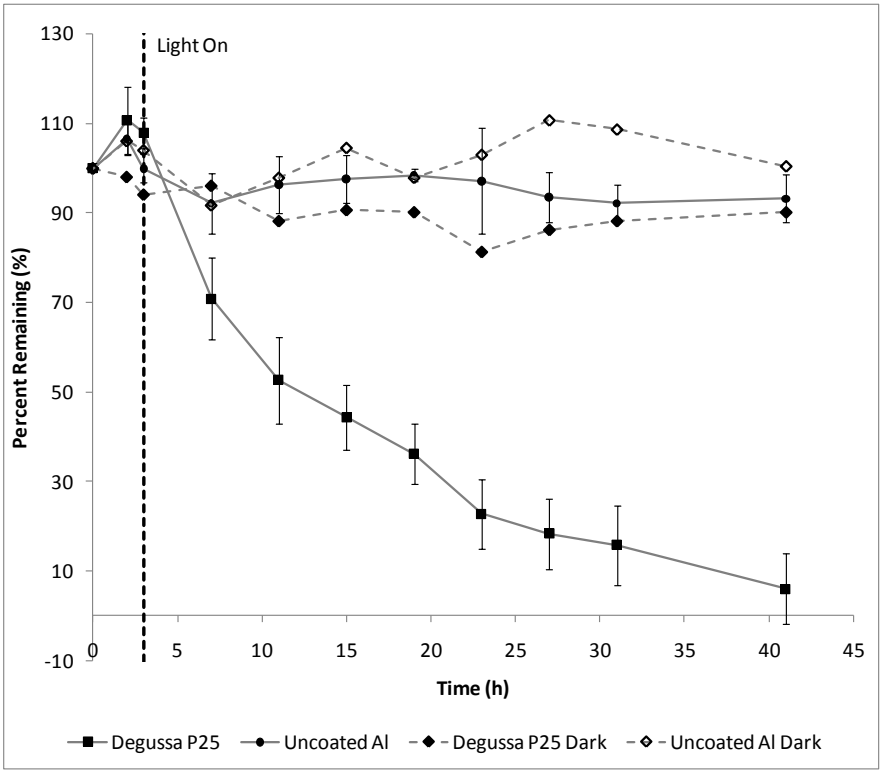

Figure 4.3 Comparison of degradation of methylene blue by Degussa P25 films in the light and in the dark. Error bars represent one standard deviation.

Although methylene blue bleaching is often directly correlated to mineralization, the photocatalytic reduction of methylene blue to *leuco*-methylene blue in oxygen limiting conditions also causes bleaching (Mills and Wang, 1999). *Leuco*-methylene blue is only stable at low oxygen concentrations, and it reverts back to methylene blue when exposed to oxygen (Tacconi et al., 1997; Karyakin et al., 1993). Therefore, to test for the presence of *leuco*-methylene, oxygen can be re-introduced into a system that has undergone a photocatalytic (oxygen consuming) reaction (Mills and Wang, 1999). Light cycling experiments were performed to determine if the setup used in this study produced oxygen limiting conditions when oxygen was consumed during the photocatalytic reaction. A photocatalytic reaction was performed for a certain time interval,

then the samples were left in the dark for a period of time to re-introduce oxygen. The results of the test can be seen in Figure 4.4.

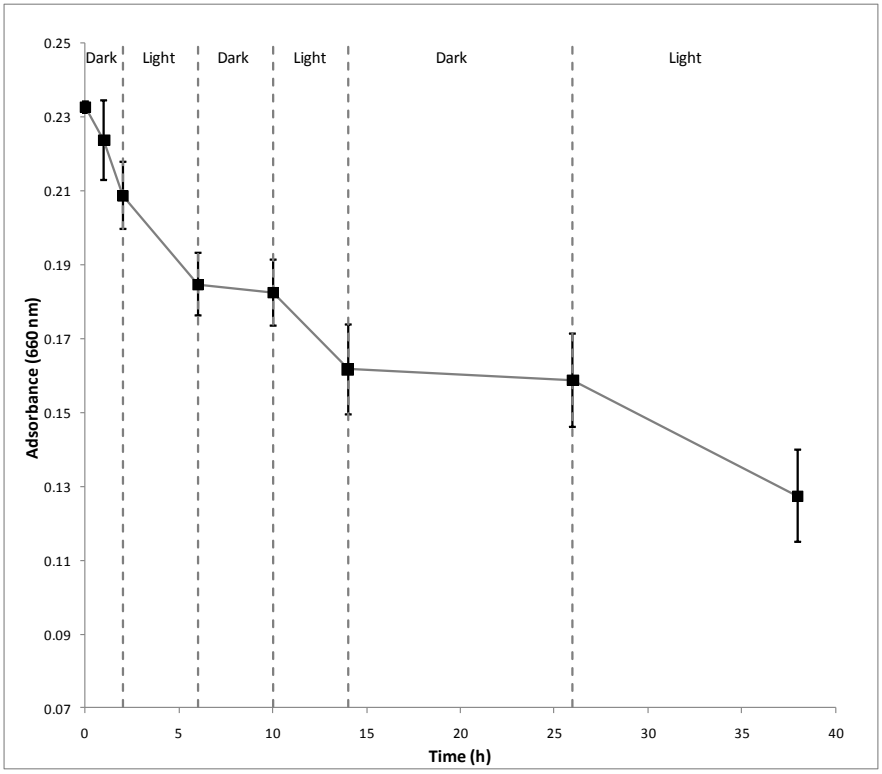

Figure 4.4 Degradation of methylene blue in light cycling experiments.

The results presented in Figure 4.4 show that there was no significant recovery of colour under dark conditions when re-oxygenation should occur. Thus, it was concluded that the current set up did not produce oxygen limiting conditions, and the bleaching of methylene blue was due to photocatalytic oxidation.

The ability of the T65 series and the Degussa P25 films to inactivate microorganisms was also tested. Bacteria in saline solution were allowed to settle and deposit onto the film surface. The film sections were then transferred to sterile saline solution where they were exposed to

UVA light. The bacterial viability on the surface was then assessed using the Live/Dead assay. The results of this experiment can be seen in Figure 4.5.

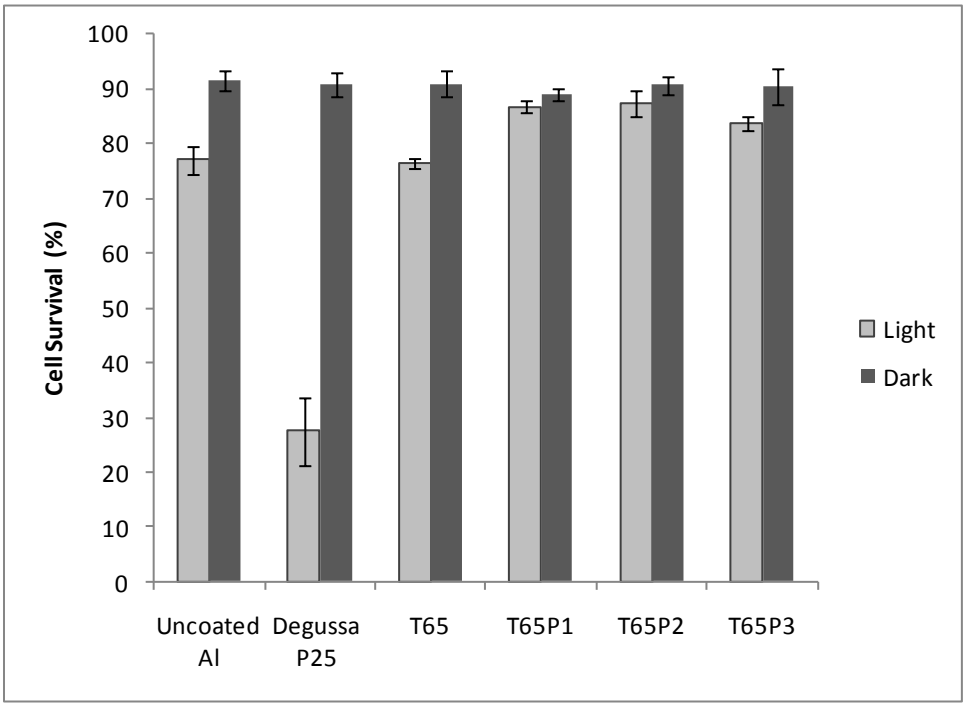

Figure 4.5 Inactivation of bacteria settled onto the surface of T65 series films when exposed to UVA light. Error bars represent one standard deviation.

After exposure to UVA light for 6 hours, it can be seen that less than 30% of the cells settled on the Degussa P25 film surface remain viable. The T65 sample showed more microbial inactivation than the samples with a silicon oxides under-layer (T65P1, T65P2, and T65P3). However, the level of inactivation of the T65 sample was not significantly different than that of the blank aluminum control. Therefore, it can be concluded that there was no photocatalytic activity with the T65 films and any inactivation was likely caused by photolysis. It can be seen that the percent cell survival is higher in the T65P1, T65P2, and T65P3 samples than the uncoated aluminum when exposed to UVA light, but the survival in the dark is similar. This suggests that

the layer of silicon oxides is reducing the exposure of the bacteria to UVA light. This may occur through direct shielding from the light, or by reduced reflectivity of the surface. The results of the bacterial inactivation experiments show that the Degussa P25 films can kill bacteria in aqueous suspension and would be an appropriate benchmark film to use. This test also shows that the T65 series samples cannot photocatalytically inactivate bacteria in water, and confirms the findings of the stearic acid test and methylene blue test.

In summary, the T65 series samples should not be used in bioaerosol inactivation experiments and improvements must be made to the flame coating process to make more effective films. These results are consistent with the SEM photographs (Chapter 3) which show that the T65 series samples have small amounts of titanium dioxide powder deposited on them. The deposition of powder formed by a gas phase reaction is a difficulty often associated with FACVD processes, so this is not an entirely unexpected result (Choy, 2003).

4.3.2 Performance of T68 Series

The T68 series films were produced using a lower air to fuel ratio, and thus a cooler flame than the T65 series, to try to improve film deposition and performance. The stearic acid test was performed on these films and the results are shown in Figure 4.6.

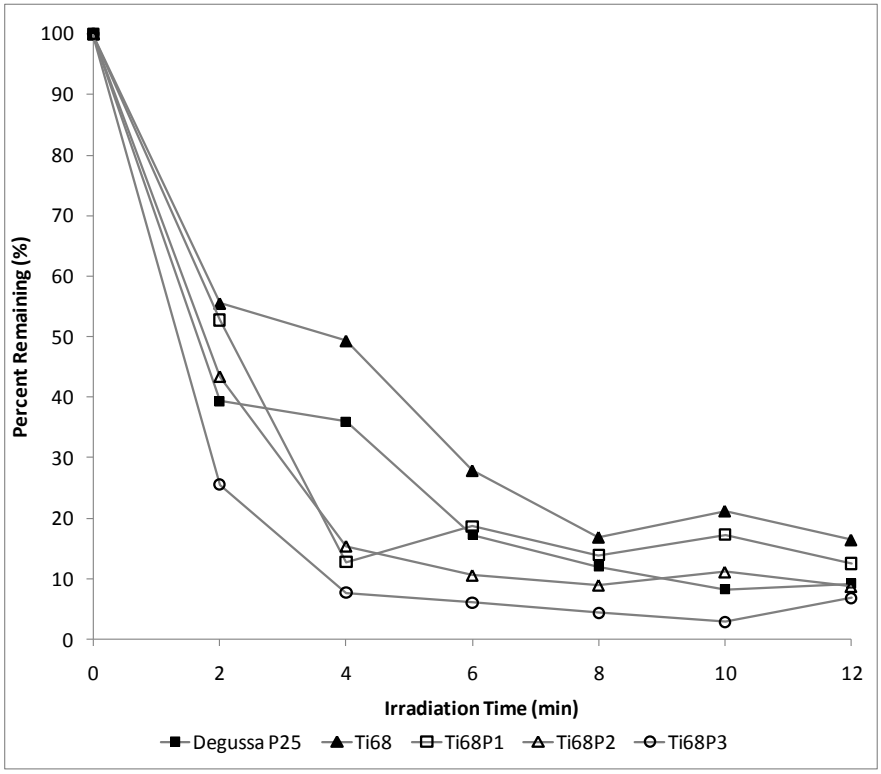

Figure 4.6 Oxidation of stearic acid on T68 sample series when exposed to UVC light.

It can be seen that all film samples tested degrade stearic acid very effectively when exposed to UVC light. Within 12 min of irradiation, all samples in the T68 series degraded over 80% of the stearic acid. It is clear that lowering the air to fuel ratio in the deposition process has significantly improved the effectiveness of the films, however from these results it is difficult to determine if the T68 series is more effective than the benchmark. In order to determine if the silicon oxides undercoating is needed, and if thickening the layer improves film performance, further experiments must be performed.

The methylene blue degradation test was performed to further investigate the effectiveness of T68 series compared to the Degussa P25 film. The test was performed and the results can be seen in Figure 4.7.

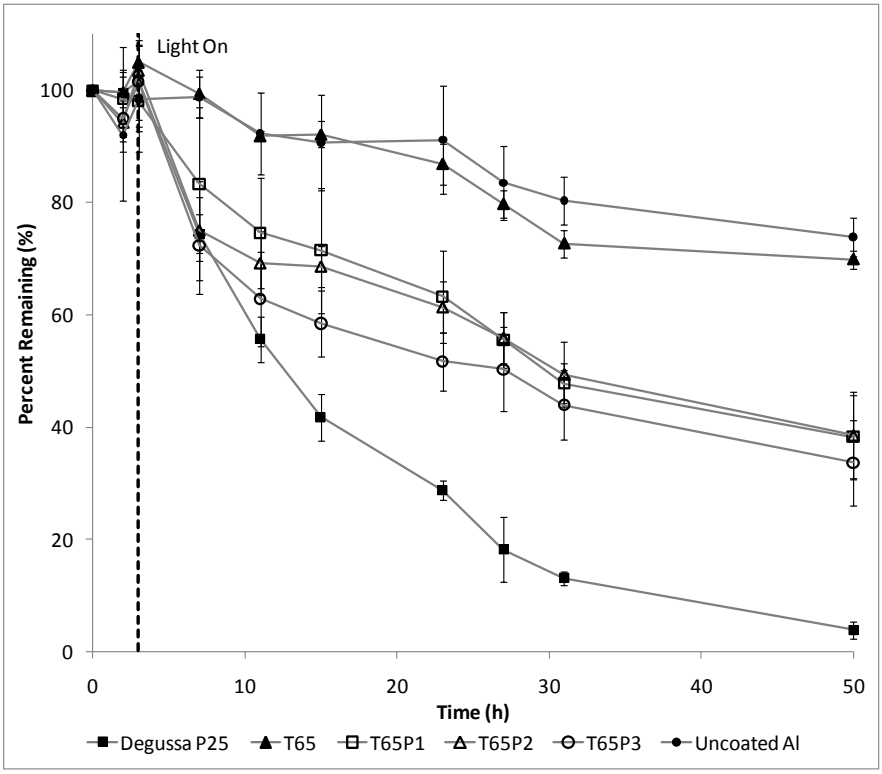

Figure 4.7 Degradation of methylene blue in aqueous solution by T68 series films exposed to UVA light. Error bars represent one standard deviation.

The Degussa P25 films have a higher rate of methylene blue degradation than any other sample tested. After 47 hours of exposure to UVA light, over 95% of the initial methylene blue has been degraded. The samples with a silicon oxides under-layer (T68P3, T68P2, and T68P1) have the next highest performance with over 60% (statistically lower than the Degussa P25 performance) of the methylene blue degraded after 47 hours of exposure to UVA light, and these films showed no activity in the dark (Figure 4.8). The difference in methylene blue degradation of these three samples is not statistically significant. Therefore, it appears that as the thickness of the silicon oxides under-layer increases, the films did not become significantly more effective. These results were not surprising after the GD-OES results (Chapter 3) indicated that as the

silicon oxides undercoating becomes thicker (from T68P1 to T68P3), no additional titanium dioxide was deposited.

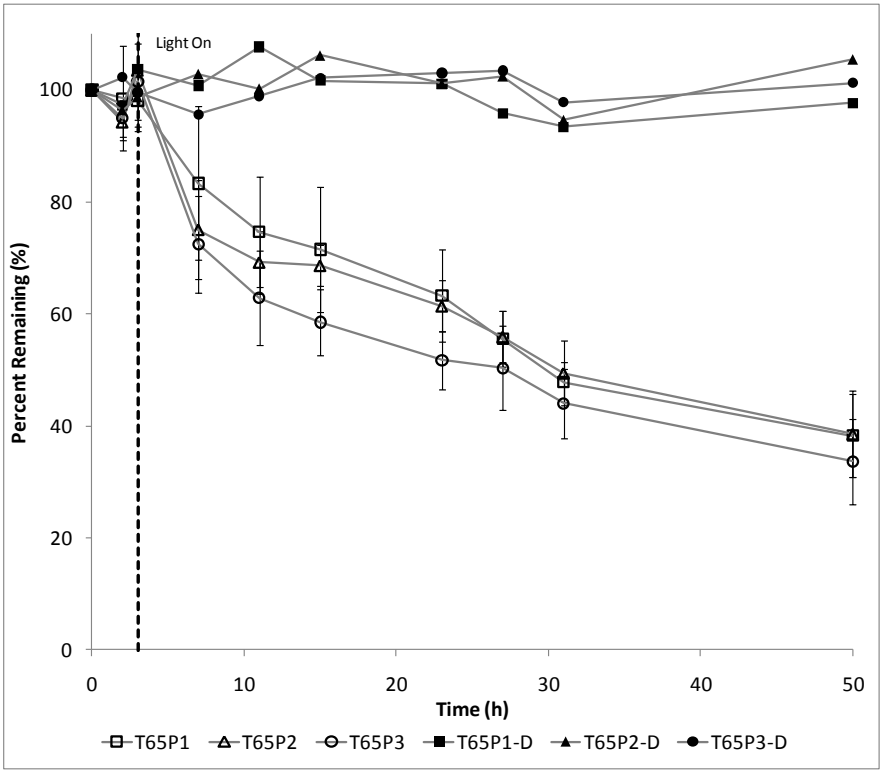

Figure 4.8 Comparison of degradation of methylene blue by T68 series films in the light and in the dark. Error bars represent one standard deviation.

When there was no silicon oxides under-layer present, the film performance is not significantly different than that of the uncoated aluminum even though a significant amount of titanium dioxide was found to be present (Chapter 3). Hence, the silicon oxides undercoating appears to improve film performance beyond allowing for moderately greater amounts of titanium dioxide to be deposited.

It is likely that the improved performance with the silicon oxides under-layer is caused by a change in titanium dioxide-substrate interaction. It has been shown that aluminum ions act as a

charge recombination site for electron hole pairs and lower photocatalytic activity (Ho et al., 2007; Choi et al., 1994) and ions can migrate into titanium dioxide films, especially during high temperature heating (Zhu et al., 2001). A passive layer of silicon dioxide has been used in past studies to block the migration of photocatalytic inhibiting sodium ions during heating processes (Watanabe et al., 1999). Past studies have also demonstrated that when titanium dioxide was deposited on SiO_2 coated stainless steel, anatase was the primary phase (Evans and Sheel, 2007). However, rutile was the primary phase when the coating was done on bare stainless steel (Evans and Sheel, 2007). Therefore, the silicon oxides layer here may be operating in a similar fashion and blocking the migration of detrimental aluminum ions and may also affect the crystalline structure by altering the deposition process.

The high activity of the Degussa P25 films without an undercoating can be explained due to the greater thickness of these films. It has been shown that as film thickness increases, the effect of aluminum support on the titanium dioxide diminishes and photocatalytic activity improves (Kwon et al., 2004). Also, ion migration is related to the temperature used during the deposition process. The electrophoretic powder deposition is performed at low temperatures, and therefore ion migration during film formation should be small. Past studies have confirmed that the activity of Degussa P25 is normally independent of the support material (Byrne et al., 1998).

Aqueous based microbial inactivation experiments were performed to further assess the performance of the T68 series films. The results can be seen in Figure 4.9.

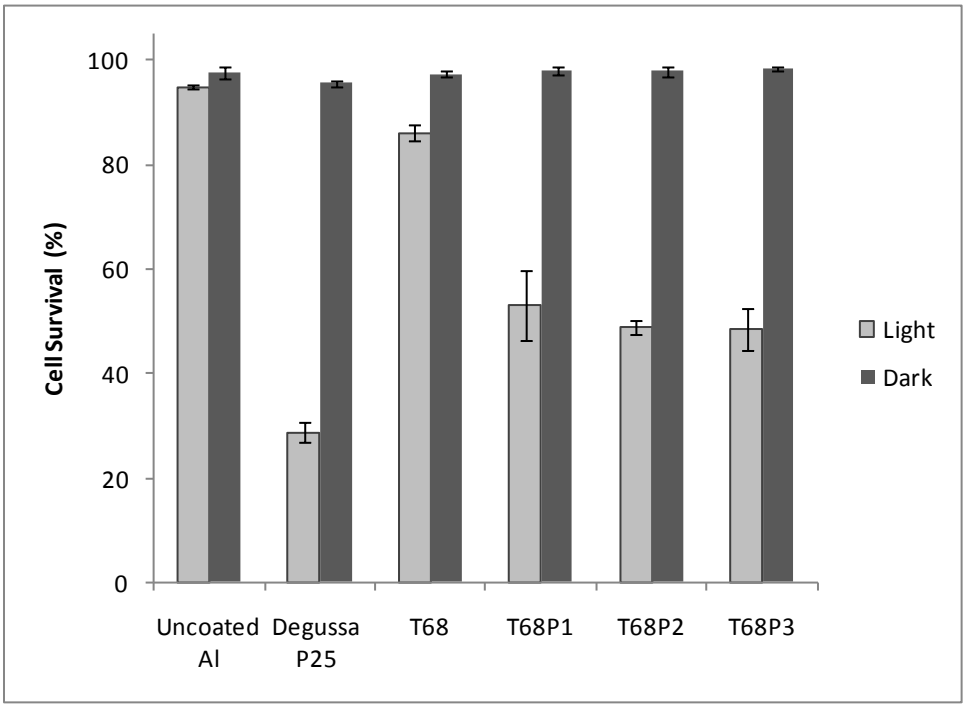

Figure 4.9 Inactivation of bacteria settled onto the surface in saline of T68 series films when exposed to UVA light. Error bars represent one standard deviation.

The Degussa P25 had the highest performance with less than 30% cell survival after 6 hours of exposure to UVA light. As in the case of the methylene blue experiment, the samples with undercoating (T68P3, T68P2, and T68P1) have the next highest performance with approximately 50% cell survival (statistically greater than the survival in the case of the Degussa P25 film). The results from these three samples are not statistically different from each other. The T68 sample comparatively shows little activity with approximately 85% cell survival, but this value is statistically significant. The results show that the T68 series films can kill bacteria in aqueous suspension with a silicon oxides under-layer and support the methylene blue results. However these results are different from the stearic acid test which showed that the T68 film with no undercoating was also effective.

To elucidate the reason for the difference in results between the stearic acid test and the aqueous based experiments, the stearic acid was repeated using the UVA lamps. The results of this experiment can be seen in Figure 4.10.

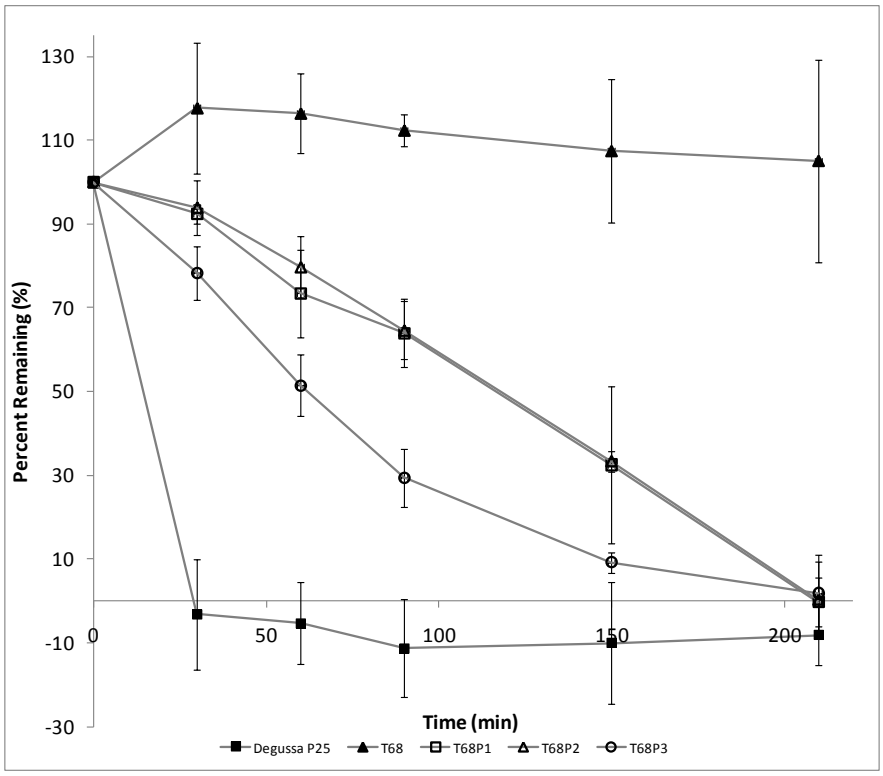

Figure 4.10 Oxidation of stearic acid on T68 sample series when exposed to UVA light.

When the stearic acid test was repeated using a UVA light source, the results agreed with the aqueous based destruction of methylene blue and inactivation of bacteria. The Degussa P25 films showed the highest activity, and the samples T65P3, T65P2, and T65P1 showed moderate activity. The sample without an undercoating showed no significant activity. It can be seen that the samples with the undercoating (T68P3, T68P2, and T68P) had lower activity under UVA light than UVC light, whereas the Degussa P25 film had similar activity under both light sources. This result is not unexpected since the GD-OES results in Chapter 3 show that the films made in the

FACVD processes were much thinner than the Degussa P25 films, and film thickness can affect the efficiency depending on the wavelength used for activation. Thin titanium dioxide films (about <100 nm) typically absorb a large amount of the UVC spectrum but little UVA (Mills et al., 2003). Thus thin films typically have a lower efficiency in UVA light than UVC light (Mills et al., 2002). The negligible activity of the T68 sample can be attributed to substrate-film interactions as discussed previously.

In summary the T68 series with silicon oxides undercoating (T68P3, T68P2, and T68P1) can act as a self-cleaning surface, degrade organic compounds in water, and inactivate bacteria in water when exposed to UVA light, with moderate performance when compared to the Degussa P25 film. Since the films are effective in these applications it is possible that they could also be successfully used in an air sterilization unit.

4.4 Conclusions

A series of tests were performed to screen for film samples that may be effective for air sterilization. The T65 series of films was not effective as self-cleaning surfaces, for the destruction of organics in water, or for the inactivation of bacteria in water. Therefore, it was concluded that this film series should not be used in bioaerosol inactivation experiments. The T68 series (produced with a lower air flow rate) was found to be moderately effective under UVA light in all tested applications, when a silicon oxides under-layer was present, compared to the Degussa P25 film. The T68 sample without an undercoating showed no activity when exposed to UVA light, and this was attributed to potential substrate-film interactions. From these results, it was determined that the T68P3, T68P2, and T68P1 samples may be appropriate for use in bioaerosol inactivation experiment.

Chapter 5

Design of Experiments for the Photocatalytic Inactivation of Bioaerosols

5.1 Introduction

Exposure to bioaerosols can lead to serious diseases, such as influenza, tuberculosis, and meningitis as well as having been found to be responsible for asthma (Lippmann, 2000). Due to the limitation of air sterilization techniques, interest has recently been growing in the application of titanium dioxide photocatalysis to sterilize air (Grinshpun et al., 2007). To have successful bioaerosol inactivation, a number of factors must be considered, such as reactor geometry, air flow rate, relative humidity, and production and capture of bioaerosols. The prediction of bioaerosol cell concentration captured is a particularly complex issue affected by many factors (as detailed previously detailed in Chapter 2).

The basic design of a reactor system for the photocatalytic inactivation of bacteria is overviewed in this chapter. Also, aerosol generation and capture experiments were performed using plate count analysis and a basic model was generated to correlate to the sampling time, nebulizer pressure (flow rate), and nebulizer optical density to the concentration of bacteria captured in the impinger. This model would provide an estimate of the amount of bacteria introduced into the air at a given set of input conditions. Ranges of the control variables were chosen to attempt to avoid problems encountered by other groups, such as excessive liquid evaporation, particle re-aerosolization, and high shear rate leading to loss of viability as detailed in Chapter 2. Alternative techniques to analyze the impinger catch solution were also examined.

5.2 Reactor System Design

The results of a photocatalytic inactivation experiment depend on the reactor design and on the operating conditions. As mentioned in Chapter 2, the three main aspects to consider are the effects of reactor geometry, system flow rate, and relative humidity.

In order to have measurable bacterial inactivation, some have shown that reactor geometry must be enhanced to increase contact between the bacteria and the photocatalytic surface (Keller et al., 2005). However, it is also possible to use a simple geometry reactor and alter operating conditions to increase bacterial inactivation. Since the purpose of this study was to evaluate performance of different film samples, and not necessarily to provide maximum bacterial inactivation, simple reactor geometry is preferable. Reactors with simple annular geometry are often used and have been shown to be effective at inactivating microorganisms (Pal et al., 2008; Paschoalino et al., 2008; Pal et al., 2005). Annular reactors are also advantageous for the assessment of film performance as the central bulb provides relatively uniform irradiation of the photocatalytic surface. For these reasons, an annular reactor was chosen. An annular UVGI reactor (Sanitron S37C, Atlantic Ultraviolet Corporation) was purchased with a working length of 81 cm and an outer diameter of 10 cm. Stainless steel inserts were fabricated to hold titanium dioxide coated aluminum. The ratio of length to width of the reactor in this study was similar to other studies using annular reactors, but the overall size was larger (Pal et al., 2005).

In order for bacterial inactivation to be measurable using a simple geometry reactor, process conditions such as humidity must be controlled. When operating a tubular reactor at a low relative humidity (<30%) no bacterial inactivation was reported (Keller et al., 2005). Using similar reactor geometries, others have reported high one-pass efficiency when relative humidity levels were increased (Pal et al., 2008; Pal et al., 2005). It has been found that the level of

humidity to obtain maximum bacterial inactivation is highly dependent on the species, but in general, higher relative humidity results in higher inactivation which is likely due to higher production of hydroxyl radicals (Yu et al., 2008; Goswami et al., 1997; Pal et al., 2008). Therefore, control of humidity is essential in bacterial inactivation experiments. A humidity control system was constructed using three mass flow controllers (RK-32907-71, Cole-Parmer) to control the flows of streams of dry air, humidified air, and bioaerosol air. The humidity levels were measured using a thermohygrometer (Traceable Hygrometer, 11-661-7B, Fisher Scientific). The conceptual layout of this system can be seen in Figure 5.1.

Air flow rate is another main factor that must be controlled to ensure measurable bacterial inactivation. Lower flow rates can provide a longer time period for bioaerosols to interact with the titanium dioxide surface (Goswami et al., 1997). In most successful single-pass experiments, the flow rates were between 0.1-10 L/min, which corresponded to reactor retention times on the order of minutes (Keller et al., 2005; Pal et al., 2008; Pal et al., 2005). To operate at similar flow rates, the equipment to generate and capture bioaerosols must be carefully selected. The Collison Nebulizer is widely accepted as a standard bioaerosol generation unit (Stone and Johnson, 2002; Reponen et al., 1997; Johnson et al., 1999; Grinshpun et al., 2007; Lin and Li, 2003). The 3-jet Collison Nebulizer (3-jet modified MRE-type Collison Nebulizer, BGI Inc.) was purchased as it can produce bioaerosols in the desired range of flow rates. All-glass impingers are widely accepted as a reference sampler (Jensen et al., 1992; Brachman et al., 1964; Ding and Wang, 1997; Grinshpun et al., 1997; Henningson et al., 1988; Burge and Solomon, 1987). However, most standard impingers operate at flow rates that are on the high end of the desired range. For example, the optimum flow rate range for the AGI-4 was found to be between 6-12.5 L/min (Willeke et al., 1995). However, the modified AGI-4 used was designed to operate at half the

flow rate as the standard AGI-4. Therefore, it may be expected that the optimal flow rate will be between 3-6 L/min. For this reason modified AGI-4 impingers (Ace Glass Inc., 7541 Impinger) were chosen as the bioaerosol capture device.

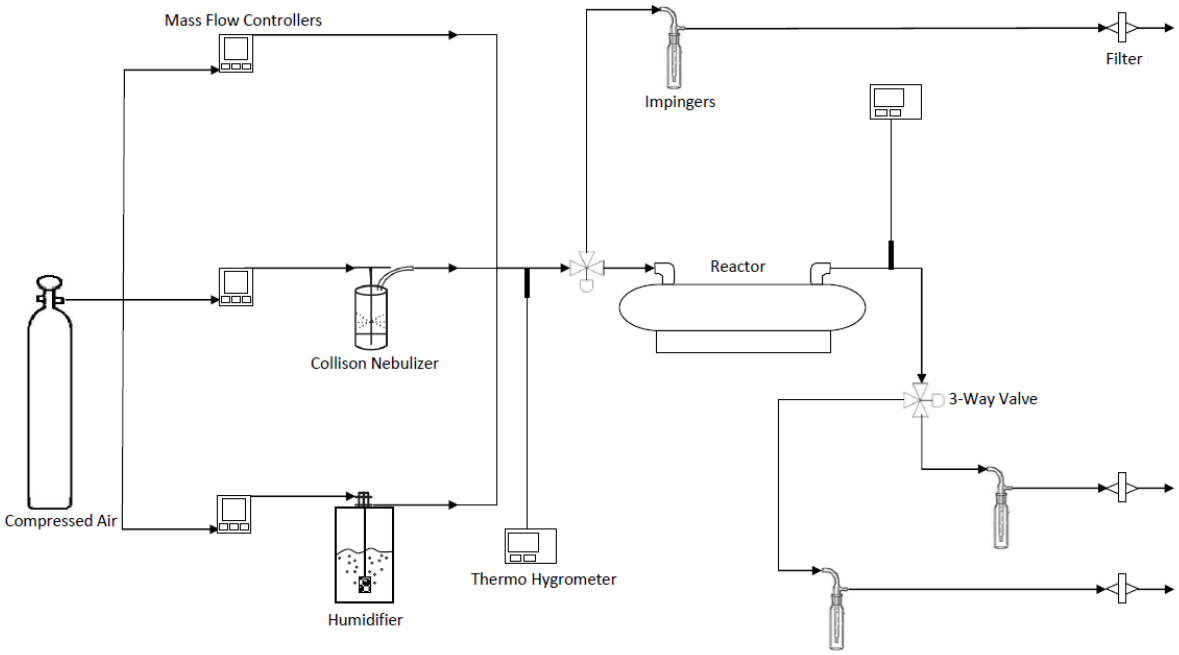

Figure 5.1 Photocatalytic Reactor System Layout.

The overall layout of the reactor system can be seen in Figure 5.1. Compressed air is fed and split into three streams; a dry stream of air, a humidified stream of air, and a bioaerosol stream. The flow rate of the three streams is controlled by individual mass flow controllers. The three streams are mixed and the temperature and humidity are measured using a thermohygrometer. The bioaerosol air stream with controlled humidity then passes through the photocatalytic reactor where temperature and humidity can be measured again. All-glass

impingers capture the bioaerosol both before and after the reactor so that microbial inactivation can be quantified.

To obtain reliable results, it is important to be able to control bioaerosol generation and have an accurate method of quantifying bioaerosols. For this reason aerosol generation and capture experiments were performed.

5.3 Bioaerosol Generation and Capture Experiments Using Plate Count Analysis

Bioaerosol generation and capture experiments were performed to analyze the feasibility of using plate count analysis to quantify bioaerosol concentration. A regression model was generated relative to control variables.

5.3.1 Experimental

5.3.1.1 Experimental Setup

The experimental setup consisted of a 3-jet Collison Nebulizer (BGI Inc., CN24) and an all-glass impinger (Ace Glass Inc., 7541 Impinger) connected using a short 3/8" OD silicon tube. A compressed air tank and valve with a pressure gauge was attached to the inlet of the nebulizer so that the air pressure supplied to the nebulizer could be controlled. A sterile air filter was connected to the impinger outlet to remove any remaining bacteria before venting to a fume hood.

5.3.1.2 Culture Storage and Preparation

Bioaerosol generation and capture experiments were performed using *Bacillus subtilis* ATCC 6051, a spore forming gram positive bacteria. This species is widely used in bioaerosol work (Stone and Johnson, 2002) and is found to have a high resistance to the stresses associated with aerosolization (Li, 1999). Working cultures were stored on nutrient agar plates. Cultures

were transferred to fresh nutrient agar plates monthly, and every 6 months cultures were refreshed from slants.

A loop of bacteria was taken from a plate and inoculated in 200 mL of nutrient broth in a 1 L flask and incubated at 30^{o}C and 200 rpm for 15 h, then harvested in the exponential growth phase. After this period the cells were centrifuged at 8000 x g for 10 minutes. The supernatant was removed, and the cells resuspended in 0.9% NaCl. The cells were washed once, and then resuspended in 0.9% NaCl . The cells were washed only once as further washing has been shown to add additional stress to the bacteria (Marthi et al., 1990). The resulting bacterial suspension was diluted with 0.9% NaCl to achieve the desired optical density measured at 600 nm (Ultrospec 1000 UV/visible spectrophotometer, Pharmacia Biotech).

5.3.1.3 Experimental Procedure

The bacterial suspension of desired optical density was added to the nebulizer chamber. Catch solution consisting of 20 mL of 0.9% NaCl in sterile distilled water was added to each impinger. Then compressed air at a specified pressure was supplied to the nebulizer to generate a bioaerosol. The nebulizer was run for at least five minutes prior to attaching the first impinger, to avoid error due to the loss of viability in the early stages of nebulization observed by other groups (Stone and Johnson, 2002). After an impinger was attached to the nebulizer, the bioaerosol air stream was passed through the silicon tube into the impinger where the bacteria were impinged in the capture solution. The air stream leaving the impinger was filtered through a 0.45 μm sterile filter before venting in the chemical hood.

After the compressed air was continuously supplied to the nebulizer until the desired sample duration was achieved it was turned off and the impinger was detached, rinsed with 10 mL of 0.9% saline solution, and put aside for later analysis. Another impinger was then attached

and the process restarted. This procedure was repeated until all available impingers (between 2 and 6) were used, and the experiment completed. The controlled pressure and sample duration were varied for each impinger as desired.

The three variables examined using this procedure included inlet nebulizer pressure, sample duration, and the optical density of the bacterial suspension added to the nebulizer. The maximum inlet nebulizer pressure was dictated by the air flow rate produced at the specified pressure, and the impinger's maximum effective air flow rate of approximately 6L/min (manufacturer specification). The pressure was varied below this value to determine the relationship between pressure and total bacteria captured. A pressure range of 10 to 20 psi was chosen, which would produce a flow rate between 4.2 and 6.1 L/min according to manufacturer's specifications. The range of sample duration was chosen to be between 2.5 and 10 min based on the minimum duration required for a detectable signal and experimental time constraints. The range of optical density, measured at 600 nm, was between 0.536 and 2.08, where the higher bound represents the maximum optical density attainable using the culture method employed.

5.3.1.4 Analysis of Impinger Catch Suspension Using Plate Counts

After experiments were completed, the impinger capture suspension was analyzed by plate count. The impinger catch was diluted in 0.9% NaCl as needed. The suspensions were mixed, and 0.1 mL from each dilution was placed on separate nutrient agar plates. A flame sealed Pasteur pipette, with approximately four centimeters of its end bent at a 90 degree angle, was used to evenly spread the suspension on the surface of the nutrient agar. The tops were secured with parafilm paper and incubated for 24 hours at 30^{o}C. The number of visible colonies on the plates was recorded. Only plates that had between 30 and 300 colonies were used to

calculate the concentration of viable bacteria in the original suspension using the known volume added to the plate and the dilution factor.

5.3.2 Results and Discussion

A total of 51 data points were obtained by varying the conditions described in the experimental section. All control variables were coded so that they ranged from -1 to 1. Figure 5.2 is a scatter plot matrix showing the relationship between the controlled variables, as well as the corresponding concentration of bacteria captured in the impinger. As seen in the bottom row in Figure 5.2 there appears to be a positive trend between the concentration of bacteria captured and all of the control variables, the most evident being sample duration (middle plot).

A least squares linear regression was performed, and inspection of the actual versus predicted plot (data not shown) and the normal probability plot shown in Figure 5.3 show this model was inadequate to describe the observed data. The data in the normal probability plot did not closely lie on a straight line indicating that the residuals were not normally distributed and therefore the model was inadequate. This lack of normal distribution was thought to be a result of the nature of the plate count analysis. As described in Chapter 3, only plates with counts between 30 and 300 colonies per plate were used, and in order to achieve this number the initial sample often had to be diluted. The count was then taken and multiplied by the dilution factor to calculate the undiluted concentration. Therefore, any error that occurred in the plate counts would also be multiplied by a factor which increased as the dilutions increased. Thus, if the predominant source of error was caused by the plate count analysis then it would be expected that the error be multiplicative and increase as the concentration of bacteria captured increased. Others have also noted the need to use the logarithm of plate count analysis from bioaerosol

experiments to compensate for the observed increase in variance in higher counts (Lembke et al., 1981).

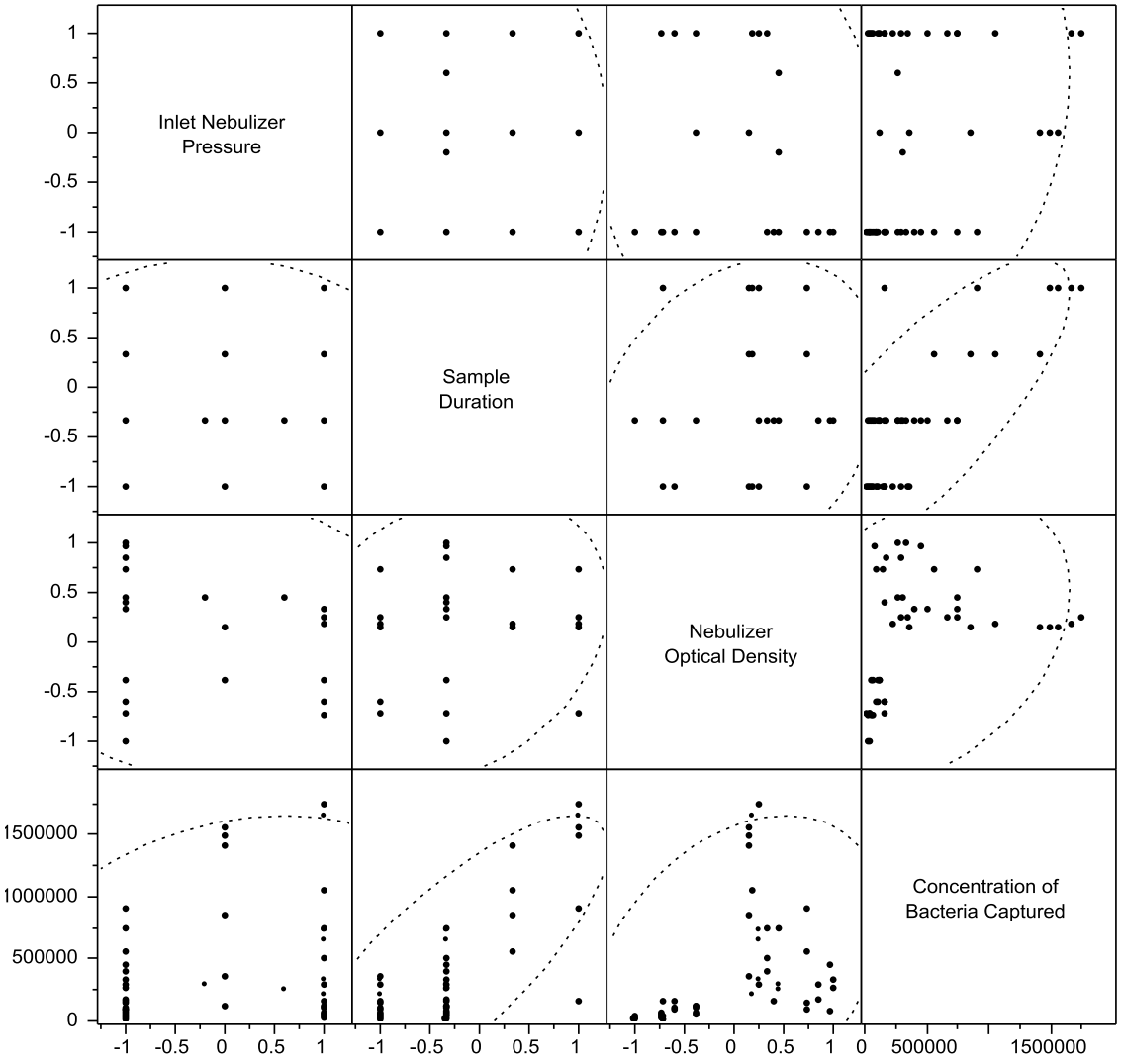

Figure 5.2 Scatterplot matrix of bioaerosol generation and capture experiment input and output variables.

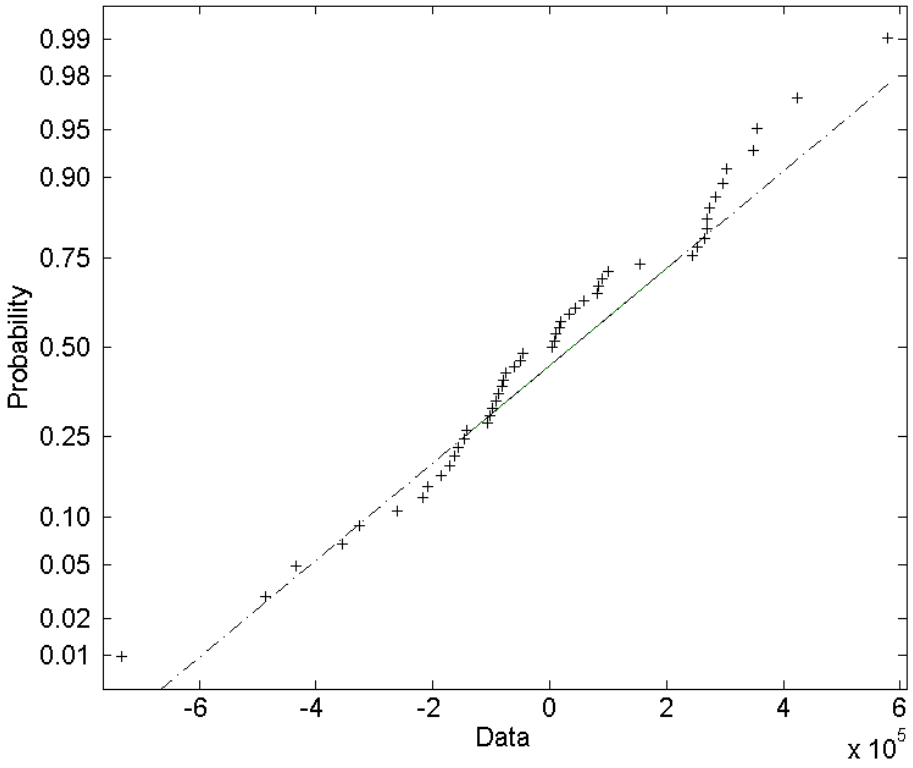

Figure 5.3 Normal probability plot of least squares linear regression.

To account for possible apparent multiplicative error, the logarithm of the concentration was taken, then a least squares linear approximation was performed in the logarithmic space. As seen in Figure 5.4, the data lie fairly well on a straight line which means the data is normally distributed, and therefore the model may be adequate.

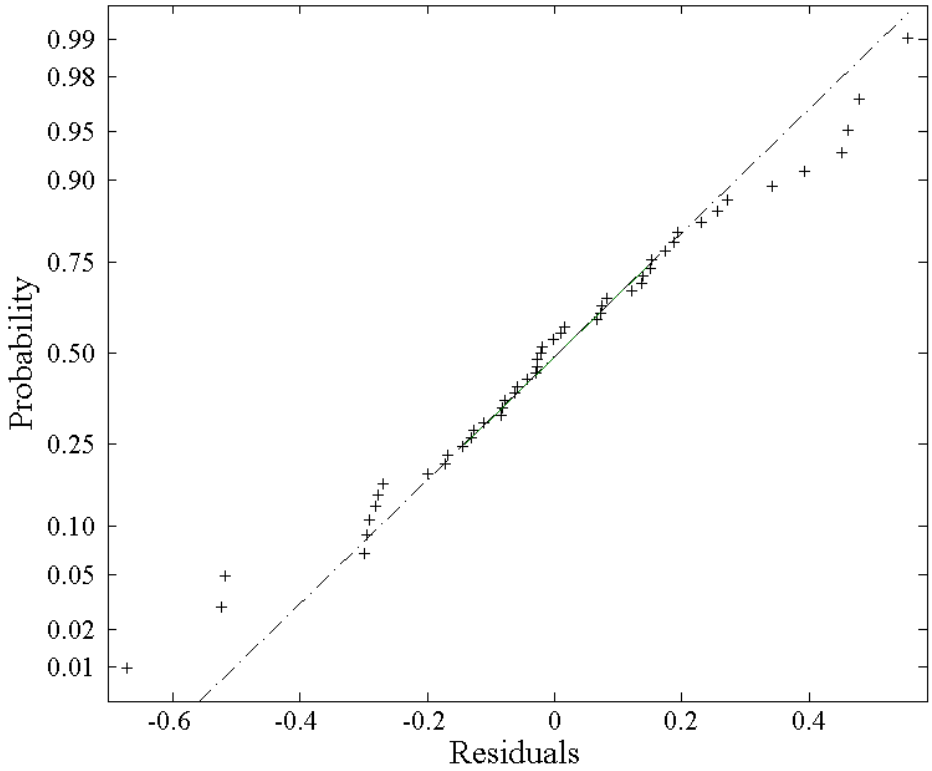

Figure 5.4 Normal probability plot of least squares linear regression in the logarithmic space of the concentration of bacteria captured.

A plot of the actual logarithm of the concentration of bacteria versus the logarithm of the concentration of bacteria captured predicted by the regression model, Figure 5.5, has been generated as a method to test the validity of the model. It can be seen that the points are scattered fairly evenly around a line of slope 1 indicating that the model is a good average representation of the data, and that there is little unmodeled trend. The points are only moderately well clustered around the line, with only about half of the points falling within the 95% mean confidence interval (region that should contain the regression curve) (Freund et al., 2003). This shows the model only provides moderate predictive ability, which may be caused by the large error associated with plate count analysis. Therefore, according to the plot of predicted

versus actual, the model appears to be adequate, providing a good average representation of the data, and moderate predictive ability.

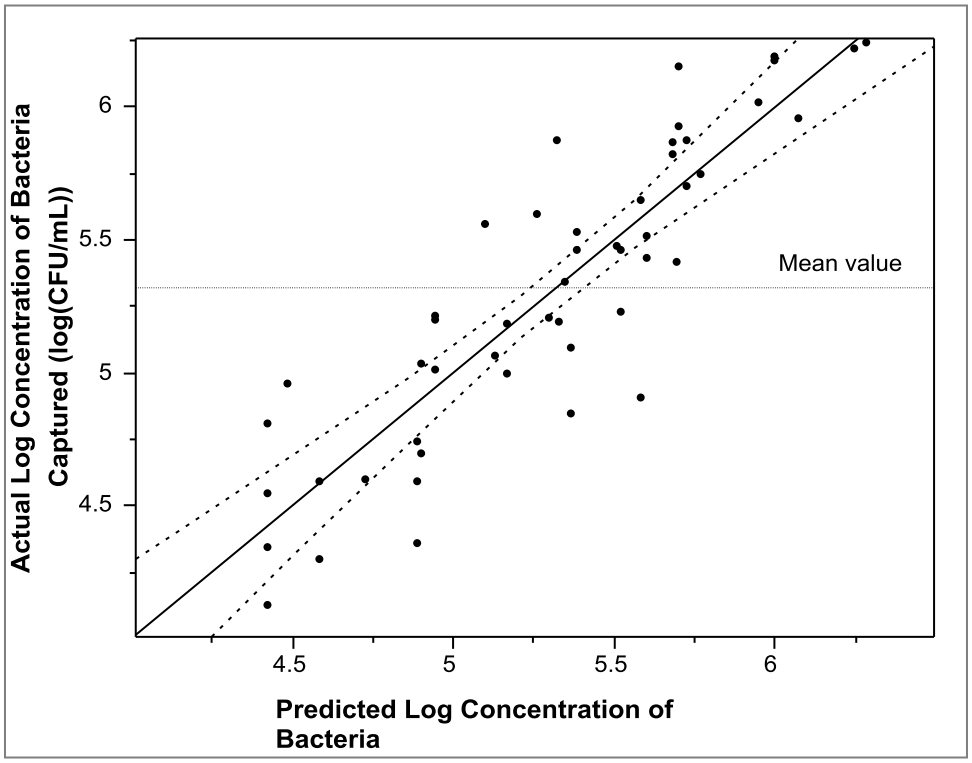

Figure 5.5 Actual versus predicted plot. Solid line represents the trend of the plot, the broken curves are the 95% confidence intervals of the mean confidence interval, and the horizontal broken line is the mean.

Further quantitative analysis was performed to test the fit of the regression model, and the results can be seen in Table 5.1 and Table 5.2. It can be seen the both the R^2 value and the adjusted R^2 value are reasonably high suggesting a moderately good fit. The F value presented in Table 5.2 is very high, and therefore according to the mean square regression ratio, the trend being modeled is strongly significant. Both quantitative tests support the previous conclusion that the model is an adequate representation of the data set.

Table 5.1 Regression statistics of least squares linear regression in the logarithmic space of the concentration of bacteria captured.

Multiple R	0.893
R Square	0.797
Adjusted R Square	0.784
Standard Error	0.266
Observations	51

Table 5.2 Analysis of variance table to test the significance of the least squares linear regression in the logarithmic space of the concentration of bacteria captured.

	Degrees of Freedom	*Sum of Squares*	*Mean Square*	*F Value*	*Significance F*
Regression	3	13.02	4.34	61.52	2.65E-16
Residual	47	3.32	0.07		
Total	50	16.34			

To confirm the validity of the model, each regression parameter estimate must be evaluated individually. The predicted parameters of the regression model are displayed in Table 5.3. The p-value for all parameters is very small, showing that all regressed parameters are strongly significant, and that they should all be kept in the model. Furthermore, the plots of residuals versus the individual parameters show good scatter around the horizontal axis. This indicates that there is little unmodeled trend, and therefore the form of the model is appropriate. A further regression was performed (data not shown) with date of experiment and order in which impingers were used as variables. Neither of these parameters improved the model, and both parameters were found to be insignificant indicating that there was no systematic trend in the experiments with time. The analysis of the parameters provides further evidence for the validity of the model and the choice of regression parameters.

Table 5.3 Parameter estimates and test of significance for parameters estimated using least square linear regression in the logarithmic space of the concentration of bacteria captured.

Parameter Estimates				
	Coefficients	*Standard Error*	*t Stat*	*P-value*
Intercept	5.474	0.042	130.17	8.89E-62
Inlet Nebulizer Pressure	0.232	0.041	5.67	8.43E-07
Sample Duration	0.452	0.059	7.63	9.28E-10
Nebulizer Optical Density	0.509	0.066	7.72	6.76E-10

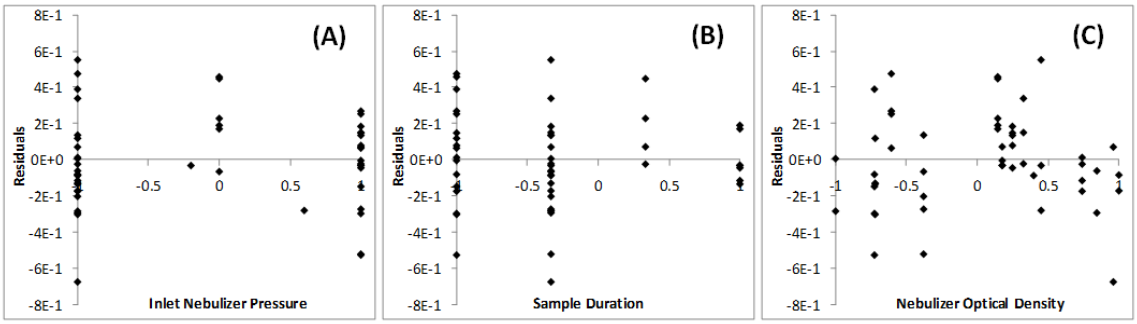

Figure 5.6 Residual plots by parameters to check for unmodeled trend. (A) residuals of inlet nebulizer pressure, (B) residuals of sample duration, (C) residuals of nebulizer optical density.

In summary, bioaerosol generation and capture experiments were completed and the analysis was performed via plate counts for the determination of the concentration of viable bacteria. A least squares linear regression model in the logarithmic space of the concentration of bacteria capture was generated. This form of model is appropriate because of the multiplicative error associated with plate count analysis. The estimated parameters in the model were shown to be significant and all test statistics indicated that the model provided adequate fit for the data set. However, as seen in the plot of actual vs. predicted, the model only provides moderate predictive ability because of the high level of error in the data set. High variability in results was expected

and has been reported by others performing similar experiments (Kesavan et al., 2010; Lembke et al., 1981). A significant fraction of the error is thought to be associated with the plate count method (Lembke et al., 1981). Others have reported that if the same impinger suspension was plated twice, the error could be expected to be as high as 30% but often ranged from 10% to 15% (Zimmerman et al., 1987). Therefore, if a different method of analysis was used it may reduce the variance of the results and provide a model with better predictive ability. This would also help eliminate some of the previously mentioned problems with plate count analysis of bioaerosols including loss of culturability of viable cells (Marthi et al., 1991; Heidelberg., 1997) and long sample processing times.

5.4 Alternate Methods for Determining the Concentration of Viable Bacteria in the Impinger Capture Suspension

Alternative methods of determining viability of the captured bioaerosol were evaluated in an attempt to reduce sampling error and sample processing time.

5.4.1 Experimental

5.4.1.1 Alternative Methods for the Evaluation of the Concentration of Viable Bacteria

Two possible methods of quantifying the concentration of viable bacteria are the Live/Dead Baclight assay (Invitrogen) and the BacTiter-Glo™ Microbial Cell Viability Assay (Promega Corporation).

The Live/Dead BacLight™ assay (Invitrogen) quantifies cell viability based on membrane intactness. It is a two-colour fluorescence assay using SYTO 9 (Invitrogen), a green-fluorescent nucleic acid stain, and propidium iodide, a red nucleic acid stain. The SYTO 9 stain labels all bacteria in a population. The propidium iodide labels the cells with damaged

membranes and causes a reduction of SYTO 9 fluorescence in cells where both dyes are present. As a result, cells that are viable will fluoresce green and non-viable cells will stain red.

The assay was prepared by mixing both components of the Live/Dead kit L13152 in 5 mL of sterile filtered water to form the stain solution. Equal volumes (100 μL) of the stain solution and the bacterial suspension were added to a black-walled-clear-bottom costar 96 well microplate and mixed by pipetting up and down several times. The plate was then incubated in a Spectramax M2^{e} Microplate Reader (Molecular Devices Inc.), in the dark at 25^{o}C for 15 min. The excitation wavelength was set at 485 nm and two readings were taken from each well centered at 530 nm (green) and 630 nm (red). The detected fluorescence could then be related to cell viability.

The BacTiter-Glo^{TM} assay works on the principle that only viable bacteria will produce ATP, and correlates cellular ATP to viable bacteria concentration. The reagent contains a proprietary formulation which causes cell lysis and extracts cellular ATP. The free ATP then reacts with a proprietary thermostable luciferase to generate a luminescent signal.

To perform the BacTiter-Glo^{TM} assay, the reagent was made by adding 100 mL of BacTiter-Glo^{TM} buffer to the proprietary substrate to reconstitute the enzyme/substrate. The reagent was mixed and allowed to equilibrate to room temperature. Equal amounts (100 μL) of reagent and the bacterial sample were added to a black-walled-clear-bottom costar 96 well microplate. The plate was then inserted into a Spectramax M2e Microplate Reader (Molecular Devices Inc.), where it was mixed and allowed to equilibrate for five minutes. The luminescent signal was then recorded using the full spectral capabilities of the plate reader.

5.4.1.2 Determining Detection Limits of Alternative Viable Bacteria Determination Methods

To determine if the nebulizer capture solution can be effectively analyzed using the Live/Dead or BacTiter-Glo™ assay, the detection limits using *Bacillus subtilis* and the available equipment must be assessed. To determine the detection limit analysis for each assay, a culture of *Bacillus subtilis* was prepared in the same fashion as for the plate count analysis experiments and the optical density was measured (Ultrospec 1000 UV/visible spectrophotometer, Pharmacia Biotech). The culture and a series of 10-fold dilutions of it were added in triplicate to a microwell plate for either Live/Dead of BacTiter-Glo™ analysis. The respective fluorescence and luminescence was recorded and used to determine the detection limits of the two assays using *Bacillus subtilis* and the available equipment.

5.4.1.3 Bioaerosol Generation and Capture Experiments to Test Alternative Methods of Catch Analysis

After the detection limit of each assay was established, the applicable assay was used in a series of bioaerosol generation and capture experiments to determine the accuracy and repeatability of the method. The results from these experiments were also compared against the plate count experiments to test for consistency and to determine the most appropriate assay to be used to analyze impinger catch.

The procedure for the general bioaerosol generation and capture experiments was the same as described earlier in the chapter, except that the Live/Dead analysis was used to analyze impinger catch instead of the plate count method. The number of experiments performed was far less extensive than that of the plate count analysis, with only two sets of experiments performed (totaling 10 data points acquired). These two experiments provided sufficient information on the repeatability of this method as well as the correlation with the plate count method. Sample

duration was varied between 2.5, 5, and 10 minutes and was the only variable changed in these experiments. The inlet nebulizer pressure was kept constant at 20 psi and the nebulizer optical density constant at 1.5.

5.4.2 Results and Discussion

5.4.2.1 Determination of Detection Limits

Serial dilutions of bacterial suspensions of known optical density were examined using the BacTiter-Glo™ and Live/Dead assays to determine the minimum detection limits. The respective luminescence and fluorescence of each well was correlated to viable cell number using the measured optical density and the previously generated calibration curve presented in Figure 5.7.

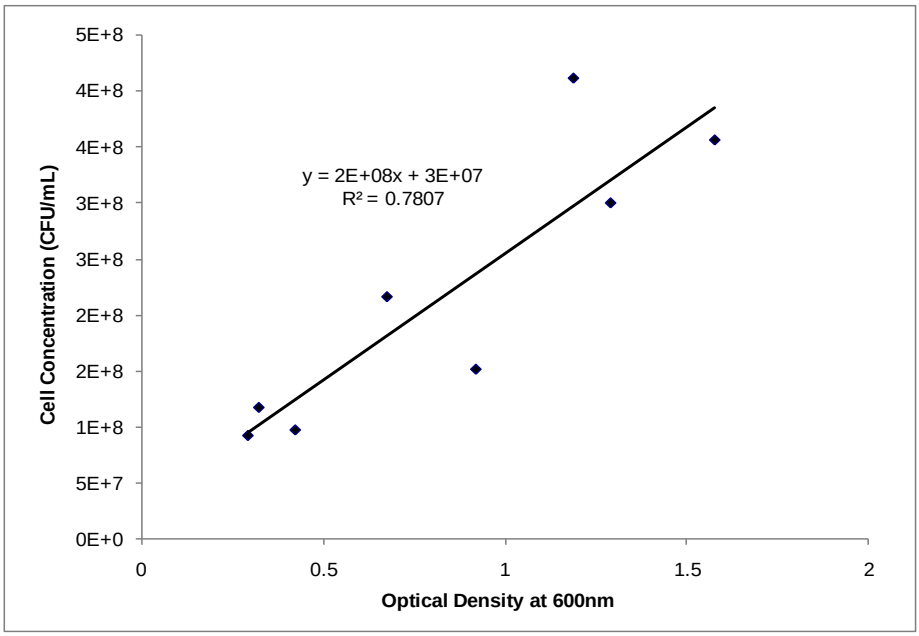

Figure 5.7 Calibration curve relating optical density of *Bacillus subtilis* measure at 600 nm to viable cell concentration found through plate count analysis.

Plots of approximate viable bacteria concentration versus luminescence, from the BacTiter-Glo™ assay, and fluorescence, from the Live/Dead assay, were then generated as seen in Figure 5.8 and Figure 5.9. In both cases a linear trend line showed very strong fit. The resultant equation from the trend line was used to calculate the approximate minimum detection limit of each assay. In the case of the Live/Dead assay only the live results are shown as the dead results were found to be far less sensitive and therefore not used.

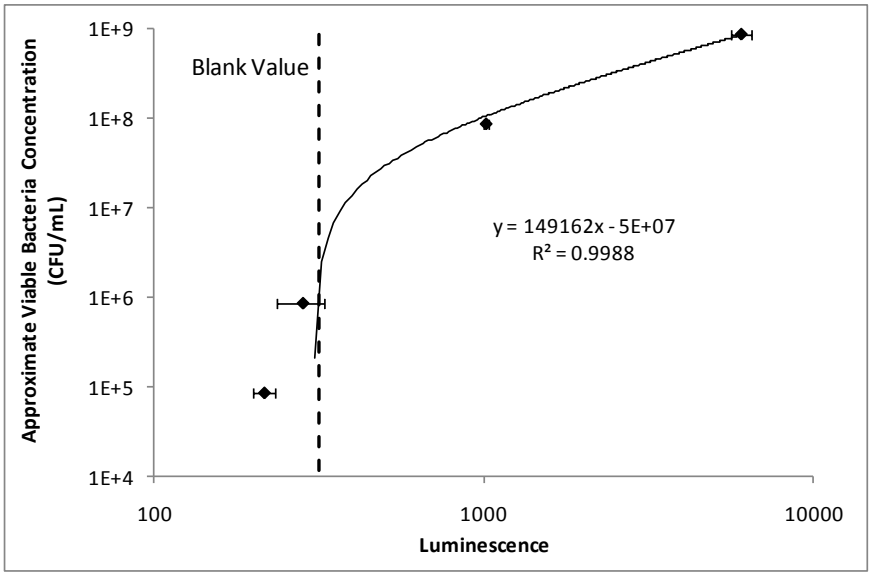

Figure 5.8 Plot of luminescence produced from the BacTiter-Glo™ assay and the corresponding approximate viable bacteria concentration. The horizontal error bars represent one standard deviation.

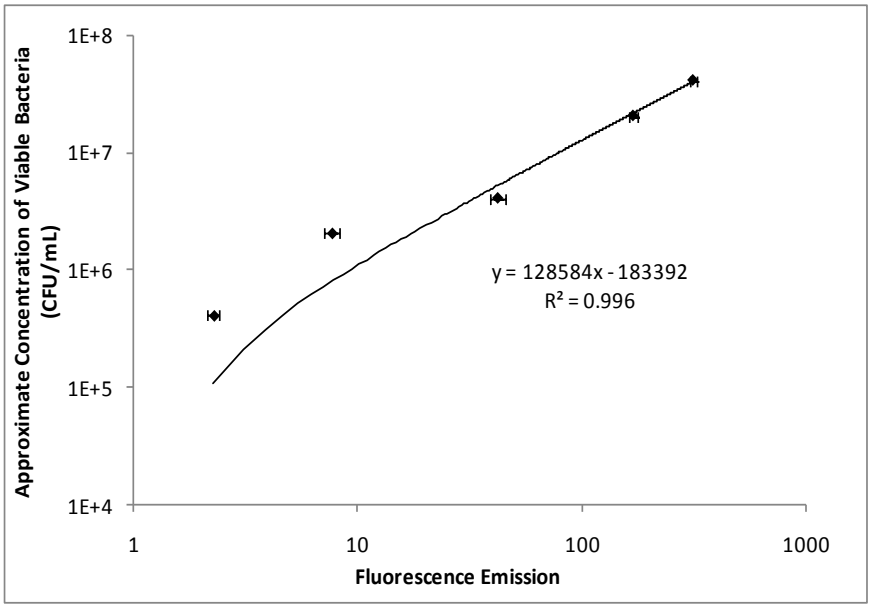

Figure 5.9 Plot of fluorescence produced from the Live/Dead assay and the corresponding approximate viable bacteria concentration. The horizontal error bars represent one standard deviation.

From the equation in Figure 5.8 the approximate minimum detection limit of the BacTiter-Glo™ assay was calculated at the blank luminescence value. Doing so yielded an approximate minimum detection value of 1.4×10^6 for the BacTiter-Glo™ assay. The same was done with the equation in Figure 5.9 to produce an approximate detection limit of 1.8×10^5 for the Live/Dead assay. It was therefore concluded that the Live/Dead assay is the more sensitive assay, having the lower detection limit. The detection limits were then compared against the data generated in the bioaerosol generation and capture experiments using plate counts. This comparison can be seen in Figure 5.10.

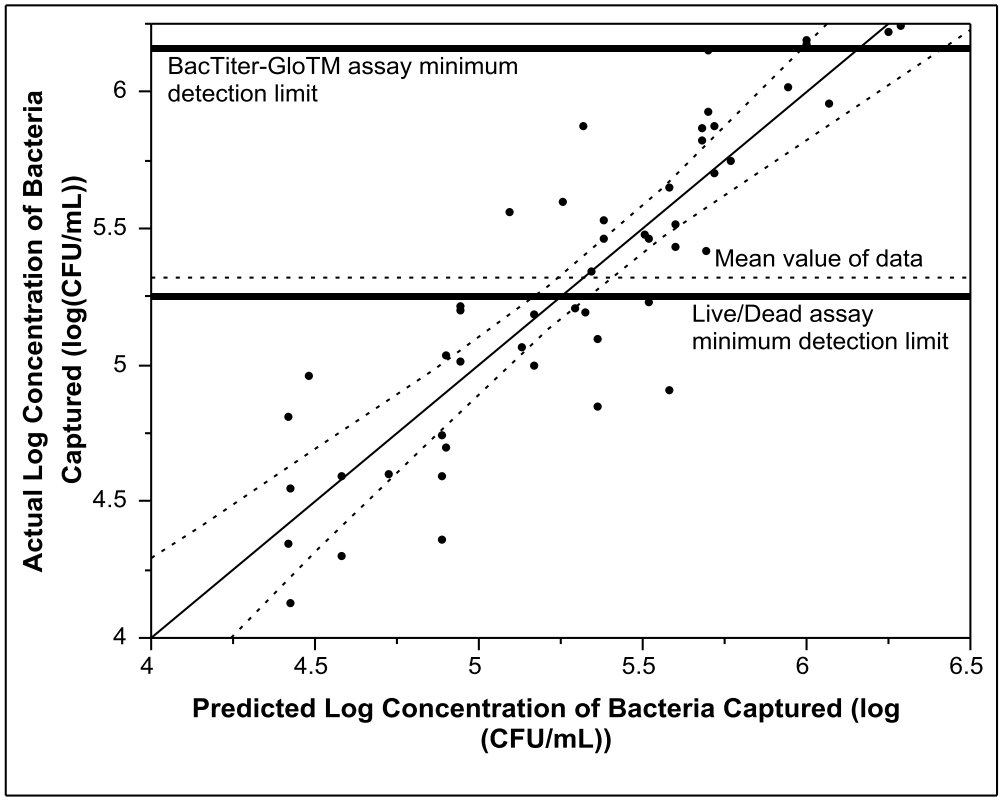

Figure 5.10 Comparison of minimum detection limits of BacTiter-Glo™ analysis and Live/Dead analysis with the data from the bioaerosol generation and capture experiments using plate counts.

From Figure 5.10 it can be seen that the minimum detection limit of the BacTiter-Glo™ assay is higher than the vast majority of the concentrations of viable bacteria captured in the previous aerosol generation and capture experiments. Therefore, if the same range of parameters is used in future experiments, then the BacTiter-Glo™ assay will not be able to effectively analyze the results using the available equipment. Others have found similar results, with the minimum detection limit occurring at approximately double the bacterial concentration used in the bioaerosol generation experiments (Yoon et al., 2010). However, when a dedicated luminometer was used for the BacTiter-Glo™ assay with *Bacillus subtilis,* the detection limit was

found to be 10^5 cells/mL (Seshadri et al., 2009). This detection limit is very similar to that of the Live/Dead assay determined here.

From Figure 5.10 it can also be seen that the minimum detection limit of the Live/Dead assay falls below the mean value of the data set. Therefore, this assay is not applicable over the entire range of experiments conducted, but may be an effective method of analysis if the upper range of parameters is used.

The detection limit of methods, alternative to plate counts, was found and the results are summarized in Table 5.4.

Table 5.4 Summary of detection limits for tested methods of determining viable bacteria concentrations.

Method of Detemining Viable Concentration	Approximate Mimimum Detection Limit (CFU/mL)
Plate counts	300*
BacTiter-GloTM assay	1.40E+06
Live/Dead BacLight assay	1.80E+05
*Theoretical value based on procedure described earlier in the chapter	

The BacTiter-Glo™ has the highest detection limit, and it was determined that this would not be an effective method of analyzing impinger catch without a dedicated luminometer. Although the detection limit of the Live/Dead assay is much higher than the theoretical detection limit of plate counts, the method was determined to be sufficient to analyze the majority of the range of the data set from the bioaerosol generation and capture experiments. Therefore, the Live/Dead test may be an appropriate method of analyzing impinger catch if the experiments with high aerosol production are used. This method of analysis does not require the cells to be cultured or diluted and therefore reduces the error associated with this method compared to plate

count analysis. This method also produces results much more quickly than with plate counts making it easier to run more experiments in a fixed period of time. However, this method may underestimate total cell number because some cells that do not appear as live using the Live/Dead test may be able to recover (Terziva et al., 1996). The potential advantages of the Live/Dead analysis and its moderate detection limit make it a method of catch analysis worth investigating.

5.4.2.2 Bioaerosol Generation and Capture Experiments Using Live/Dead Analysis

Aerosol generation and capture experiments were run as described in the experimental section. The results of the experiments and the predicted results using the fit developed for the plate count analysis experiments are presented in Figure 5.11.

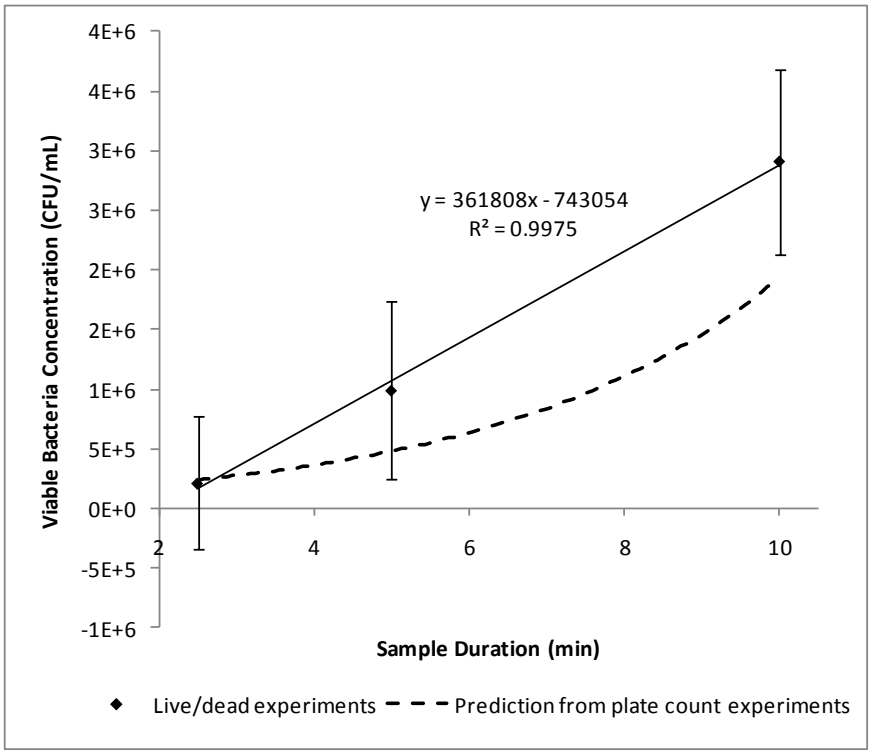

Figure 5.11 Results from bioaerosol generation and capture analysis using Live/Dead analysis, and comparison to predicted trend from plate count analysis. The error bars represent 1 standard deviation.

The trend line in Figure 5.11 shows very strong fit indicating that it is a good prediction of the average value of the experimental results. This fit is much better than that of the plate count analysis, and the use of a power function was not needed as the error from the Live/Dead analysis is not expected to be multiplicative. However, it can be seen that the deviation is still quite high. Upon further examination, it was found that the source of deviation was between the two experimental runs, and that replicates in the same experimental run showed very little deviation. It was therefore concluded that there is likely little error associated with the Live/Dead method, as seen in past results, and that the major source of error came from the experimental setup.

From Figure 5.11, it can also be seen that the results from the Live/Dead analysis is in good agreement with the prediction from the plate count experiments, especially towards the lower end of the range tested. This further confirms the validity of the Live/Dead assay in testing the impinger catch. Even though Live/Dead analysis has a higher minimum detection limit than plate count analysis, it has lower associated error and produces results much more quickly. Therefore, in cases where a high catch value is expected, the Live/Dead analysis should be used, and if possible, experiments should be designed to allow the use of this test.

5.5 Conclusions

The basic design of a reactor system for the photocatalytic inactivation of bioaerosols was described. A simple geometry reactor was chosen for ease in assessment of film performance and a humidity control method was developed using a stream of dry air, humidified air, and a bioaerosol air. A Collison 3-jet Nebulizer was chosen as the bioaerosol generating device, and modified AGI-4 impinger as the capture device. Bioaerosol generation and capture

experiments were completed and analysis was performed via plate counts for the determination of the concentration of viable bacteria. A least squares linear regression model in the logarithmic space of the concentration of bacteria captured was generated but high deviation was seen in the results. To attempt to reduce this deviation, different methods of analyzing the impinger catch were assessed. The detection limit of the Live/Dead assay is much higher than the theoretical detection limit of plate counts, but the limit was sufficient to analyze the majority of the range of the data set from the bioaerosol generation and capture experiments. Aerosol generation and capture experiments were performed using Live/Dead analysis and the results were in good agreement with the prediction from the plate count experiments. The Live/Dead assay is much quicker to perform and has less associated variability. Therefore, in cases where a high catch value is expected, the Live/Dead analysis should be used, and if possible experimental runs should be designed to allow for the use of this test.

Chapter 6

Conclusions and Future Work

The performance of films produced by Novelis Inc. by a flame assisted chemical vapour deposition (FACVD) process was compared with films coated with industry standard Degussa P25. Degussa P25 films were deposited on aluminum substrate by electrophoretic deposition. FACVD films were produced by Novelis Inc. and the effects of varying air flow rate and using different thicknesses of silicon oxides under-layers were assessed.

All films were analyzed by scanning electron microscopy (SEM), energy-dispersive X-ray spectroscopy (EDS), glow discharge optical emission spectroscopy, and Raman spectroscopy. The Degussa P25 films were shown to have thick, high surface area coatings of titanium dioxide primarily in the anatase form, as determined by Raman spectroscopy. The FACVD film series produced with a high air flow rate (T65 series) had a sparse coating of titanium dioxide powder. The films produced at a lower air flow rate (T68 series) had titanium dioxide deposits on all films, however more titanium dioxide was present on films that had silicon oxides under-layer. The amount of deposited titanium dioxide did not increase as the silicon oxides layer was made thicker. The crystallinity of the T65 and T68 series films could not be confirmed due to the small amount of titanium dioxide.

A series of tests were performed to determine which films may be effective for air sterilization. The performance of the films as self-cleaning surfaces, for the destruction of aqueous phase organic compounds, and for the inactivation of aqueous phase microorganisms was tested. The T65 series of films was not effective as self-cleaning surfaces, for the destruction of organics in water, or for the inactivation of bacteria in water. Therefore, it was concluded that

this film series should not be used in bioaerosol inactivation experiments. The Degussa P25 films were shown to have high activity in all applications, confirming that it is a good standard for comparison.

When the air flow rate to in the deposition process was lowered (T68 series), the films were seen to be active. However, only films with a silicon oxides under-layer were effective under UVA light. This was attributed to potential substrate-film interactions such as the migration of aluminum ions, which can act as electron hole recombination centers and decrease photocatalytic activity. The T68 samples with silicon oxides under-layers showed moderate activity when compared to the Degussa P25 films. When UVC light was used, all samples in the T68 series were shown to be as effective as the Degussa P25 film at mineralizing stearic acid. The observation of high performance under UVC light and lower performance under UVA light is commonly made when thin films are used. From these results, it was determined that the T68P3, T68P2, and T68P1 samples may be appropriate for use in bioaerosol inactivation experiment, and that the Degussa P25 films served as an appropriate standard.

The basic design of a reactor system for the photocatalytic inactivation of bioaerosols was described with consideration to reactor geometry, air flow rate, and relative humidity. A simple geometry reactor was chosen for ease of assessment of film performance. A humidity control method was developed using a stream or dry air, humidified air, and bioaerosol impregnated air. A Collison 3-jet Nebulizer was chosen as the bioaerosol generating device, and modified AGI-4 impinger as the capture device. Bioaerosol generation and capture experiments were completed and analysis was performed via plate counts for the determination of the concentration of viable bacteria. The model provided adequate prediction of the trend, but there was high variation between samples. To reduce this deviation, different methods of analyzing the

impinger catch were assessed. The detection limit of the BacTiter-Glo™ assay was found to be higher and therefore not used. The detection limit of the Live/Dead assay is much higher than the theoretical detection limit of plate counts, but the limit was sufficient to analyze the majority of the range of the data set from the bioaerosol generation and capture experiments. Aerosol generation and capture experiments were performed using Live/Dead analysis and the results were in good agreement with the prediction from the plate count experiments. The Live/Dead assay is much quicker to perform and has less associated variability and it should therefore be used in future bioaerosol testing.

The FACVD process was improved to produce films with moderate photocatalytic activity compared to Degussa P25. A test system and protocols for bioaerosol testing was developed. Future work should test bioaerosol inactivation ability of Novelis Inc.'s FACVD films versus the Degussa P25 films. Further work should also be done to try and improve the film thickness produced by the FACVD system to increase photocatalytic activity in the UVA range.

References

Akhtar, M.K., Pratsinis, S.E., Mastrangelo, S.V.R. (1992). *Dopants in Vapor-Phase Synthesis of Titania Powders.* Journal of the American Ceramic Society. 75: 12, 3408-3416.

Akhtar, M.K., Pratsinis, S.E., Mastrangelo, S.V.R. (1992). *Vapor Phase Synthesis of Al-Doped Titania Powders.* Journal of Materials Research. 9: 5, 1241-1249.

Al-Rasheed, R., Cardin, D.J. (2003). *Photocatalytic Degradation of Humic Acid in Saline Waters. Part 1. Artificial Seawater: Influence of TiO_2, Temperature, pH, and Air-Flow.* Chemosphere. 51: 9, 925-933.

Baird, C., Cann, M. (2005). *Environmental Chemistry*. 3rd ed. New York: W.H. Freeman and Company.

Bessergenev, V.G., Khmelinskii, I.V., Pereira, R.J.F., Krisuk, V.V., Turgambaeva, A.E., Igumenov, I.K. (2002). *Preparation of TiO_2 Films by CVD Method and its Electrical, Structural, and Optical Properties.* Vacuum: 64, 275-279.

Bessergenev, V.G., Pereira, R.J.F., Mateus, M.C., Khmelinskii, I.V., Vasconcelos, D.A., Nicula, R., Burkel, E., Botelho do Rego, A.M., Saprykin, A.I. (2006). *Study of Physical and Photocatalytic Properties of Titanium Dioxide Thin Films Prepared from Complex Precursors by Chemical Vapour Deposition.* Thin Solid Films. 503: 29-39.

Bhatkhande, D.S., Pangarkar, V.G., Beenackers, A.A. (2001). *Photocatalytic Degradation for Environmental Applications – a Review.* Journal of Chemical Technology and Biotechnology. 77: 1, 102-116.

Bickley, R.I., Teresita, G.C., Lees, J.S., Palmisano, L., Tilley, R.J.D. (1991). *A Structural Investigation of Titanium Dioxide Photocatalysis.* Journal of Solid State Chemistry. 92: 178-190.

Blake, D.M., Maness, P., Huang, Z., Wolfrum, E.J., Huang, J., Jacoby, W.A. (1999). *Application of the Photocatalytic Chemistry of Titanium Dioxide to Disinfection and the Killing of Cancer Cells.* Separation & Purification Reviews. 28:1, 1-50.

Brachman, P.S., Ehrlich, R., Eichenwald, H.F., Gabelli, V.J., Kethley, T.W., Madin, S.H., Maltman, J.R., Middlebrook, G., Morton, J.D., Silver, I.H., Elwood K. (1964). *Standard Sampler for Assay of Airborne Microorganisms.* Science, New Series. 144: 3624, 1295.

Burge, H.A., Solomon, W.R. (1987). *Sampling and Analysis of biological Aerosols*. Atmospheric Environment. 21:2, 451-456.

Buttner, M.P., Stetzenbach, L.D. (1991). *Evaluation of Four Aerobiological Sampling Methods for the Retrieval of Aerosolized Pseudomonas syringae.* Applied and Environmental Microbiology. 57:4, 1268-1270.

Byrne, J.A., Eggins, B.R., Brown, N.M.D., McKinney, B., Rouse, M. (1998). *Immobilisation of TiO_2 Powder for the Treatment of Polluted Water.* Applied Catalysis B: Environmental. 17: 25-36.

Byun, D., Jin, Y., Kim, B., Lee, J.K., Park, D. (2000). *Photocatalytic TiO_2 Deposition by Chemical Vapor Deposition.* Journal of Hazardous Materials. 73: 2, 199-206.

Carey, J.H., Lawrence, J., Tosine, H.M. (1976). *Photodecholrination of PCB's in the Presence of Titanium Dioxide in Aqueouse Suspensions*. Bulletin of Environmental Contamination and Toxicology. 16: 6, 697-701.

Carp, O., Huisman, C.L., Reller, A. (2004). *Photoinduced Reactivity of Titanium Dioxide*. Progress in Solid State Chemistry. 32: 33-177.

Carraway, E.R., Hoffman, A.J., Hoffman, M.R. (1994). *Photocatalytic Oxidation of Organic Acids on Quantum-Sized Semiconductor Colloids.* Environmental Science and Technology. 28: 5, 786-793.

Chang, C.W., Grinshpun, S.A., Willeke, K., Macher, J.A., Donnelly, J., Clark, S., Juozaitis, A. (1995). *Factors affecting microbiological colony count accuracy for bioaerosol sampling and analysis*. American Industrial Hygiene Association Journal. 56:10, 979–986.

Chang, C.W., Hwang, Y.H., Grinshpun, S.A., Macher, J.A., Willeke, K. (1994). *Evaluation of counting error due to colony masking in bioaerosol sampling*. Applied and Environmental Microbiology. 60:10, 3732–3738.

Chen, D., Ray, A.K. (1999). *Photocatalytic Kinetics of Phenol and its Derivatives Over UV Irradiated TiO_2.* Applied Catalysis B: Environmental. 23: 143, 157.

Chen, F., Yang, X., Xu, F., Wu, Q., Zhang, Y. (2009). *Correlation of Photocatalytic Bactericidal Effect and Organic Matter Degradation of TiO_2 Part I: Observation of Phenomena.* Environmental Science and Technology. 43: 4, 1180-1184.

Cho, M., Chung, H., Choi, W., Yoon, J. (2004). *Linear Correlation Between Inactivation of E. coli and OH Radical Concentration in TiO_2 Photocatalytic Disinfection.* Water Research. 38. 1069-1077.

Choi, W., Termin, A., Hoffman, M.R. (1994). *Role of Metal Ion Dopnats in Quantum-Sized TiO_2: Correlation Between Photoreactivity and Charge Carrier Recombination Dynamics.* Journal of Physical Chemistry. 98:51, 13669-13679.

Choy, K.L., (2003). *Chemical Vapour Deposition of Coatings*. Progress in Materials Science. 48: 57-170.

Choy, K., Bai, W., Charojrochkul, S., Steele, B.C.H. (1998). *The Development of Intermediate-Temperature Solid Oxide Fuel Cells for the Next Millennium.* Journal of Power Sources. 71: 1-2, 361-369.

Chuaybamroong, P., Chotigawin, R., Supothina, S., Sribenjalux, P., Larpkiattaworn, S., Wu, C.Y. (2010). *Efficacy of Photocatalytic HEPA Filter on Microorganism Removal.* Indoor Air. 20: 246-254.

Coleman, H.M., Eggins, B.R., Bryne, J.A., Palmer, F.L., King, E. (2000). *Photocatalytic Degradation of 17-β-oestradiol on Immobilised TiO_2.* Applied Catalysis B: Environmental. 24: 1, L1-L5.

Colwell, R.R., Brayton, P.R., Grimes, D.J., Roszak, D.B., Huq, S.A., Palmer, L.M. (1985). *Viable but Non-Culturable Vibrio cholera and Related Pathogens in the Environment: Implications for Release of Genetically Engineered Microorganisms.* Bio/Technology. 3: 817-820.

Crittenden, J.C., Liu, J., Hand, D.W., Perram, D.L. (1997). *Photocatalytic Oxidation of Chlorinated Hydrocarbons in Water*. Water Research. 31: 3, 429-438.

de Lasa, H., Serrano, B., Salaices, M. (2005). *Photocatalytic Reaction Engineering*. New York: Springer Science+Business Media.

de Tacconi, N.R., Carmona, J., Rajeshwar, K. (1997). *Reversibility of Photoelectrochromism at the TiO_2/ Methylene Blue Interface.* Journal of the Electrochemical Society. 144: 7, 2486-2490.

DeCosemo, G. A. L., Stewart, I.W., Griffiths, W.D., Deans, J.S. (1992). *The assessment of airborne microorganisms*. Journal of Aerosol Science. 23(Suppl. 1):S683-S686.

Ding, P.H., Wang, C.S. (1997). *Effect of Sampling Time on the Sampling Efficiency of All Glass Impinger-30 Samplers for E-coli Aerosol.* Journal of Aerosol Science. 28(Suppl. 1): S671-S672.

Ding, P.H., Wang, C.S. (2001). *Effect of Sampling Time on the Total Recovery Rate of AGI-30 Impingers for E-coli Aerosols*. Aerosol and Air Quality Research. 1:1, 31-36.

Ding, Z., Lu, G.Q., Greenfield, P.F. (2000). *Role of the Crystallite Phase of TiO_2 in Heterogeneous Photocatalysis for Phenol Oxidation in Water.* Journal of Physical Chemistry B. 104:18, 4815-4820.

Draper, R.B., Fox, M.A. (1990). *Titanium Dioxide Photosensitized Reactions Studied by Diffuse Reflectance Flash Photolysis in Aqueous Suspensions of TiO_2 Powder.* Langmuir. 6: 8, 1396-1402.

Dunlop, P.S.M., Byrne, J.A., Manga, N., Eggins, B.R. (2002). *The Photocatalytic Removal of Bacterial Pollutants from Drinking Water.* Journal of Photochemistry and Photobiology A: Chemistry. 148: 355-363.

Evans, P., Sheel, D.W. (2007). *Photoactive and Antibacterial TiO_2 Thin Films on Stainless Steel.* Surface & Coatings Technology. 201: 9319-9324.

Fernandez, A., Lassaletta, G., Jimenez, V.M., Justo, A., Gonzalez-Elipe, A.R., Herrmann, J.M., Tahiri, H., Ait-Ichou, Y. (1995). *Preparation and Characterization of TiO_2 Photocatalysts Supported on Various Rigid Supports (Glass, Quartz and Stainless Steel). Comparative Studies of Photocatalytic Activity in Water Purification.* Applied Catalysis B: Environmental. 7: 49-63.

Foarde, K.K., VanOsdell, D.W., Steiber, R.S. (1997). *Investigation of Gas-Phase Ozone as a Potential Biocide.* Applied Occupational and Environmental Hygiene. 12:8, 535-542.

Fox, M.A., Dulay, M.T. (1993). *Hetergeneous Photocatalysis.* Chemical Reviews. 93:1, 341-357.

Freund, R., Littell, R., Creighton, L. (2003). Regressions in JMP. In: *Regression Using JMP*. Online: SAS Institute and John Wiley and Sons. 25-43.

Fujishima, A., Zhang, X., Tryk, D.A. (2008). *TiO_2 Photocatalysis and Related Surface Phenomena*. Surface Science Reports. 63:12, 515-582.

Gogate, P.R., Pandit, A.B. (2004). *A Review of Imperative Technologies for Wastewater Treatment I: Oxidation Technologies at Ambient Conditions.* Advances in Environmental Research. 8: 501-551.

Goswami, D.Y., Trivedia, D.M, Block, S.S., (1997). *Photocatalytic Disinfection of Indoor Air*. Journal of Solar Energy Engineering. 119:92-96.

Griffiths, W.D., DeCosemo, G.A.L. (1994). *The Assessment of Bioaerosol: A Critical Review.* Journal of Aerosol Science. 25: 8, 1425-1458.

Grinshpun, S.A., Adhikari, A., Honda, T., Kim, K.Y., Toivola, M., Roa, K.S., Reponen, T. (2007). *Control of Aerosol Contaminants in Indoor Air: Combining the Particle Concentration with Microbial Inactivation*. Environmental Science and Technology. 41: 2, 606-612.

Grinshpun, S.A. , Willeke, K., Ulevicius, V., Juozaitis, A., Terzieva, S., Donnelly, J., Stelma, G.N. and Brenner, K.P.(1997). *Effect of Impaction, Bounce and Reaerosolization on the Collection Efficiency of Impingers*. Aerosol Science and Technology. 26: 4, 326 — 342.

Hashimoto, K., Irie, H., Fujishima, A. (2005). *TiO_2 Photocatalysis: A Historical Overview and Future Prospects.* Japanese Journal of Applied Physics. 44: 8269-8285.

Heft, A., Tolke, T., Pfuch, A., Erbe, C. (2006). *Photocatalytically Active Thin Films on Float Glass with Ehanced Hydrophilicity and Transmission for Photovolataic Applications.* Solar Energy Materials and Solar Cells. 90: 17, 2846-2854.

Heller, A. (1995). *Chemistry and Applications of Photocatalytic Oxidation of Thin Organic Films.* Accounts of Chemical Research. 28:12, 503-508.

Henningson, E.W., Fangmark, I., Larsson, E., Wikstrom, L.E. (1988). *Collection Efficiency of Liquid Samplers for Microbiological Aerosols.* Journal of Aerosol Science. 19:7, 911-914.

Herrmann, J.M., Guillard, C., Arguello, M., Aguera, A., Tejedor, A., Piedra, L, Fernandez-Alba, A. (1999). *Photocatalytic Degradation of Pesticide Pirimiphosmethyl: Determination of the Reaction Pathway and Identification of Intermediate Products by Various Analytical Methods.* Catalysis Today. 54: 353-367.

Hiedelberg, J. F., Shahamat, M., Levin, M., Rahman, I., Stelma, G., Grim, C., Colwell, R.R. (1997). *Effects of Aerosolization on Culturability and Viability of Gram Negative Bacteria*. Applied and Environmental Microbiology. 63:9, 3585-3588.

Hitchman, M.L., Tian, F. *Studies of TiO_2 Thin Films Prepared by Chemical Vapour Deposition for Photocatalytic and Photoelectrocatalytic Degradation of 4-Chlorophenol.* Journal of Electroanalytical Chemistry. 539-539: 165-172.

Ho, W., Yu, J.C., Lee, S. (2007). Photocatalytic Activity and Photo-induced Hydrophilicity of Mesoporous TiO_2 Thin Films Coated on Aluminum Substrate. Applied Catalysis B: Environmental. 73:135-143.

Hoffmann, M.R., Martin, S.T., Choi, W. (1995). *Environmental Applications of Semiconductor Photocatalysis.* Chemistry Reviews. 95:1, 69-96.

Huoas, A., Lachheb, H., Ksibi, M., Elaloui, E., Guillard, C., Herrmann, J. (2001). *Photocatalytic Degradation Pathway of Methylene Blue in Water.* Applied Catalysis B: Environmental. 31: 145-157.

Inagaki, M., Nakazawa, Y., Hirano, M., Kobayashi, Y., Toyoda, M. (2001). *Preparation of Stable Anatase-Type TiO_2 and its Photocatalytic Performance.* Internation Journal of Inorganic Materials. 3: 809-811.

Jacobsen, A.E. (1949). *Titanium dioxide Pigments: Correlation Between Photochemical Reactivity and Chalking.* Industrial Engineering and Chemistry. 41: 3, 523-526.

Jacoby, W.A., Maness, P.C., Wolfrum, E.J., Blake, D.M., Fennel, J.A. (1998). *Mineralization of Bacterial Cell Mass on a Photocatalytic Surface in Air.* Environmental Science & Technology. 32: 17, 2650-2653.

Jang, H.D., Kim, S., Kim, S. (2001). *Effect of Particle Size and Phase Composition of Titanium Dioxide Nanoparticles on the Photocatalytic Properties.* Journal of Nanoparticle Research. 3: 141-147.

Jankowska, E., Reponen, T., Willeke, K., Grinsjpu, S.A., Choi, K. (2000). *Collection of Fungal Spores on Air Filters and Spore Reentrainment from Filter into Air*. Journal of Aerosol Science. 31: 8, 969-978.

Jensen, P.A. , Todd, W. F. , Davis, G. N., and Scarpino, P.V.(1992). *Eight Bioaerosol Samplers Challenged with Aerosols of Free Bacteria.* American Industrial Hygiene Association Journal, 53: 10, 660 — 667.

Johnson, D. L.(1999). *The Effect of Phosphate Buffer on Aerosol Size Distribution of Nebulized Bacillus subtilis and Pseudomonas fluorescens Bacteria.* Aerosol Science and Technology. 30: 2, 202 — 210.

Josset, S., Taranto, J., Keller, N., Keller, V., Lett, M. (2010). *Photocatalytic Treatment of Bioaerosols: Impact of Reactor Design.* Environmental Science and Technology. 44: 7, 2605-2611.

Juozaitis, A., Willeke, K., Grinshpun, S.A., Donnelly, J. (1994). *Impaction onto a glass slide or agar versus impingement into a liquid for the collection and recovery of airborne microorganisms*. Applied and Environmental Microbiology. 60:3, 861–870.

Kaliwoh, N., Zhanf, J., Boyd, I.W. (2002). *Characterisation of TiO_2 Deposited by Photo-Induced Chemical Vapour Deposition*. Applied Surface Science. 186: 241-245.

Kalogerakis, N., Pashchali, D., Lekaditis, V., Pantidou, A., Eleftheriadis, K., Lazaridis, M. (2005). *Indoor Air Quality – Bioaerosol Measurements in Domestic and Office Premises.* Aerosol Science. 36: 751-761.

Kanno, T., Oguchi, T., Sakuragi, H., Tokumaru, K. (1980). *Semiconductor-Catalyzed Photooxygenation of Aromatic Olefins.* Tetrahedron Letters. 21: 5, 467-470.

Karyakin, A.A., Strakhova, A.K., Karyakina, E.E., Varfolomeyev, S.D., Yatsimirsky, A.K. (1993). *The Electrochemical Polymerization of Methylene Blue and Bioelectrochemical Activity of the Resulting Film.* Bioelectrochemistry and Bioenergetics. 32: 1, 35-43.

Keller, V., Keller, N., Ledoux, M.J., Lett, M. (2005). *Biological Agent Inactivation in a Flowing Air Stream by by Photocatalysis*. Chemical Communication. 2918-2920.

Kesavan, J., Schepers, D., McFarland, A.R.(2010). *Sampling and Retention Efficiencies of Batch-Type Liquid-Based Bioaerosol Samplers*. Aerosol Science and Technology, 44: 10, 817 — 829.

Konstantinou, I.K., Sakkas, V.A., Albanis, T.A. (2001). *Photocatalytic Degradation of Herbicides Propanil and Molinate Over Aqueous TiO_2 Suspensions: Identification of Intermediates and the Reaction Pathway.* Applied Catalysis B: Environmental. 34:3, 227-239.

Kuhn, K.P., Chaberny, I.F., Massholder, K., Stickler, M., Benz, V.W., Sonntag, H., Erdinger, L. (2003). *Disinfection of Surfaces by Photocatalytic Oxidation with Titanium Dioxide and UVA Light.* Chemosphere. 53: 71-77.

Kwon, C.H., Shin, H., Kim, J.H., Choi, W.S., Yoon, K.H. (2004). *Degradation of Methylene Blue Via Photocatalysis of Titanium Dioxide.* Materials Chemistry and Physics. 86: 78-82.

Legrini, O., Oliveros, E., Braun, A.M. (1993). *Photocatalytic Processes for Water Treatment*. Chemical Reviews. 93: 2, 671-698.

Lembke, L.L., Kniseley, R.N., Van Nostrand, R.C., Hale, M.D. (1981). *Precision of the All-Glass Impinger and the Andersen Microbial Impactor for Air Sampling in Solid-Waste Handling Facilities.* Applied and Environmental Microbiology. 42:2, 222-225.

Li, C.S. (1999). *Sampling Performance of Impactors for Bacterial Bioaerosols.* Aerosol Science and Technology. 30: 3, 280-287.

Li, C.S., Hao, M.L., Lin, W.H., Chang, C.W., Wang, C.S. (1999). *Evaluation of Microbial Samplers for Bacterial Microorganisms.* Aerosol Science and Technology. 30:2, 100-108.

Li, C., Tseng, C., Lai, H., Chang, C. (2003). *UItraviolet Germicidal Irradiation and Titanium Dioxide Photocatalyst for Controlling Legionella pneumiphila.* Aerosol Science and Technology. 37: 12, 961-966.

Lin, C.Y., Li, C.S.(2003). *Effectiveness of Titanium Dioxide Photocatalyst Filters for Controlling Bioaerosols.* Aerosol Science and Technology. 37:2, 162 — 170.

Lippmann, M. (2000). *Environmental Toxicants: Human Exposures and Their Health Effects*. 2nd ed. New Jersey: John Wiley & Sons, Inc.. p449-480, 889-901.

Liu, H., Ma, H.T., Li, X.Z., Li, W.Z., Wu, M., Boa, X.H. (2003). *The Enhancement of TiO_2 Photocatalytic Activity by Hydrogen Thermal Treatment.* Chemosphere. 50: 1, 39-46.

Maeda H, Miyamoto H, Mizuno K. (2004). Synthesis of 3,3,6,6-Tetraaryl-1,2-Dioxanes via TiO_2-Catalyzed Photooxygenation of 1,1-Diarylethenes in the Presence of $Mg(ClO_4)_2$. Chemistry Letters. 33:4, 462.

Maness, P., Smolinski, S., Blake, D.M., Huang, Z., Wolfrum, E.J., Jacoby, W.A. (1999). *Bactericidal Activity of Photocatalytic TiO_2 Reaction: Toward an Understanding of its Killing Mechanism.* Applied and Environmental Microbiology. 65: 9, 4094-4098.

Mao, Y., Schoneich, C., Asmus, K.D. (1991). *Identification of Organic Acids and Other Intermediates in Oxidative Degradation of a Chlorinated Ethanes on Titania Surfaces en Route to Mineralization: a Combined Photocatalytic and Radiation Chemical Study*. Journal of Physical Chemistry. 95: 24, 10080-10089.

Mardare, D., Tasca, M., Deliba, M., Rusu, G.I.. (2000). *On the Strucutural Properties and Optical Transmittance of TiO_2 R.F. Sputtered Thin Films*. Applied Surface Science. 156: 200-206.

Marthi, B., Fieland, V.P., Walter, M., Seidler, R.J. (1990). *Survival of Bacteria during Aerosolization.* Applied and Environmental Microbiology. 56:11, 3463-3467.

Marthi, B., Shaffer, B.T., Lighthart, B., Ganio, L. (1991). *Resuscitation Effects of Catalase on Airborne Bacteria.* Applied and Environmental Microbiology. 57:9, 2775-2776.

Matsunaga, T., Tomoda, R., Nakajima, T., Wake, H. (1985). *Photoelectrochemical Sterilization of Microbial Cells by Semiconductor Powders.* FEMS Microbiology Letters. 29: 211-214.

Matthews, D., Kay, A., Gratzel, M. (1994). *Electrophoretically Deposited Titanium Dioxide Thin Films for Photovolataic Cells.* Australian Journal of Chemistry. 47. 1869-1877.

May, K.R., Harper, G.J. (1957). *The Effect of Various Liquid Impinger Samplers in Bacterial Aerosols.* British Journal of Industrial Medicine. 14:287-297.

Michler, J., Aeberhard, M., Velten, D., Winter, S., Payling, R., Breme, J. (2004). *Depth Profiliing by GDOES: Application of Hydrogen and D.C. Bias Voltage Corrections to the Analysis of Thin Oxide Films.* Thin Solid Films. 447-448: 278-283.

Mills, A., Elliott, N., Parkin, I.P., O'Niell, S.A., Clark, R.J. (2002). *Novel TiO_2 CVD Films for Semiconductor Photocatalysis.* Journal of Photochemistry and Photobiology A: Chemistry. 151: 171-179.

Mills, A., Hill, G., Bhopal, S., Parkin, I.P., O'Niell, S.A. (2003). *Thick Titanium Dioxide Films for Semiconductor Photocatalysis.* Journal of Photochemistry and Photobiology A: Chemistry. 160: 185-194.

Mills, A., Le Hunte, S. (1997). A*n Overview of Semiconductor Photocatalysis.* Journal of Photochemistry and Photobiology A: Chemistry. 108: 1-35.

Mills, A., Wang, J. (1998). *Photomineralisation of 4-Chlorophenol Sensitised by TiO_2 Thin Films.* Journal of Photochemistry and Photobiology A: Chemistry. 118: 53-63.

Mills, A., Wang, J. (1999). *Photobleaching of Methylene Blue Sensitised by TiO_2: an Ambiguous System?.* Journal of Photochemistry and Photobiology A: Chemistry. 127: 123-134.

Mills, G., Hoffman, M.R. (1993). *Photocatalytic Degradation of Pentachlorophenol on TiO_2 Particles: Identification of Intermediates and Mechanism of Reaction*. Environmental Science and Technology. 27:8, 1681-1689.

Minabe, T., Tryk, D.A., Sawunyama, P., Kikuchi, Y., Hashimoto, K., Fujishima, A. (2000). *TiO_2-Mediated Photodegradation of Liquid and Solid Organic Compounds.* Journal of Photochemistry and Photobiology A: Chemistry. 137: 53-62.

Mitchell, J.P.. (1995). Aerosol Generation for Instrument Calibration. In: Cox, C.S., Wathes, C.M. *Bioaerosols Handbook*. Boca Raton: Lewis Publishers.

Mohamed, O.S., Gaber, A.E.M., Abdel-Wahab, A.A. (2002). *Photocatalytic Oxidation of Selected Aryl Alcohols in Acetonitrile.* Journal of Photochemistry and Photobiology A: Chemistry. 148: 205-210.

Montgomery, D.C., Runger, G.C. (2003). *Applied Statistics and Probability for Engineers*. 3rd ed. New York: John Wiley & Sons.

Nevalainen, A., Pastuszka, J., Liebhaber, F., Willike, K. (1992). *Performance of Bioaerosol Samplers: Collection Characteristics and Sampler Design Considerations.* Atmospheric Environment. 26A:4, 531-540.

O'Regan, B., Gratzel, M. (1991). *A Low-Cost, High-Efficiency Solar Cell Based on Dye-Sensitized Colloidal TiO_2 Films.* Nature. 353: 737-740.

O'Shea, K.E., Cardona, C. (1994). *Hammett Study on the TiO_2-Catalyzed Photooxidation of Para-Substituted Phenols. A Kinetic and Mechanistic Analysis.* Journal of Organic Chemistry. 59:17, 5005-5009.

Ohno, T., Masaki, Y., Hirayama, S., Matsumura, M. (2001). *TiO_2-Photocatalyzed Epoxidation of 1-Decene by H_2O_2 Under Visible Light.* Journal of Catalysis. 204: 1, 163-168.

Okudera, H., Yokogawa, Y. (2001). *Formation of TiO_2 Thin Films by Hydrolysis of Ti-Tetraethoxide in Ethanol: Kinetics, Surface Morphology, Constituent Phases and their formation Mechanism.* Thin Solid Films. 401: 124-130.

Ozkan, A., Ozkan, M.H., Gurkan, R., Akcay, M., Sokmen, M. (2004). *Photocatalytic Degradation of a Textile Azo Dye, Sirius Gelb GC on TiO_2 or Ag-TiO_2 Particles in the Absence and Presence of UV Irradiation: the Effects of Some Inorganic Anions on the Photocatalysis.* Journal of Photochemistry and Photobiology A: Chemistry. 163: 29-35.

Pal, A., Min, X., Yu, L.E., Pehkonen, S.O., Ray, M.B. (2005). *Photocatalytic Inactivation of Bioaerosols by TiO_2 Coated Membrane.* International Journal of Chemical Reactor Engineering. 3: A45, 1-12.

Parra, S., Olivero, J., Pacheco, L., Pulgarin, C. (2003). *Structural Properties and Photoreactivity Relationships of Substituted Phenols in TiO_2 Suspensions.* Applied Catalysis B: Environmental. 43: 3, 293-301.

Paschoalino, M.P., Jardim, W.F. (2008). *Indoor Air Disinfection Using a Polyester Supported TiO_2 Photo-reactor.* Indoor Air. 18:473-479.

Peccia, J., Werth, H.M., Miller, S., Hernandez, M. (2001). *Effects of Relative Humidity on the Ultraviolet Induced Inactivation of Airborne Bacteria.* Aerosol Science and Technology. 35: 728-740.

Pozzo, R.L., Baltana, M.A., Cassano, A.E. (1997). *Supported Titanium Oxide as Photocatalyst in Water Decontamination: State of the Art.* Catalysis Today. 39: 219-231.

Reponen, T., Willeke, K., Ulevicius, V., Grinshpun, S.A., Donnelly, J.(1997). *Techniques for Dispersion of Microorganisms into Air.* Aerosol Science and Technology. 27: 3, 405-421.

Riley, R.L., Kaufman, J.E. (1972). *Effect of Relative Humidity on the Inactivation of Airborne Serratia marcescens by Ultraviolet Radiation.* Applied Microbiology. 23:6, 1113-1120.

Ritala, M., Leskela, M., Nykanen, E., Soininen, P., Niinisto, L. (1993). *Growth of Titanium Dioxide Thin Films by Atomic Layer Epitaxy.* Thin Solid Films. 225: 288-295.

Rule, A.M. , Schwab, K.J. , Kesavan, J., Buckley, T. J.(2009). *Assessment of Bioaerosol Generation and Sampling Efficiency Based on Pantoea agglomerans.* Aerosol Science and Technology. 43: 6,

620 — 628.

Saito, T., Iwase, T., Horie, J., Morioka, T. (1992). *Mode of Photocatalytic Bactericidal Action of Powdered semiconductor TiO_2 on Mutans Streptococci*. Journal of Photochemistry and Photobiology B: Biology. 14:4, 369-379.

Sawunyama, P., Jiang, L., Fujishima, A., Hashimoto, K. (1997). *Photodecomposition of a Langmuir-Blodgett Film of Strearic Acid on TiO_2 Film Observed by In Situ Atomic Force Microscopy and FT-IR.* Journal of Physical Chemistry B. 101:51, 11000-11003.

Serrano, B., de Lasa, H. (1997). *Photocatalytic Degradation of Water Organic Pollutants. Kinetic Modeling and Energy Efficiency.* Industriak & Engineering Chemistry Research. 36: 11, 4705-4711.

Seshadri, S., Han, T., Krumins, V., Fennell, D.E., Mainelis, G. (2009). *Applications of ATP Bioluminescence to Characterize Performance of Bioaerosol Sampling Devices.* Aerosol Science. 40:113-121.

Sivakumar, S., Pillai, P.K., Mukundan, P., Warrier, K.G.K. (2002). *Sol-Gel Synthesis of Nanosized Anatase from Titanyl Sulfate.* 57: 2, 330-335.

Soana, F., Sturini, M., Cermenati, L., Albini, A. (2000). *Titanium Dioxide Photocatalyzed Oxygenation of Naphthalene and Some of its Derivatives.* Journal of the Chemical Society Perkins Transactions. 2: 699-704.

Stetzenbach, L.D. (1997). *Aerobiology.* In: Hurst, C.J., Knudsen, G.R., McInerney, M.J., Stetzenbach, L.D., Walter, M.V. *Manual of Environmental Microbiology.* Washington: ASM Press.

Stewart, L. S., Grinshpun, S.A., Willeke, K., Terzieva, S., Ulevicius, V., Donnelly, J. (1995). *Effect of impact stress on microbial recovery on an agar surface*. Applied and Environmental Microbiology. 56: 4, 3468–3472.

Stone, R. C., Johnson, D. L. (2002). *A Note on the Effect of Nebulization Time and Pressure on the Culturability of Bacillus subtilis and Pseudomonas fluorescens*. Aerosol Science and Technology, 36: 5, 536 — 539.

Sunada, K., Kikuchi, Y., Hashimoto, K., Fujishima, A. (1998). *Bactericidal and Detoxification Effects of TiO_2 Thin Film Photocatalysis.* Environmental Science and Technology. 32: 5, 726-728.

Sunada, K., Watanabe, T., Hashimoto, K. (2003). *Studies on Photokilling of Bacteria on TiO_2 Thin Film.* Journal of Photochemistry and Photobiology A: Chemistry. 156: 227-233.

Tanaka, K., Capule, M.F.V., Hisanaga, T. (1991). *Effect of Crystallinity of TiO_2 on its Photocatalytic Action.* Chemical Physics Letters. 187:1-2, 73-76.

Terzian, R., Serpone, N., Minero, C. (1991). *Photocatalyzed Mineralization of Cresols in Aqueous Media with Irradiated Titania.* Journal of Catalysis. 128: 2, 352-365.

Terziva, S., Donnelly, J., Ulevicius, V.,Grinshpun, S. A., Willeke, K., Sterlma, G. N., Brenner, K.P. (1996). *Comparisons of Methods for Detection of Airborne Microorganisms by Liquid Impingement*. Applied and Environmental Microbiology. 62 : 7, 2264-2272.

Turchi, C.S., Ollis, D.F. (1990). *Photocatalytic Degradation of Organic Water Contaminants: Mechanisms Involving Hydroxyl Radical Attack.* Journal of Catalysis. 122: 1, 178-192.

Vohra, A., Goswami, D.Y., Deshpande, D.A., Block, S.S. (2005). *Enhanced Photocatalytic Inactivation of Bacterial Spores on Surfaces in Air*. Journal of Industrial Microbiology & Biotechnology. 32: 6, 364-370.

Vohra, A., Goswami, D.Y., Deshpande, D.A., Block, S.S. (2006). *Enhanced Photocatalytic Disinfection of Indoor Air*. Applied Catalysis B: Environmental. 65:57-65.

Walter, M.V., Marthi, B., Fieland, V.P., Ganio, L.M. (1990). *Effect of Aerosolization on Subsequent Bacterial Survival*. Applied and Environmental Microbiology. 56: 11, 3468–3472.

Wang, J., Zhu, W., Zhang, Y., Liu, S. (2007). *An Efficient Two-Step Technique for Nitrogen-Doped Titanium Dioxide Synthesizing: Visible-Light-Induced Photodecomposition of Methylene Blue*. Journal of Physical Chemistry. 111: 2, 1010-1014.

Wang, R., Hashimoto, K., Fujishima, A., Chikuni, M., Kojima, E., Kitamura, A., Shimohigoshi, M., Watanabe, T. (1998). *Photogeneration of Highly Amphphilic Surface.* Advanced Materials. 10: 135-138.

Wang, Z., Reponen, T., Grinshpun, S.A., Gorny, R.L., Willeke, K. (2001). *Effect of Sampling Time and Air Humidity on the Bioefficiency of Filter Samplers for Bioaerosol Collection*. Aerosol Science. 32:661-674.

Watanabe, T., Nakajima, A, Wang, R., Minabe, R., Koizumi, S., Fujishima, A., Hashimoto, K. (1999). *Photocatalytic Activity and Photoinduced Hydrophilicity of Titanium Dioxide Coated Glass.* Thin Solid Films. 351: 260-263.

Willeke, K., Grinshpun, S.A., Ulevicius V., Terzieva, S., Donnelly, J., Stewart, S., Juozaitis, A. (1995). *Microbial stress, bounce and re-aerosolization in bioaerosol samplers*. Journal of Aerosol Science. 26:S883–S884.

Wold, A. (1993). *Photocatalytic Properties of TiO_2.* Chemistry of Materials. 5:3, 280-283.

Wolfrum, E.J., Huang, J., Blake, D.M., Maness, P., Huang, Z., Fiest, J. (2002). *Photocatalytic Oxidation of Bacteria, Bacterial and Fungal Spores, and Model Biofilm Components to Carbon Dioxide on Titanium Dioxide-Coated Surfaces.* Environmental Science and Technology. 36: 15, 3412-3419.

Xu, Y., Yan, X. (2010). *Chemical Vapour Deposition: An Integrated Engineering Design for Advanced Materials*. New York: Springer.

Ye, S., Fan, M., Song, X., Luo, S. (2010). *Enhanced Photocatalytic Disinfection of P. expansum in Cold Storage Using a TiO_2/ACF Film*. International Journal of Food Microbiology. 136: 332-339.

Yoon, K.Y., Park, C.W., Byeon, J.H., Hwang, J. (2010). *Design and Application of an Inertial Impactor in Combination with an ATP Bioluminescence Detector for In Situ Rapid Estimation of the Efficacies of Air Controlling Devices on Removal of Bioaerosols.* Enivronmental Science & Technology. 44:5, 1742-1746.

Yu., K., Lee, G.W., Lin, S., Huang, C.P. (2008). *Removal of Bioaerosols by the Combination of a Photocatalytic Filter and Negative Air Ions.* Aerosol Science. 39: 377-392.

Zhu, Y., Zhang, L., Wang, L., Tan, R., Cao, L. (2001). *Interface Diffusion and Reaction Between TiO_2 Film Photocatalyst and Aluminum Alloy Substrate*. Surface and Interface Analysis. 32: 218-223.

Zimmerman, N.J., Reist, P.C., Turner, A.G. (1987). *Comparison of Two Biological Sampling Methods.* Applied and Environmental Microbiology. 53:1, 99-104.